# Central Gulf of Aden conjugate margins (Yemen-Somalia): Tectono-sedimentary and magmatism evolution in hybrid-type margins

Chloé Nonn, Sylvie Leroy, Marc Lescanne, Raymi Castilla

Manuscript: Nonn C., Leroy S., Castilla, R., Lescanne M. 2019. Central Gulf of Aden conjugate margins (Yemen-Somalia): tectono-stratigraphic and magmatic evolution of hybrid-type margins. Marine & Petroleum Geology. 105. 100-123. 10.1016/ j.marpetgeo.2018.11.053

# Central Gulf of Aden conjugate margins (Yemen-Somalia): tectono-sedimentary and magmatism evolution in hybrid-type margins

Chloé NONN [1], Sylvie LEROY [1], Marc LESCANNE [2], Raymi CASTILLA[2]

*1* - Sorbonne Université, CNRS-INSU, Institut des Sciences de la Terre Paris, ISTeP UMR 7193, F-75005 Paris, France.

*2 - Total, CSTJF, Research & Development, Av Larribau Pau, France.*

Magma-rich and magma-poor passive margins are generally studied separately. Yet, the spatial evolution from one type to another is not well understood. Central Gulf of Aden margins are at the transition between these two types of margins. Based on new seismic data, published wells and gravity data, we determine seismic stratigraphy and structural patterns. We map the distinct crustal domains (continental, Ocean-Continent Transition (OCT), oceanic domains) and propose a tectonic evolution of the Yemeni and Somalian conjugate margins in an oblique rifting context. The most striking results are the significant segmentation, narrowness and asymmetry of conjugate margins, as well as the gradual eastward decrease in the intensity of magmatic activity of these hybrid-type margins. West of Bosaso-Hami Fracture Zone (BHFZ), the Hami-Ahl Medo segment presents magmatic-type margin features in the distal Yemeni margin related to the strong influence from the Afar plume: Seaward dipping reflectors develop since the late syn-rift stage (~21 - 18 Ma) near the Xiis-Al Mukalla Fracture Zone. Conversely, east of BHFZ, the Bosaso-Sayhut margins segment is characterized by magma-poor margins for which the exhumation stage is characterized by the unroofing of mantle along multiple detachment faults in the OCT and shortly followed by diachronous volcanism (~18 Ma). The central Gulf of Aden is affected by a major uplift during the final syn-rift stage and up to OCT formation. This event is associated with the formation of erosional surfaces in the east and with gravitational deformation taking place on decoupling surfaces at the base of the syn-rift sequence (lower Ghaydah Fm) that lead to the sliding of syn-rift units on top of the exhumed mantle rocks in the OCT.

***Key words:*** *hybrid margins, Gulf of Aden, crustal domains, tectono-stratigraphic evolution, asymmetry, magmatism.*

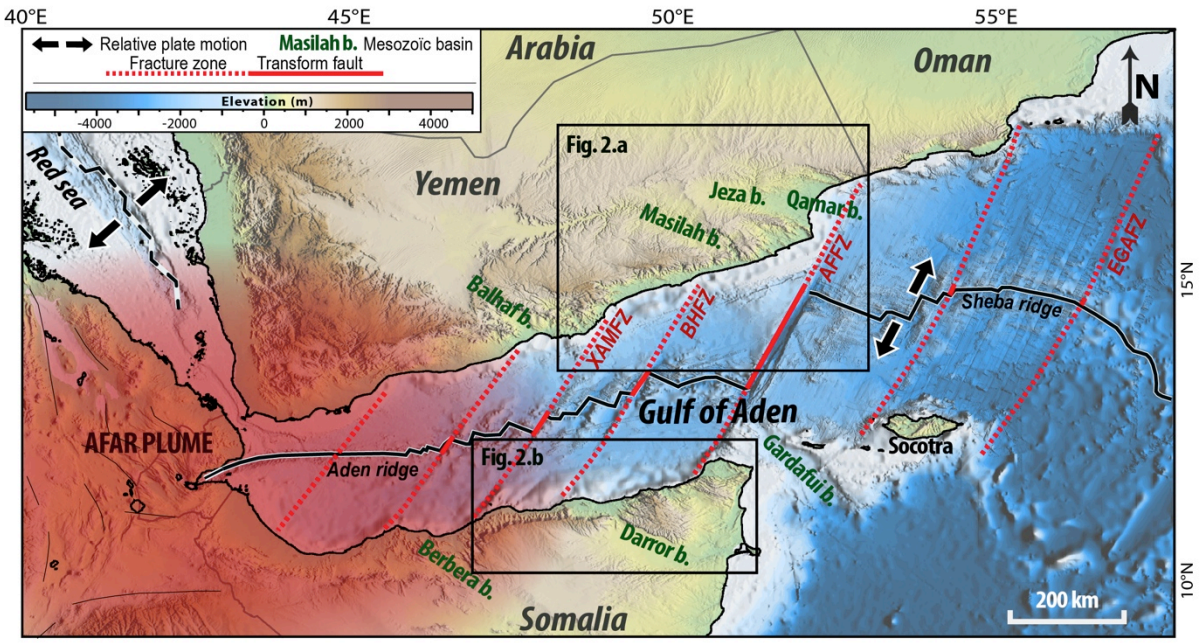


*Figure 1- Topographic and bathymetric map of the Gulf of Aden (modified from Nonn et al., 2017) showing the first-order fracture zones. Black arrows represent the relative plate motion; the studied area is framed in black in the central Gulf of Aden, between the Xiis Al Mukalla Fracture Zone (XAMFZ) and the Alula Fartak Fracture Zone (AFFZ). The Mesozoic basins correspond to: (i) the Balhaf, the Masilah, the Jeza and the Qamar basins (b.) in Yemen; (ii) the Berbera, the Darror and the Gardafui basins (b.) in Somalia. BHFZ: Bosaso-Hami Fracture Zone. EGAFZ: Eastern Gulf of Aden Fracture Zone.*

## 1. Introduction

To improve our understanding of how the deformation localized in distal part of the margins, towards the future area of lithospheric breakup, we need to better figure out the actual architecture of crustal domains in present-day passive margins. Despite of variable tectonic and magmatic processes involved during their formation, magma-poor and magma-rich rifted margins present major crustal domains displaying structural similarities at first-order (Péron-Pinvidic et al., 2013). The continental domain is characterized by unequivocal continental crust that is progressively thinned in distal parts of the margins. The Ocean-Continent Transition (OCT) corresponds to the gradual transition from the thinned continental domain to the stable oceanic crust. The rifting process is driven by lithospheric mantle dynamic until the OCT formation (Lagabrielle, 2009; Jolivet et al., 2015; Péron-Pinvidic and Osmundsen, 2016). Subsequently, the formation of steady-state oceanic crust is driven by asthenospheric mantle dynamic. The geological and geophysical attributes of the OCT contrast from one margin to another, as does the amount of volcanic supply (Péron-Pinvidic and Osmundsen, 2016; Stab et al., 2016).

During and after rifting, magmatism is an essential process in the formation of continental passive margins. The question of whether conjugate passives margins are magma-poor or magma-rich, and the along strike variation from one to another, are significant issues for the understanding of rift systems with lateral

52 changes in thermal state. The distinction between margins that are magma-rich (related to large volumes of
53 magma) or magma-poor (related to lithospheric detachment faulting) is based on the timing and degree of
54 mantle melting associated with lithospheric thinning as well as with crustal and lithospheric break-up (White
55 and McKenzie, 1989; Coffin and Eldholm, 1994; Courtillot et al., 1999; Geoffroy et al., 2015). However, the
56 occurrence of hybrid margins, for which the volume of volcanic products varies along strike from magma-poor
57 to magma-rich settings (Reston and Manatschal, 2011), show that these definitions are still ambiguous. In any
58 case, significant and localized magma supply can contribute to focusing the extension (e.g. Buck, 1991; Ebinger
59 and Casey, 2001; Péron-Pinvidic et al., 2013), while diffuse volcanic supply can lead to a wider distribution of
60 the extensional stress (Corti et al., 2003).
61 In the present study, we focus on the type of stratigraphic, structural and magmatic architectures that
62 can develop on a hybrid continental margin. We focus on the central Gulf of Aden located between the Xiis-Al
63 Mukalla (XAMFZ) and Alula Fartak (AFFZ) Fracture Zones (area Framed in black, Fig. 1). In this oceanic basin, the
64 Somalia-Yemen conjugate margins were formed by a polyphase and oblique divergence of the Arabian and
65 African plates during the Mesozoic and Cenozoic. The little-known studied area is located between magma-rich
66 margins in the western part (influenced by the Afar plume; Tard et al., 1991; Beydoun et al., 1998; Leroy et al.,
67 2012; Stab et al., 2016) and magma-poor margins in the eastern part (Leroy et al., 2004, 2012, d'Acremont et
68 al., 2005, 2006; Autin et al., 2010b; Watremez et al., 2011; Nonn et al., 2017). The aim of this paper is to
69 explore the Cenozoic syn- to post-rift tectonic history of the central Gulf of Aden conjugate margins. Based on
70 interpretations of a dense grid of seismic profiles combined with wells, bathymetric, gravimetric data, we
71 correlate the onshore and offshore stratigraphy; we map the structures and the crustal domains in order to
72 correlate the conjugate margin and constrain their spatial evolution. We attempt to address questions on the
73 nature of the seismic basement in various crustal domains and on the relationships between the tectono-
74 stratigraphic and magmatic evolution of the conjugate margins in an area of along strike transition from
75 volcanic to non-volcanic margins. The mapping of crustal domains shows the narrowness and the asymmetrical
76 style of these hybrid-type margins. The observation of the sedimentary sequences reveals the activity of
77 decoupling surface at the base of the syn-rift sequence from the late syn-rift period to the syn-OCT period. We
78 observed that the period of formation of the OCT is marked by a phase of significant uplift of the whole
79 margins also recorded by significant erosion in the central Gulf of Aden distal margins.
80
81 **2. Geological setting**

### 2.1 Kinematic context

The continental rifting of Gulf of Aden started 34 Ma ago between the Arabian and Somalian plates (Figs. 1, 2) with a direction of extension (N20°E) oblique to the trend of the rift (N70°E) (Roger et al., 1989; Watchorn et al., 1998; Leroy et al., 2012; Pik et al., 2013; Robinet et al., 2013). The obliquity led to a significant segmentation characterized by various fault sets including several major fracture zones parallel to the divergence such as the XAMFZ, the AFFZ and the Bosaso Hami Fracture Zone (BHFZ) (in grey, Figs. 1, 2). None inherited zones of weakness trending ~N70°E parallel to the Gulf is reactivated (Autin et al., 2010a, 2013; Bellahsen et al., 2013a). Oceanic seafloor spreading started during the Burdigalian at ~17 Ma in the Gulf of Aden (e.g. Leroy et al., 2004; d'Acremont et al., 2006, 2010; Leroy et al., 2010; Nonn et al., 2017). The oceanic spreading rate increases from the west (13 mm yr-1 along N35°E) towards the eastern Sheba-Ridge (18 mm yr-1 along N25°E, Jestin et al., 1994; Fournier et al., 2001) (Fig. 2). Extension resulted in magma-rich margins in the western part near the Afar plume (Tard et al., 1991; Beydoun et al., 1998; Leroy et al., 2012; Stab et al., 2016) and magma-poor margins in the eastern Gulf of Aden, leading to mantle exhumation from the AFFZ to the EGAFZ (Leroy et al., 2004, 2010a; d'Acremont et al., 2005, 2006; Autin et al., 2010b; Watremez et al., 2011; Leroy et al., 2012; Nonn et al., 2017) (Fig. 1).

### 2.2 Structural framework onland and crustal thickness

In the central Gulf of Aden, significant outcrops of Cenozoic pre-rift units (in orange, Figs. 2, 3.a) occur in series of grabens and horsts on the conjugate margins. On the Yemeni margin, the EW to N110°E-trending Masilah basin is bounded to the southwest by the Mukalla High, to the northeast by the Fartak High and to the north by the Hadramaut Arch (Fig. 2.a). Along the coastline, the Hami graben is limited to the north by the highest relief of the Yemeni margin that reaches an elevation of ~2000 m and trends EW (Lat. 15°N, Long. 50°E, Fig. 2.a). Basins, plateaus and mountains also form the morphology of the onshore Somalian margin (Fig. 2.b). In the western part, the EW trending Ahl Medo High (2000 m of elevation) borders the Ahl Medo and Bosaso basins (Lat. 11°10'N, Long. 49°E, Fig. 2.b). In the eastern part, the Ahl Miskat and the Ahl Bari highs border the major WNW-ESE Darror (10°30'N, 49°30'E, Fig. 2.b), the Qandala El Gal and Alula basins (Lat. 11°25'N, Long. 50°10'E and Lat. 11°50'N, Long. 50°50'E, Fig. 2.b).

On the onshore conjugate margins, the continental crust is thinned of ~30-50% towards the ocean (Fig. 2): Moho depths range from 20 km near the coastline to 35 km at a distance of ~75 km from the coastline to 42 km in the outer parts of the rift system (Ali and Watts, 2013; Korostelev et al., 2016).

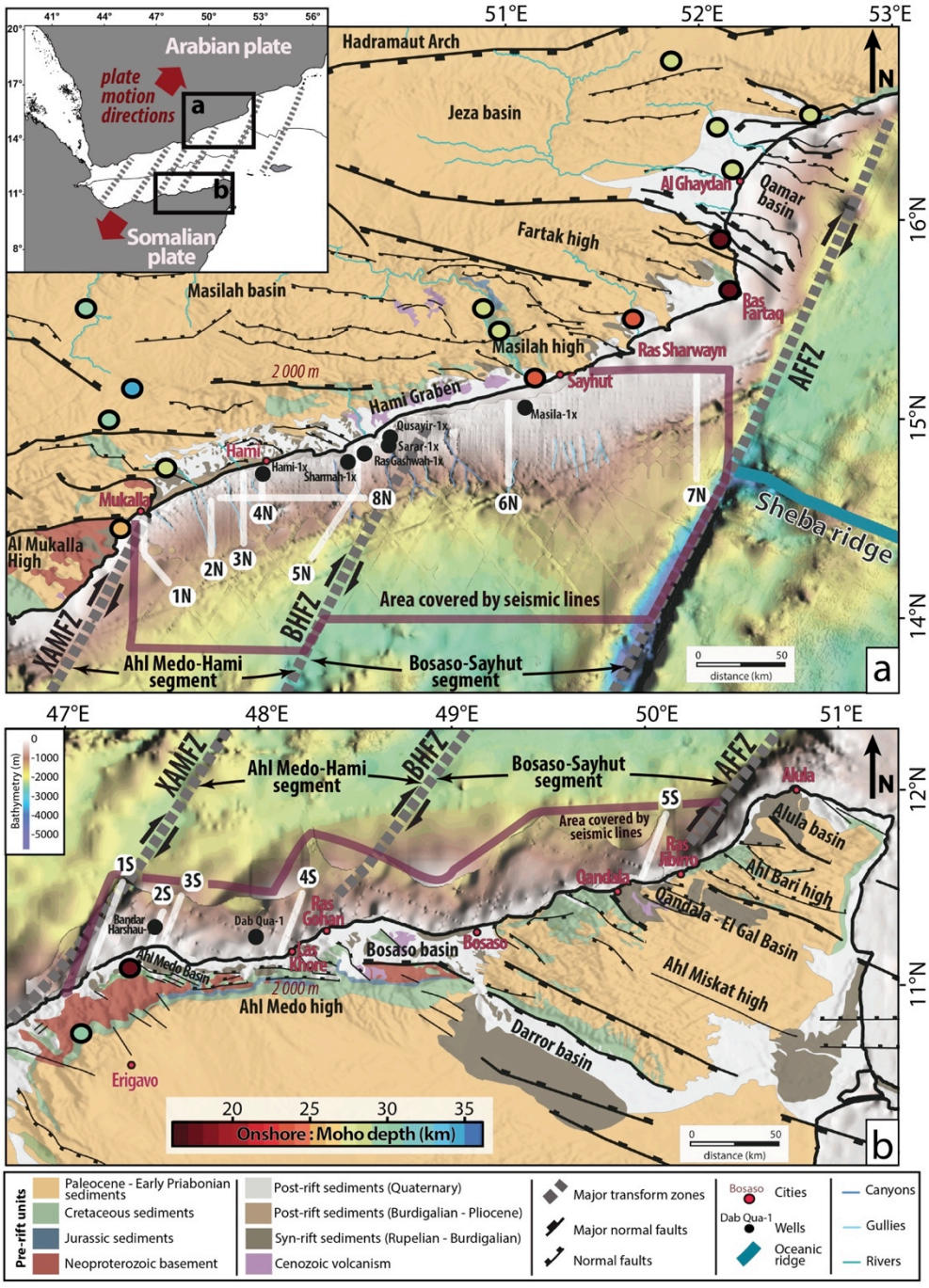


***Figure 2*** *- Simplified geological map of the Central Gulf of Aden conjugate margins (Ellis et al., 1996; Birse et al., 1997; Beydoun, 1970; Bott et al., 1992; Bosence, 1997; Brannan et al., 1997; Fantozzi and Sgavetti, 1998; Nichols and Watchorn, 1998; Watchorn et al., 1998; Fantozzi and Ali-Kassim, 2002; Leroy et al., 2012; Ali, 2015) (location on Figure 1) showing bathymetry from GEBCO 30 arc-second global grid (2014) and interpretation of seismic data, with topographic map in background, for the northern (a) and southern (b) margins. The offshore areas covered by seismic profiles are surrounded by the dark purple lines and the conjugate coastlines (represented in black). The colour coding of the geological map is the same as on Figure 3: in red, the Neoproterozoic crystalline basement (metamorphic and igneous rocks (e.g. Menzies et al., 1992, 1994, 1997; Redfern and Jones, 1995) crops out with a global EW structural trend (e.g. Fantozzi and Ali-Kassim, 2002) near the Mukalla High in Yemen (Bosence et al., 1996; Watchorn et al., 1998), near Erigavo and Bosaso cities in Somalia (Warden and Horkel, 1984; Kröner and Sassi, 1996). In blue, Jurassic basement; in green, Cretaceous basement; in light orange, Cenozoic pre-rift units (Palaeocene – Eocene); in dark brown, syn- rift units (Priabonian – Burdigalian); in light brown, post-rift units (Burdigalian – Pliocene); in white, Quaternary units; in violet, Oligo-Miocene volcanic formations. Colourful circles: Onshore crustal thicknesses (a) from receiver function analysis (Korostelev et al., 2016) and (b) derived from gravity and flexure modelling (Ali and Watts, 2013). The hydrological network is inferred from sea bottom observations. The location of wells is derived from Ahlbrandt (2002), Ali and Watts (2013) and Bott et al. (1992) and other references therein. Top-left inset: simplified regional map indicating the relative motions of the Arabian and Somalian plates (red arrows), the fracture zones (in dashed grey) and the location of Figures a and b. AFFZ: Alula Fartak Fracture Zone. XAMFZ: Xiis Al Mukalla Fracture Zone. BHFZ: Bosaso Hami Fracture Zone.*

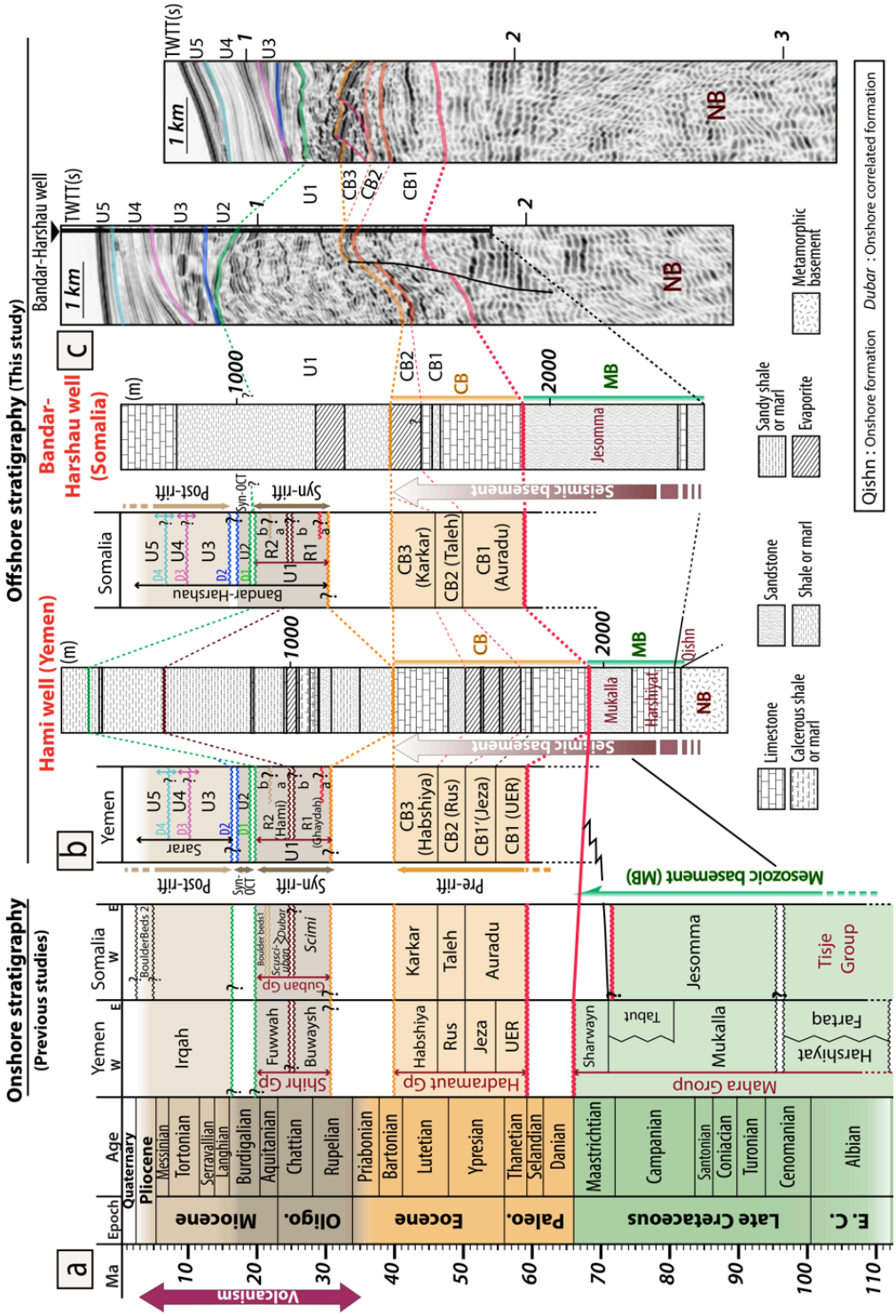


*Figure 3 - Synthesis of onshore stratigraphy and correlation with various units proposed for the stratigraphy of offshore profiles. (a) Synthesis of onland stratigraphy of the central Gulf of Aden conjugate margins taking into account the spatial distribution (Azzaroli, 1958; Menzies et al., 1992, 1997; Ali Kassim, 1991; Bott et al., 1992; Redfern and Jones, 1995; Kröner and Sassi, 1996; Bosence et al., 1996; Beydoun et al., 1996, 1998; Beydoun, 1997; Bosence, 1997; Fantozzi and Sgavetti, 1998; Fantozzi and Ali-Kassim, 2002; Nichols and Watchorn, 1998; Watchorn et al., 1998; Ahlbrandt, 2002; Bosworth et al., 2005; Hakimi et al., 2010; Ali and Watts, 2013; Ali, 2015) (b) Summary of different units in Yemen and Somalia suggested as correlating with the offshore stratigraphy. Correlation with Hami well (Yemen) (Bott et al., 1992) and Bandar-Harshau well (Somalia) (Ali, 2015; Bott et al., 1992). (c) Correlation with segment of seismic line in Somalia published by (Ali and Watts, 2013; Ali, 2015) showing the seismic facies and various units mentioned here. The working correlation is based on well data, seismic facies, sediment geometries and location of sedimentary units in the stratigraphic column in accordance with the tectono-sedimentary evolution of the Gulf of Aden. See text for explanation. CB: Cenozoic basement. Gp: Group. MB: Mesozoic basement. NB: Neoproterozoic basement. UER: Umm Er Radhuma.*

164 **2.3 Tectono-stratigraphic record: previous works in the central Gulf of Aden**

165 Previous field works and well studies show the relationships between the sedimentary record and tectonic events of
166 the central segment of the Gulf of Aden, along the conjugate margins bordering Yemen (e.g. Brannan et al., 1997;
167 Huchon and Khanbari, 2003) and Somalia (e.g. Fantozzi and Ali-Kassim, 2002; Ali and Watts, 2016) (Fig. 3). Note that
168 the terms 'pre-rift', 'syn-rift', and 'post-rift' are used here with respect to the Oligo-Miocene rifting of the Gulf of
169 Aden. In this work, the Mesozoic series are included in the pre-rift sequence.

170

171 *2.3.1 Pre-rift sequence: Mesozoic and Cenozoic sequences*

172 The Cenozoic pre-rift succession, which is widely exposed in the central Gulf of Aden segment (Fig. 2), lies
173 unconformably on the Mesozoic basement. Its eastward thickening expresses the eastward increase of
174 subsidence (Beydoun, 1970, 1997; Brannan et al., 1997; Ali and Watts, 2013). In Yemen, the Hadramaut Group
175 represents the Palaeocene to Eocene sequence and is composed of the Umm Er Radhuma (UER), Jeza, Rus and
176 Habshiya Fms (in orange, Figs. 2, 3.a, b) (Beydoun, 1997; Bosence, 1997; Brannan et al., 1997; Watchorn et al.,
177 1998).

178 A first major transgression is recorded by the shallow marine reefal carbonates of the UER (Thanetian –
179 Ypresian) and marly carbonates of the Jeza Fms (Ypresian) in Yemen (Beydoun et al., 1998) correlated to the
180 limestone of the Auradu Fm (Thanetian – Ypresian) in Somalia (Figs. 3.a, b) (Beydoun, 1970; Fantozzi and Ali-
181 Kassim, 2002). A second period of regression (middle Ypresian – early Lutetian) is associated with the
182 evaporites of the Rus Fm in Yemen and Taleh Fm in Somalia (Beydoun, 1970; Brannan et al., 1997; Beydoun et
183 al., 1998) (Figs. 3.a, b). The latest transgression (Lutetian) led to the accumulation of the Habshiya Fm in Yemen
184 and Karkar Fm in Somalia (Figs. 3.a, b), which are made up of shallow marine reefal carbonates (Beydoun,
185 1970; Fantozzi and Ali-Kassim, 2002). The Eocene is characterized by a major uplift of the conjugate margins
186 recorded by broad erosion at the top of the carbonates of the Habshiya and Karkar Fms (Brannan et al., 1997;
187 Leroy et al., 2012) (Figs. 3.a, b).

188

189 *2.3.2 Syn-rift sequence*

190 On the northern margin, the onshore syn-rift succession (Shihr Group, Upper-Priabonian – Burdigalian, Fig. 3.a)
191 (Watchorn et al., 1998; Beydoun et al., 1998; Ahlbrandt, 2002) crops out along the coast to the East of Al
192 Mukalla city (Fig. 2). On the southern margin, the syn-rift sequence (Guban Group and lower Bandar-Harshau

193 Fms, Fig. 3.a) (Azzaroli, 1958; Fantozzi and Ali-Kassim, 2002) is restricted to the Darror basin and along the
194 coastline east of Qandala city (Lat. 11°N, Long. 49°E, Fig. 2).

195 During the Oligocene, the rifting is characterized by a phase of tectonic subsidence as shown by a
196 transition from clastic to carbonate deposits on the conjugate margins. In onshore Yemen, the Buwaysh Fm is
197 composed of alternating shales, sandstones, conglomerates and anhydrites (Beydoun et al., 1998; Ahlbrandt,
198 2002) (Fig. 3.a). Offshore Yemen, the Ghaydah Fm (Rupelian – Early Chattian) is characterized by sandstones
199 and conglomerates in the lower part and anhydrites and marls in the upper part (Fig. 3. b); this unit is more
200 evaporitic towards the west and mainly carbonate-bearing towards the east (Beydoun, 1970; Bott et al., 1992;
201 Bosence et al., 1996; Beydoun et al., 1998; Watchorn et al., 1998). In Somalia, the base of the syn-rift sequence
202 seen onshore is composed of sandstones and conglomerates correlated with the Scimi Fm (e.g. Fantozzi and
203 Ali-Kassim, 2002; Bosworth et al., 2005; Ali and Watts, 2016) (Fig. 3.a). Offshore Somalia, the lower part of
204 Bandar-Harshau Fm comprises anhydrites and shales recorded in the Bandar-Harshau-1 (Bott et al., 1992; Ali
205 and Watts, 2013) (Fig. 3.b).

206 During the Chattian – Burdigalian, rifting intensified and is associated with the development of major
207 faults (Leroy et al., 2012). Onshore Yemen, carbonate marls and conglomerates form the base and a carbonate
208 platform forms the top of the Fuwwah Fm (Beydoun et al., 1998; Ahlbrandt, 2002) (Fig. 3.a). Offshore Yemen,
209 this sequence is equivalent to the Hami Fm defined by alternations of carbonate marls and sandstones passing
210 up into limestones (Beydoun, 1970; Bott et al., 1992; Bosence et al., 1996; Beydoun et al., 1998; Watchorn et
211 al., 1998) (Fig. 3.b). The onshore Somalia succession corresponds to reefal carbonates (correlated with the
212 Dubar Fm) which passes laterally into lagoon and fluvial facies (correlated with the Scusciuban Fm) (Azzaroli,
213 1958; Ali Kassim, 1991; Bott et al., 1992; Fantozzi and Sgavetti, 1998; Fantozzi and Ali-Kassim, 2002; Bosworth
214 et al., 2005; Ali and Watts, 2016) (Fig. 3.a). Offshore Somalia, the Bandar-Harshau Fm corresponds to deep-
215 marine deposits (Hughes and Beydoun, 1992) (Figs. 3.b, c).

216

217 *2.3.3 Syn-OCT development sequence*

218 The end of rifting is characterized by a regional uplift and late-stage tilting of the conjugate margins (Leroy et
219 al., 2012). On the Somalian margin, the upper part of the syn-rift sequence displays regressive facies overlain
220 by syn-tectonic conglomeratic deposits of the Boulder beds 1 Fm (Fig. 3.a) near the coast of Somalia with
221 alluvial fan deposits along normal faults (Fantozzi and Ali-Kassim, 2002).

222

223 *2.3.4 Post-rift sequence*

224 On the emerged Yemen margin, the middle Miocene-Pliocene post-rift sequence (Beydoun et al., 1998)
225 unconformably overlies the Shihr Group (Fig. 3) and is composed of marine sandstones, conglomerates and
226 siltstones of the Irqah Fm (Bosence et al., 1996; Nichols and Watchorn, 1998; As-Saruri et al., 2010). However,
227 this unit is restricted to the coastline and is poorly documented onshore (Fig. 2.a). The post-rift sequence
228 records at least three uplift pulses (Watchorn et al., 1998). Offshore Yemen, the Sarar Fm (Figs. 2.a, 3.a)
229 consists of various lithologies including turbidite sands, shales and marls (Bott et al., 1992). On the emerged
230 Somalian margin, the post-rift sequence is recorded on the coastline and in the Darror basin (Figs. 2.b, 3). It is
231 composed of a conglomeratic unit, named Boulder beds 2 Fm, dated as probably Pliocene (Fantozzi and Ali-
232 Kassim, 2002) (Fig. 3.b). Offshore Somalia, the upper part of the Bandar-Harshau Fm (Figs. 2, 3.b, c) is
233 characterized by shale, carbonates and evaporites observed in the Dab-Qua-1 and Bandar-Harshau-1 wells
234 (Bott et al., 1992; Ali and Watts, 2013). Plio-Quaternary volcanic formations dated from ~3 - 6 Ma to present,
235 are recorded in the Hami graben (Yemeni, Fig. 2.a), in the Bosaso and the Qandala basins (Somalia, Fig. 2.b) and
236 are located in the prolongation of the BHFZ and AFFZ (Bott et al., 1992; Fantozzi and Sgavetti, 1998; Watchorn
237 et al., 1998; Leroy et al., 2010b).
238
239 **3. Data of the central Gulf of Aden conjugate margins**

240 This study is based on investigations of oil industry data including deep reflection seismic surveys and
241 published information on wells (Bott et al., 1992; Ahlbrandt, 2002; Ali and Watts, 2013; Ali, 2015) (Fig. 2). This
242 analysis benefits from access to a large number of seismic reflection profiles across and along the conjugate
243 central margins of the Gulf of Aden (see area covered by seismic profiles, Fig. 2). The offshore seismic data
244 were acquired during a large-scale and dense seismic survey carried out in the 1980s. Unfortunately, we are
245 not able to show the seismic profiles. Further control on this interpretation is obtained through well data (Figs.
246 3.b, c, 4) and field observations of onshore stratigraphy derived from literature (Bott et al., 1992; Fantozzi,
247 1996; Bosence et al., 1996; Beydoun et al., 1996; Beydoun, 1997; Beydoun et al., 1998; Watchorn et al., 1998;
248 Fantozzi and Sgavetti, 1998; Nichols and Watchorn, 1998; Fantozzi and Ali-Kassim, 2002; Bosworth et al., 2005;
249 Ali and Watts, 2013; Ali, 2015). The depth to basement and thickness maps are compiled from interpretations
250 of all densely spaced seismic data available in the area. The Sismage® software was used to perform grids
251 obtained by interpolating interpreted horizons with a spacing of 10 to 15 km. The depth conversions for the
252 maps and seismic interpretations are carried out according to estimated P-waves velocities from processing

253 stack velocities (Dix formula; Dix, 1955) (1500 m.s-1 for the water and surface sediments, 1800 to 2200 m.s-1
254 for post-rift and syn-OCT units, 2500 m.s-1 for the syn-rift sequence, 5500 m.s-1 for the continental basement,
255 6500 m.s-1 for the transitional basement and 7000 m.s-1 for the whole oceanic crust).
256
257 **4. Results from seismic stratigraphy and crustal domains mapping of the central Gulf of Aden conjugate**
258 **margins**
259 For both the northern and southern margins of the central Gulf of Aden segment, we describe the offshore
260 seismic stratigraphy using the seismic units and major discontinuities based on a compilation of seismic and
261 well data (Figs. 3, 4) correlated with the offshore and previous onshore geological studies (e.g. Bott et al., 1992;
262 Fantozzi and Ali-Kassim, 2002; Bosworth et al., 2005). We summarize the seismic units patterns (boundaries,
263 geometries, continuity, amplitude, frequency and ages), and the onshore-offshore correlations in Figure 3 and
264 Table 1. In a second section, we describe the major features of acoustic basement morphology of offshore
265 conjugate margins thanks to the depth to basement maps (Figs. 5.a, b).
266
267 **4.1 Seismic stratigraphy**
268 *4.1.1 Pre-rift sequence*
269 At the top of the tilted blocks in the continental domains, we identify three main sequences (Figs. 2, 3, 4; Tab.
270 1): the Neoproterozoic crystalline basement, the Mesozoic basement and the Cenozoic basement (CB1 to CB3).
271 In the Cenozoic basement, the CB1 subunit can be correlated to carbonates of the Umm Er Radhuma and Jeza
272 Fms on the Yemeni margin and to the Auradu Fm on the Somalian margin using the well data (Figs. 3.c, d).
273 Wells data show that CB2 corresponds to the evaporitic Rus Fm on the northern margin and the Taleh Fm on
274 the southern margin (Fig. 3). CB3 is composed of double reflectors that are very remarkable, deposited
275 unconformably above the eroded CB2 subunit (Fig. 3.c; Tab. 1), and locally cut by small-offset normal faults
276 that are rooted at a common decollement layer on CB2 (Right segment of seismic line, Fig. 3.c). According to
277 the wells considered, CB3 corresponds to the carbonates of the Habshiya and the Karkar Fms in offshore
278 Yemen and Somalia, respectively (Figs. 3.b, c, 4.a).

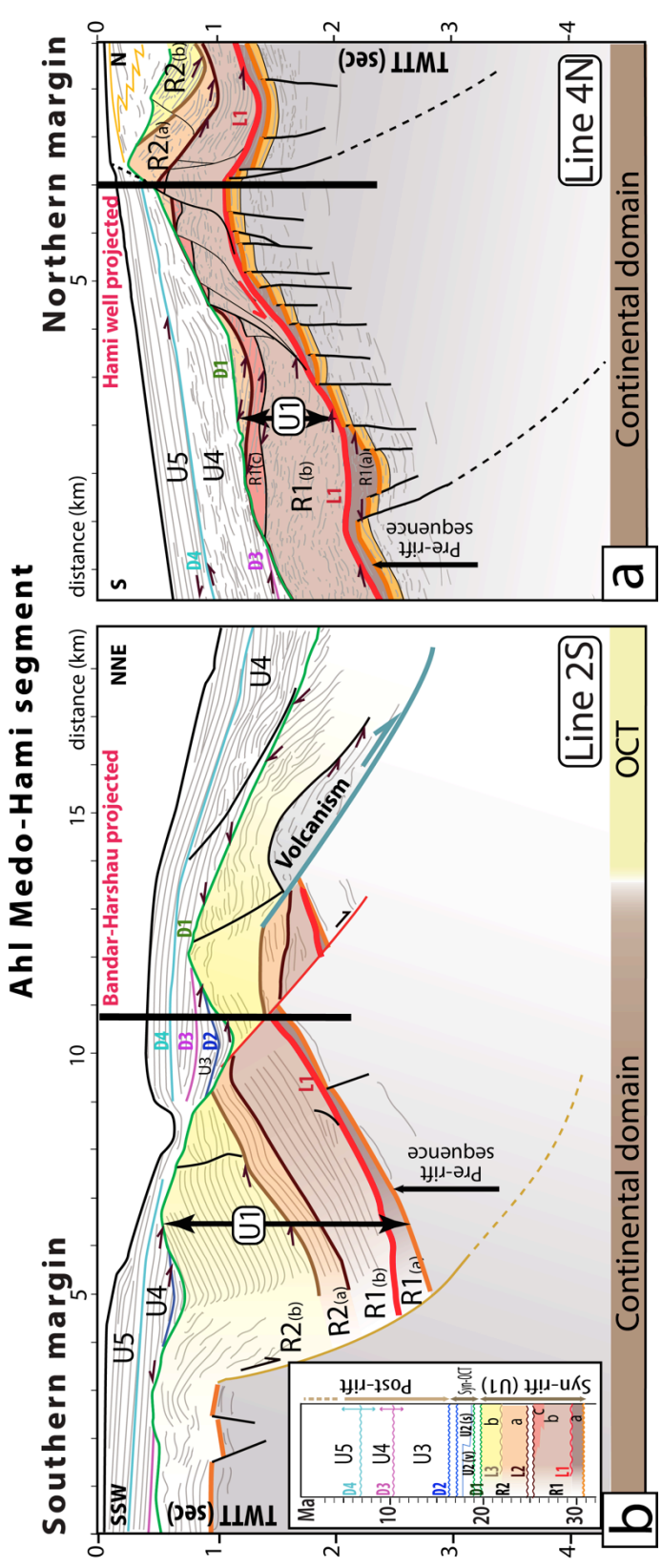


***Figure 4*** *- Interpreted line drawing of (a) the northern part of the seismic line 5N in the northern margin (Location on Figure 2.a) (b) the seismic line 2S in the southern margin (in the Ahl Medo-Hami segment) with the different sedimentary sequences identified on the seismic profiles in the continental domain and Ocean-Continent Transition (OCT) (vertical exaggeration ~1.8) and the projected Hami well and Bandar-Harshau well. The pre-rift sequence (CB1-2 and the Mesozoic basement) and the upper crust are represented in grey and the top of the pre-rift sequence is represented in orange (CB3).*

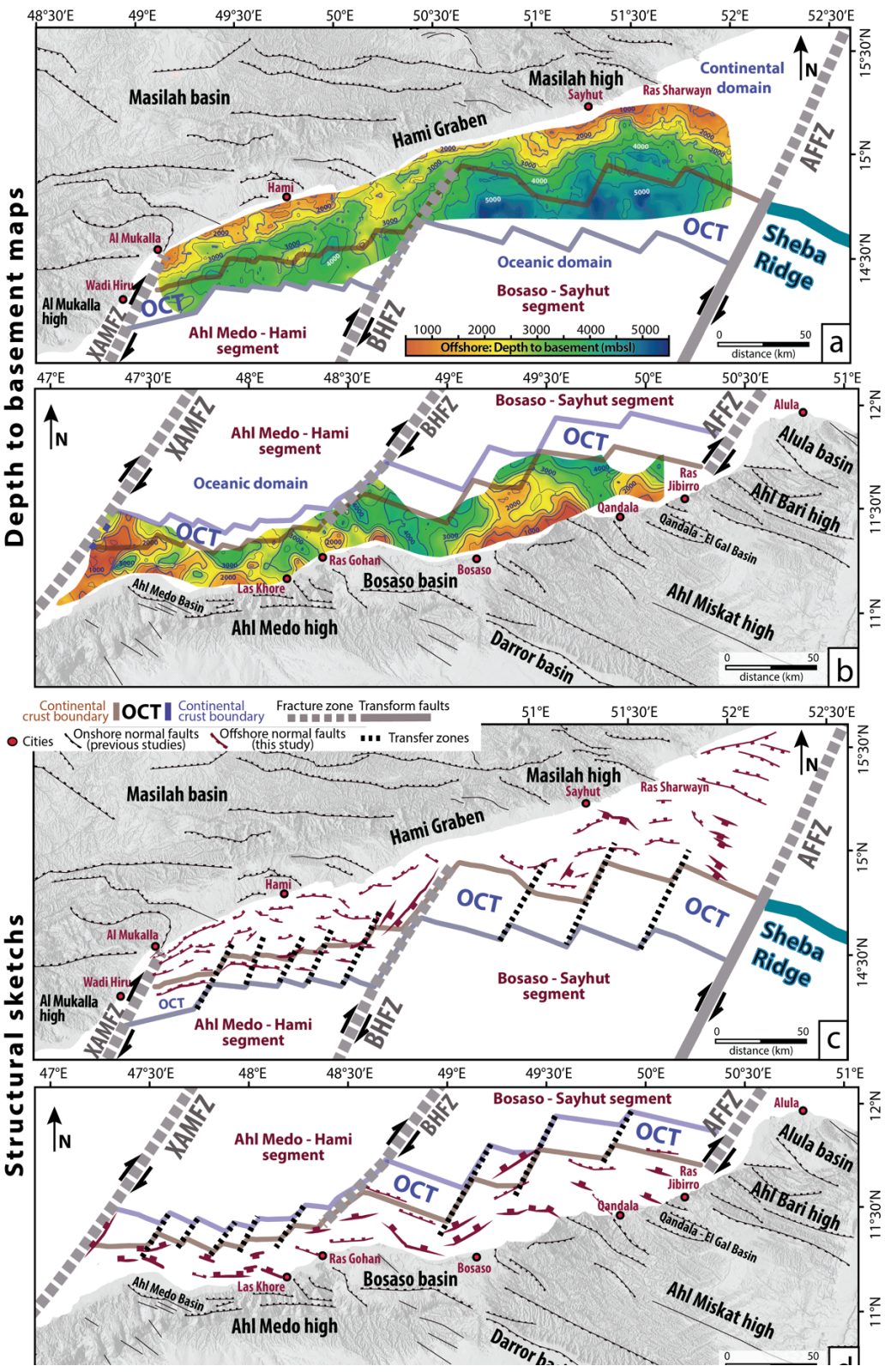


***Figure 5*** *– Upper panels: Depth to seismic basement maps of (a) the Yemeni and (b) Somalian margins established from seismic reflection data. Onshore first-order structures (after Beydoun, 1970; Bott et al., 1992; Bosence, 1997; Brannan et al., 1997; Fantozzi and Sgavetti, 1998; Nichols and Watchorn, 1998; Watchorn et al., 1998; Fantozzi and Ali-Kassim, 2002; Leroy et al., 2012; Ali, 2015) and other references therein. Lower panels: Structural sketches of the northern (c) and southern (d) margins with different crustal domains and major structures that affect the continental and transitional seismic basements. Thicker lines represent major faults. Note that structures are drawn at the foot of the faults. OCT: Ocean-Continent Transition. AFFZ: Alula Fartak Fracture Zone. BHFZ: Bosaso Hami Fracture Zone. XAMFZ: Xiis Al Mukalla Fracture Zone. Shaded topography is shown onshore (SRTM, Jarvis et al., 2008).*

| Seismic units | Reflection characteristics | | | | | Ages |
|---|---|---|---|---|---|---|
| | Boundaries | Geometry | Continuity | Amplitude | Frequency | |
| **Post-rift units (U3 to U5)** | | | | | | |
| **U5** | Top: toplaps, erosional truncations at the seafloor<br>Base: onlaps on D4 | Draping, parallel, locally prograding | Continuous | Low to middle | High | ~7 Ma |
| **U4** | Top: toplaps, truncations on D4 (channels)<br>Base: onlaps on D3 | Parallel, prograding, hummocky, chaotic | Continuous to chaotic | Low to middle | Middle to high | ~10 - 7 Ma |
| **U3** | Top: toplaps on D3<br>Base: onlaps on D2 | Draping, parallel | Continuous | Middle to high | Middle | ~17 - 10 Ma |
| **Syn-OCT units (U2)** | | | | | | |
| **U2(s)** | Top: toplaps on D2<br>Base: onlaps, downlaps on D1, SDR<br>or on the surface of the transitional basement | Draping, parallel | Continuous to chaotic | Low to high, locally transparent | Low to middle | ~20 – 17.6 Ma |
| **U2(v)** | | Parallel, divergent To chaotic | Continuous to chaotic | High | Low to middle | |
| **SDR** | Top: conformable on U2(v)<br>Base: onlaps, dowlaps on the surface of the transitional basement | Divergent | Continuous to chaotic | High | Low | |
| **Syn-rift units (U1)** | | | | | | |
| **R2(b)** | Top: toplaps on D1<br>Base: onlaps, downlaps on L2 and L3 | Divergent | Continuous | Middle to high | Low to middle | Burdigalian >20 Ma |
| **R2(a)** | Top: toplaps, concordant on L3<br>Base: onlaps or downlaps on L2 | Divergent | Continuous or discontinuous | Low to high, locally transparent | Low to middle | Mid. Chattian? - Low. Burdigalian? |
| **R1(c)** | Top: toplaps on L2<br>Base: onlaps at the top of R1(b) | Parallel to slightly divergent | Discontinuous | Low, transparent | Middle | Middle Chattian? |
| **R1(b)** | Top: toplaps on L2<br>or at the base of R1(c)<br>Base: onlaps on L1 | Slightly divergent | Discontinuous | Low to middle<br>Transparent at the top | Low to middle | Mid. Rupelian? – Low. Chattian? |
| **R1(a)** | Top: toplaps on L1<br>Base: downlaps on CB | Parallel to slightly divergent | Discontinuous | Low, transparent | Low | Middle Rupelian |
| **Cenozoic basement (CB)** | | | | | | |
| **CB3** | Top: conformable or toplaps<br>Base: conformable or onlaps | Parallel | Continuous | Very high | Middle | Lutetian - Barthonian |
| **CB2** | Top: conformable<br>Base: conformable | Parallel | Discontinuous | Low to middle | Middle | Upper Ypresian - Lutetian |
| **CB1** | Top: conformable<br>Base: onlaps, downlaps on MB | Parallel | Discontinuous | Middle to high | Low to middle | Thanetian - Ypresian |
| **Mesozoic basement (MB) and Neoproterozoic basement (NB)** | | | | | | |
| **MB** | Top: toplaps on CB<br>Base: onlaps on NB | Parallel to chaotic | Continuous to discontinuous | Low to high | Low | Mesozoic |
| **NB** | Top: angular unconformity | Chaotic | Chaotic | Low | Low | Neoproterozoic |

D4
D3
D2
D1
L3
L2
L1

*Table 1 - Summary of key observations of the seismic units, with their reflection characteristics and ages.*

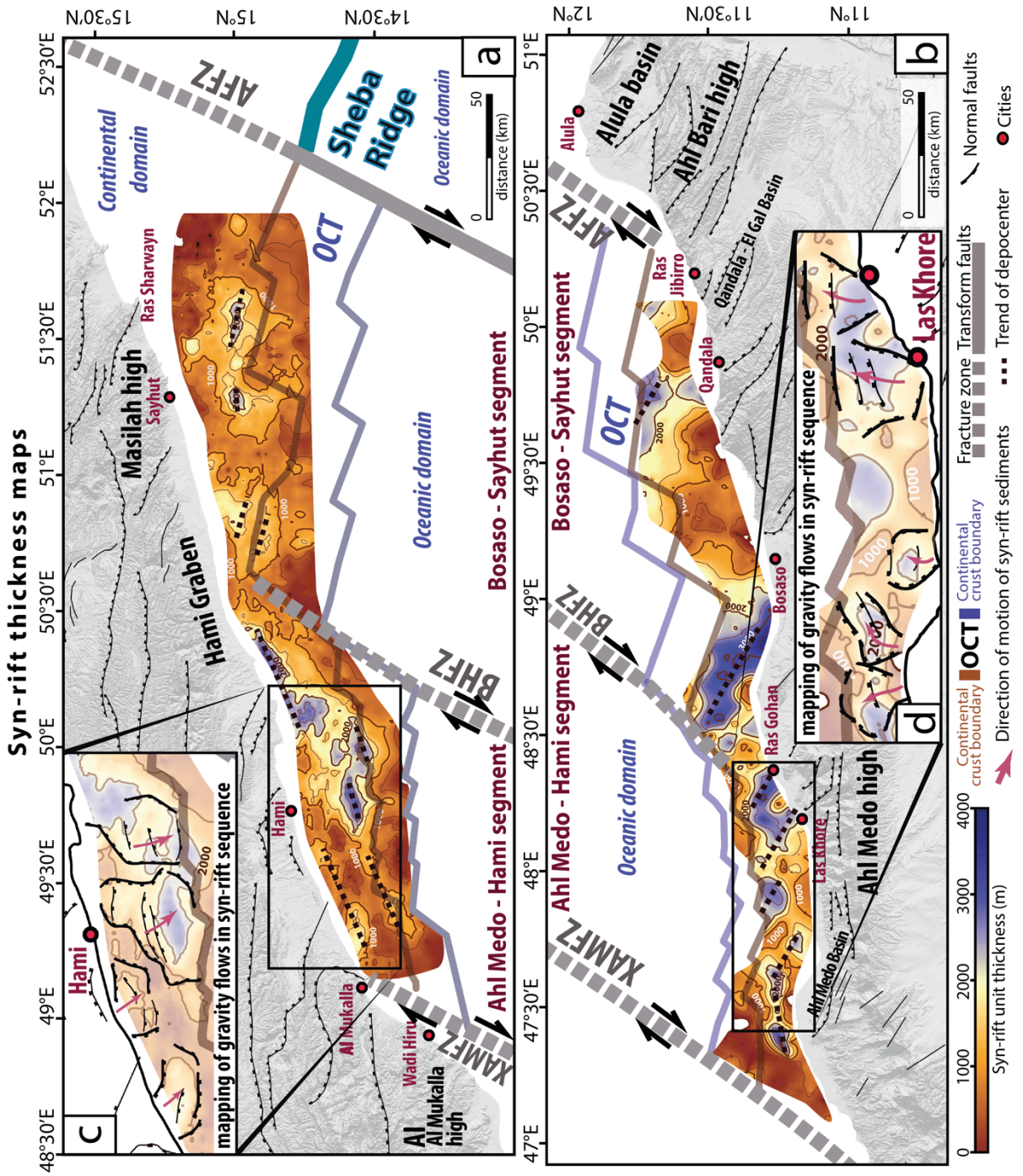


***Figure 6*** *- Isopach map of the syn-rift unit (U1) inferred from our interpretation of the datasets for (a) the Yemeni margin and (b) the Somalian margin. In black insets: mapping of gravity flows in the syn-rift sequence U1 and direction of motion; major normal faults are represented by thick lines and no evidence of reverse faults is observed. OCT: Ocean-Continent Transition. AFFZ: Alula Fartak Fracture Zone. BHFZ: Bosaso Hami Fracture Zone. XAMFZ: Xiis Al Mukalla Fracture Zone. Onshore topography is shaded (SRTM, Jarvis et al., 2008).*

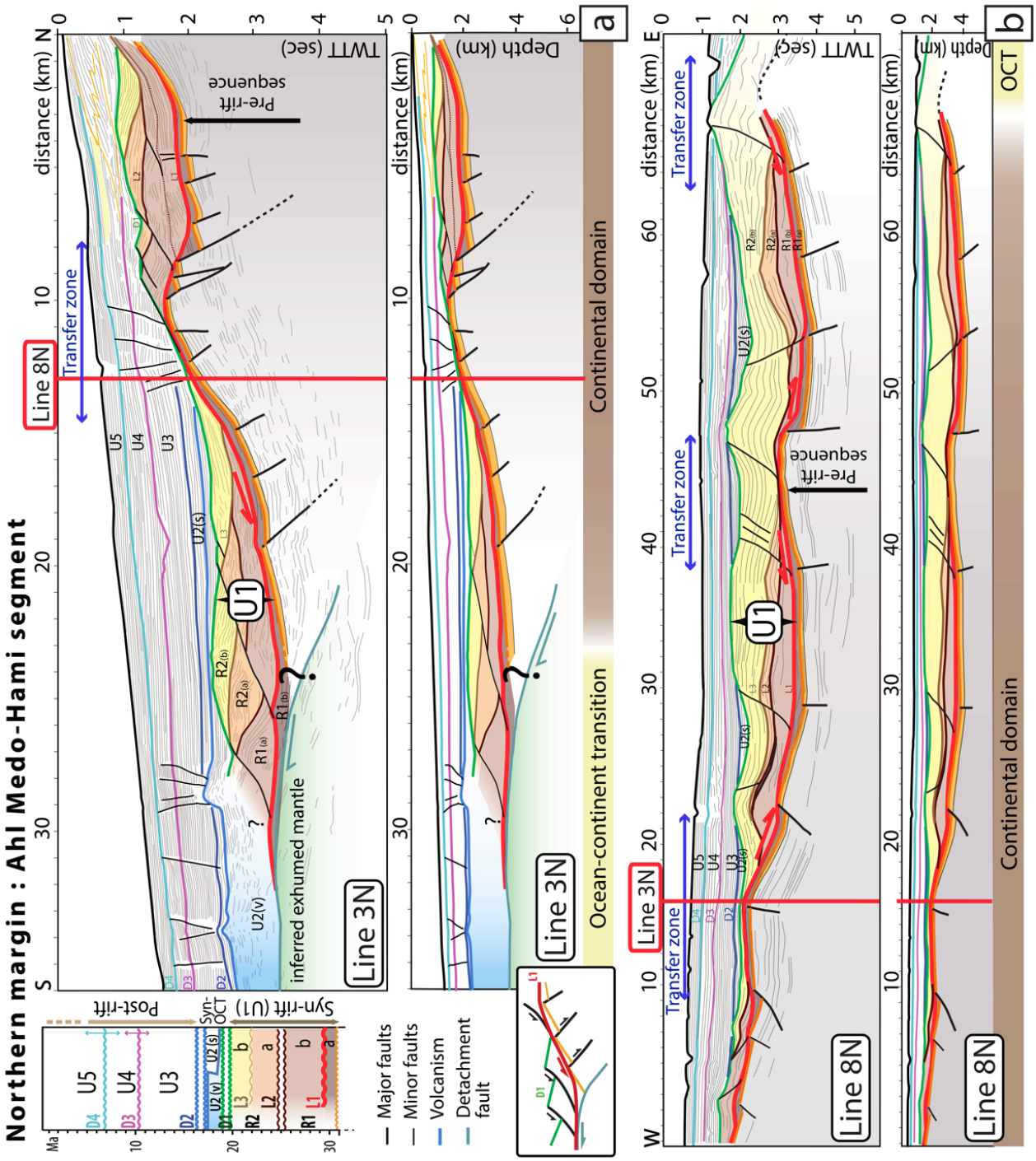


*Figure 7 - Interpreted line drawing of (a) the seismic profiles 4N and (b) the along-strike seismic line 9N in the northern margin (in the Ahl Medo-Hami segment) with the different sedimentary sequences identified on the profiles and interpretation of crustal domains (vertical exaggeration ~1.8). See location on Figure 2.a. (a) Seismic profiles 4N: Some intra-R1(b) decollement layers are recorded. Lower pannel: depth converted seismic line and its interpretation, with no vertical exaggeration. (b) seismic line 9N: the transfer zones are characterized by positive relief delimiting syn-rift basins. Lower panel: depth converted seismic line 9N and its interpretation, with no vertical exaggeration. In grey under the orange unit (CB3), the top of the pre-rift sequence CB1-2 and the Mesozoic basement (~2 km of thickness, characterized by sub-parallel to chaotic reflections), the Neoproterozoic basement and the upper crust are in contact with the exhumed mantle in distal part of the margin (at a distance of 16 – 25 km from the North of the cross-section). Inset: Sketch of the line 4N showing the geometry of the faults and their chronology. Left panel: Simplified seismic stratigraphic column.*

426 *4.1.2 Syn-rift sequence*

427 The syn-rift sequence U1 in the central Gulf of Aden is dated as Oligo-Miocene (Fig. 3) and composed of a
428 clastic to carbonate deposits in the Hami well (Yemen, Figs. 3.b, 4.a) and Bandar-Harshau well (Somalia, Figs.
429 3.b**,** 4.b). The thickness of U1 varies from 0 to 3500 m in the continental domain (Figs. 6 to 10) and decrease
430 westwards from the Ahl Medo-Hami (Figs. 6 to 8, 10.a, b, c) to the Bosaso-Sayhut segment (Figs. 6, 9, 10.d). U1
431 is thinner on the northern margin (reaching 2500 m, Figs. 6.a) in interpreted profiles 2N to 8N (Figs. 4.a, 7 to 9),
432 than on the southern margin (reaching 3500 m, Fig. 6.b) in interpreted profiles 1S to 5S (Figs. 4.b, 10).

433 The deformation of U1 is decoupled from the basement structures (Figs. 3.c, 4.a, 6.c, d, 7 to 9). U1 is
434 mainly recorded in the centre of the syn-rift sub-basins (that trend N70°E to N80°E, EW to N120°E; Figs. 6.a, b)
435 and between the areas of positive topography corresponding to and N30°E to N40°E transfer fault zones (Figs.
436 5, 7):

437 • **N70°E to N80°E-trending depocenter:** On the Yemeni margin in the Ahl Medo-Hami segment, U1 displays
438 N70°E-trending depocenter and is up to 2500 m thick (Figs. 6.a, 7, 8). Four main submarine landslides are
439 mapped with a global SE direction of flow (orthogonal to the depressions along a N70°E-axis parallel to the
440 coastline; Fig. 6.c). On the Somalian margin, U1 displays a N80°E-elongate depocenter east of the XAMFZ
441 (Fig. 6.b).

442 • **EW to N120°E-trending depocenter:** On the Yemeni margin in the Bosaso-Sayhut segment, U1 fills *en*
443 *echelon* N110°E-elongated basins and reaches up to ~2000 m (e.g. South of Ras Sharwayn, Figs. 6.a, 9.b).
444 On the Somalian margin, from north of the Ahl Medo basin to the northwest of the Bosaso city, several *en*
445 *echelon* sedimentary packages (up to ~3200 m thick, Fig. 6.b) trending N120°E are obvious (Figs. 10.a, b, c).
446 Five main submarine landslides are observed with global NE direction of flow (orthogonal to depressions
447 along a EW to N120°E-axis; Fig. 6.d).

448 • **N30°E to N40°E-trending highs:** On the Yemeni margin, U1 is 1500 m thick with a N30°E-trend southwest
449 of the Hami graben and along the western border of the BHFZ (Fig. 6.a). On the Somalian margin, U1 is less
450 than 500 m thick in N40°E-trending zones northeast of Bosaso city (Fig. 6.b). U1 reaches less than 100 m
451 and is eroded with a N40°E-trend at the eastern border of the XAMFZ in the eroded basement high (Figs.
452 6.b, 10.a).

453

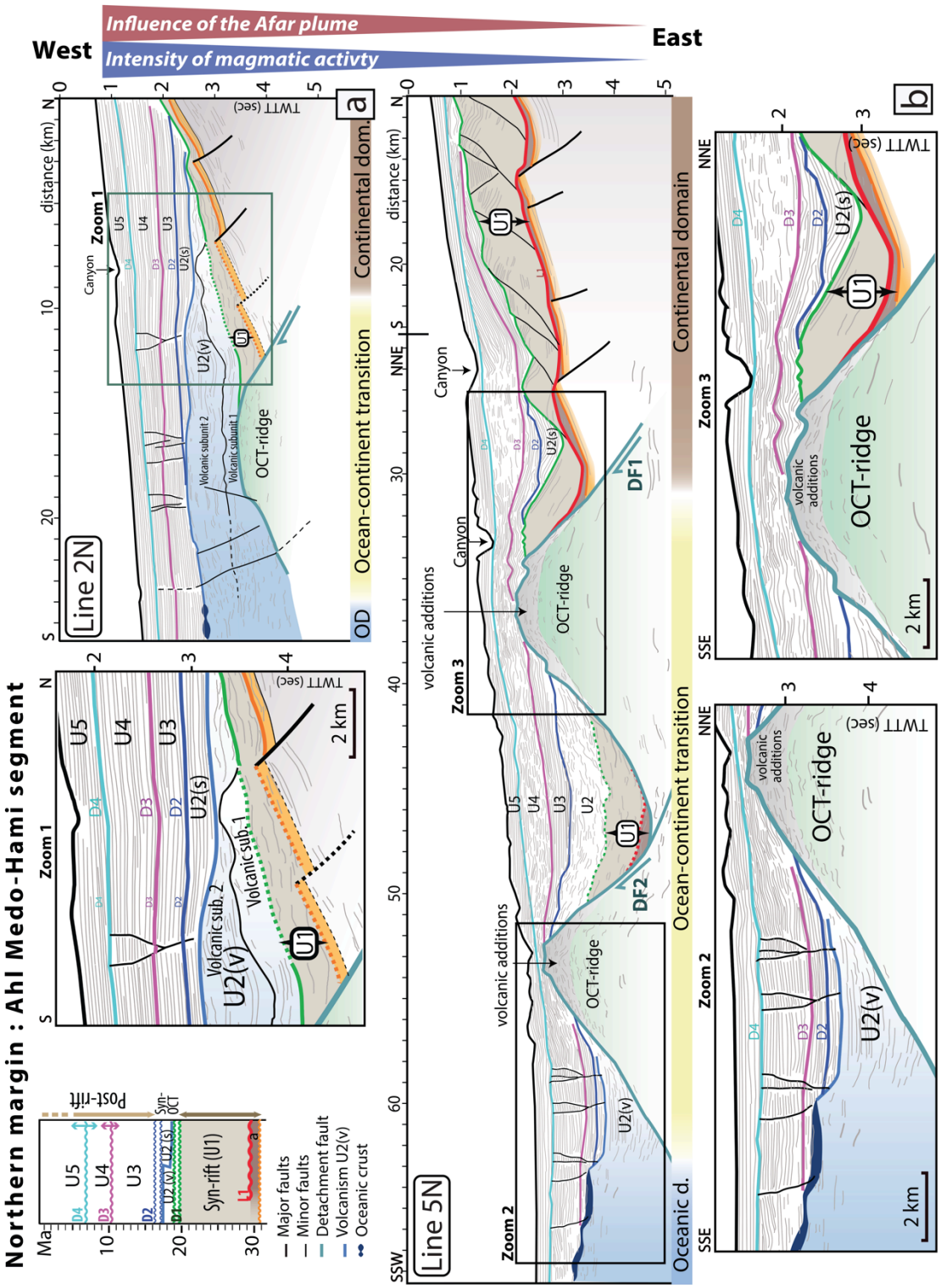


*Figure 8 - Interpreted line drawing of the seismic profiles (a) 2N and (b) 5N in the Ahl Medo-Hami segment in the northern margin with the different sedimentary sequences identified on the seismic profiles and interpretation of crustal domains in the Ahl Medo-Hami segment (vertical exaggeration ~1.8). See location on Figure 2.a. (a) Zoom 1: Close-up view of line 2N showing the interpretation of basement structures, volcanic and sedimentary units in the OCT. (b) Zoom 2: Close-up view of line 5N showing the interpretation of an OCT-ridge and associated volcanic formations. Zoom 3: Close-up view of line 5N showing the interpretation of an OCT-ridge and structural relation between the pre- and syn-rift units in the continental domain and OCT domain. Left panel: simplified seismic stratigraphic column. OD: Oceanic domain.*

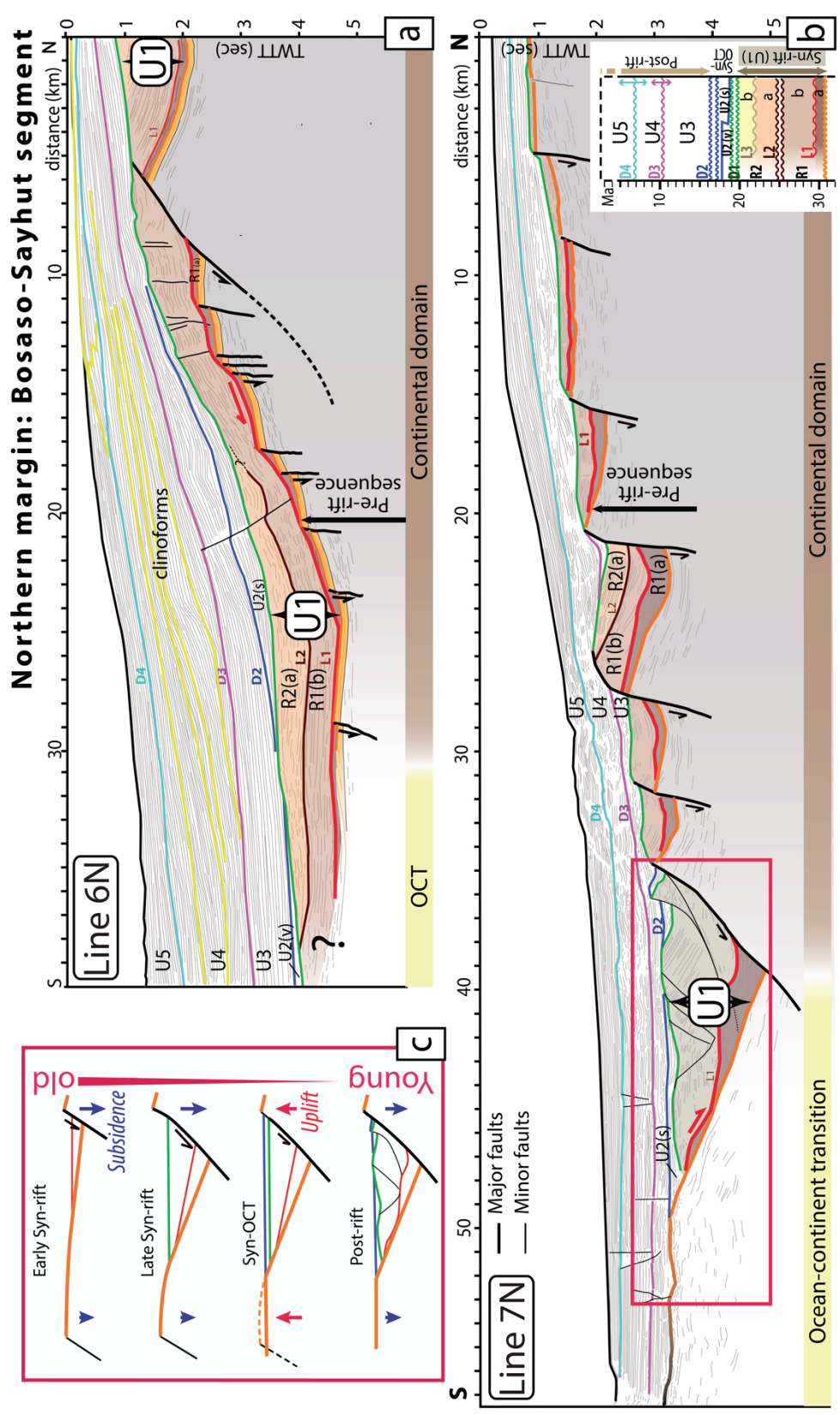


***Figure 9*** *- Interpreted line drawing (a) of the seismic line 6N and (b) of the seismic line 7N in the northern margin (in the Bosaso-Sayhut segment) with the different sedimentary sequences identified on the profiles and our interpretation of crustal domains (vertical exaggeration ~1.8). Upper left inset: sketch of OCT evolution from the syn-rift (at top) to post-rift phases (at bottom). Bottom right panel: simplified seismic stratigraphic column. In grey: the top of the pre-rift sequence (CB1-3 and the Mesozoic basement for the seismic line 6N and CB1-CB2 and the Mesozoic basement for the seismic line 7N) and the upper crust.*

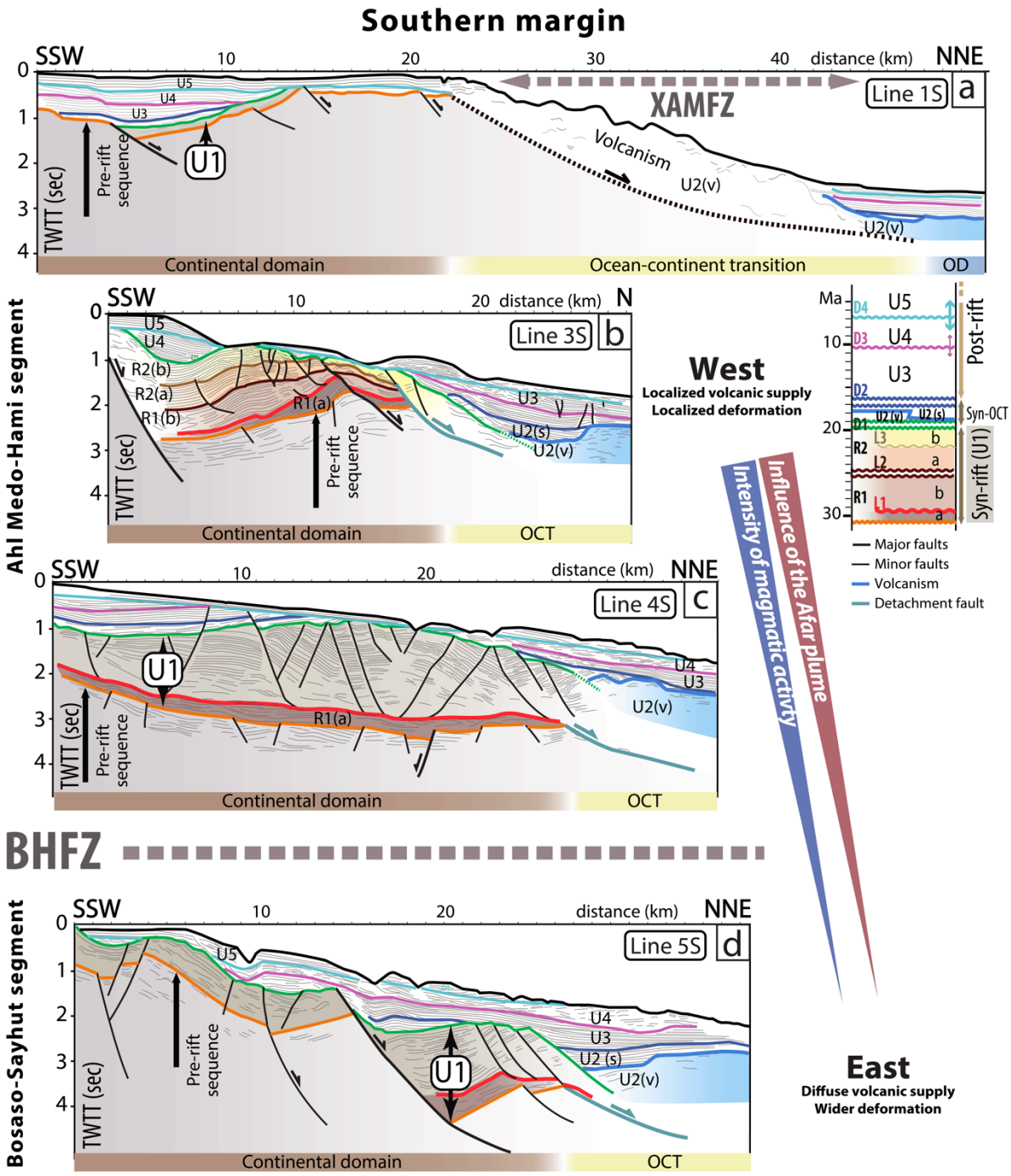


*Figure 10 - (a) to (d) Interpreted line drawing of the seismic profiles 1S, 3S, 4S and 5S in the southern margin, with the different sedimentary sequences identified on the profiles and our interpretation of crustal domains (vertical exaggeration ~1.8). Location of seismic profiles on Figure 2.b. OD: Oceanic Domain. OCT: Ocean Continent Transition. Right panel: simplified seismic stratigraphic column. In grey: the top of the pre-rift sequence (CB1-2 and the Mesozoic basement) and the upper crust.*

U1 is composed of two units (R1 and R2, Fig. 3, Tab. 1) and subunits mainly recorded in the Ahl Medo-Hami segment, on the Yemeni (Figs. 4.a, 7) and Somalian margins (Figs. 4.b, 10.b), and in the Bosaso-Sayhut segment on the Yemeni margin (Figs. 9, 3.b, c). The seismic horizons of U1 are in general parallel and do not display significant fan-shape as expected for deposits contemporaneous with fault activity (Fig. 4).

In the Ahl Medo-Hami segment, unit R1 corresponds to the Ghaydah Fm on the northern margin (Hami well; Figs. 3.b, 4.a; Tab. 1) and to the base of the Bandar-Harshau Fm on the southern margin (Bandar-Harshau well; Figs. 3.b, c, 4.b). The unit R1 is composed of three distinct subunits named R1(a), R1(b) and R1(c) (Figs. 3.a, 4; Tab. 1). The L1 discontinuity delimits the onlaps at the base of the R1(b) subunit and the toplaps of R1(a) subunit (Fig. 4, Tab. 1). On the northern margin, some intra-R1(b) decollement layers are recorded on Line 3N (Fig. 7.a). South of Hami city, the R1(c) subunit is locally observed and onlaps onto the top of R1(b) on a local boundary under the L2 discontinuity (in black, Fig. 7.a; Tab. 1). Extensional faults affecting the R1(b) unit are rooted on L1, L2 discontinuities and/or attenuated in R1(a) and R1(c) (Fig. 4.a). R2 is composed of the R2(a) and R2(b) subunits delimited by the L3 discontinuity (Figs. 3, 4). The whole syn-rift sequence (U1) is affected by normal faults (in black, Figs. 4, 7, 8.b line 5N, zoom 3, 9.a, 10.b, c, d) and rooted on the L1 discontinuity at the base of U1.

*4.1.3 Syn-OCT sequence*

The syn-OCT sequence (U2) was deposited during a period of complex transition between the end of the syn-rift phase and the onset of the steady-state oceanic spreading (~17 Ma; Leroy et al., 2010a; Nonn et al., 2017) (Fig. 3, Tab. 1). U2 is characterized by onlaps that directly cover the OCT basement and the pre- and syn-rift sediments in the continental domain (see dark blue horizon for top of U2, Figs. 3.c, 7 to 10, 11.b). U2 is absent on the steady-state oceanic crust (Figs. 8, 11.a, zoom 1 on Fig. 11.b). The syn-OCT sequence may correspond to the sedimentary subunit U2(s) (Figs. 3.c, 7 to 10; Tab. 1) and/or to the volcanic deposits of U2(v) (Fig. 7, zoom 1 on Fig. 8.a, zoom 2 on Fig. 8.b, Figs. 10, 11; Tab. 1). U2(v) onlaps on top of exhumed basement and displays wedge-shape horizons towards the OCT ridge in the western part (zoom 2, Fig. 8.b). In the Yemeni margins on the Ahl Medo-Hami segment, two volcanic subunits are recorded on U2(v) (zoom 1, Fig. 8.a). U2(s) onlaps, in some place, on top of U2(v) at the end of the syn-OCT period (Figs. 7, 8, 10, zoom 2 on Fig. 11). Near the XAMFZ, the U2 is more complex and composed of seaward dipping reflectors (SDR1 and SDR2; Fig. zoom 2 on 11.b) emplaced during the deformation of highly intruded continental crust. The SDR1 and SDR2 display fan-shape growth structures controlled by low-angle normal faults, dipping toward the continent with high-amplitude/low-frequency facies. The top of U2(s) correspond to the erosional discontinuity D2 (Figs. 3, 7, 8, 10.b, 11).

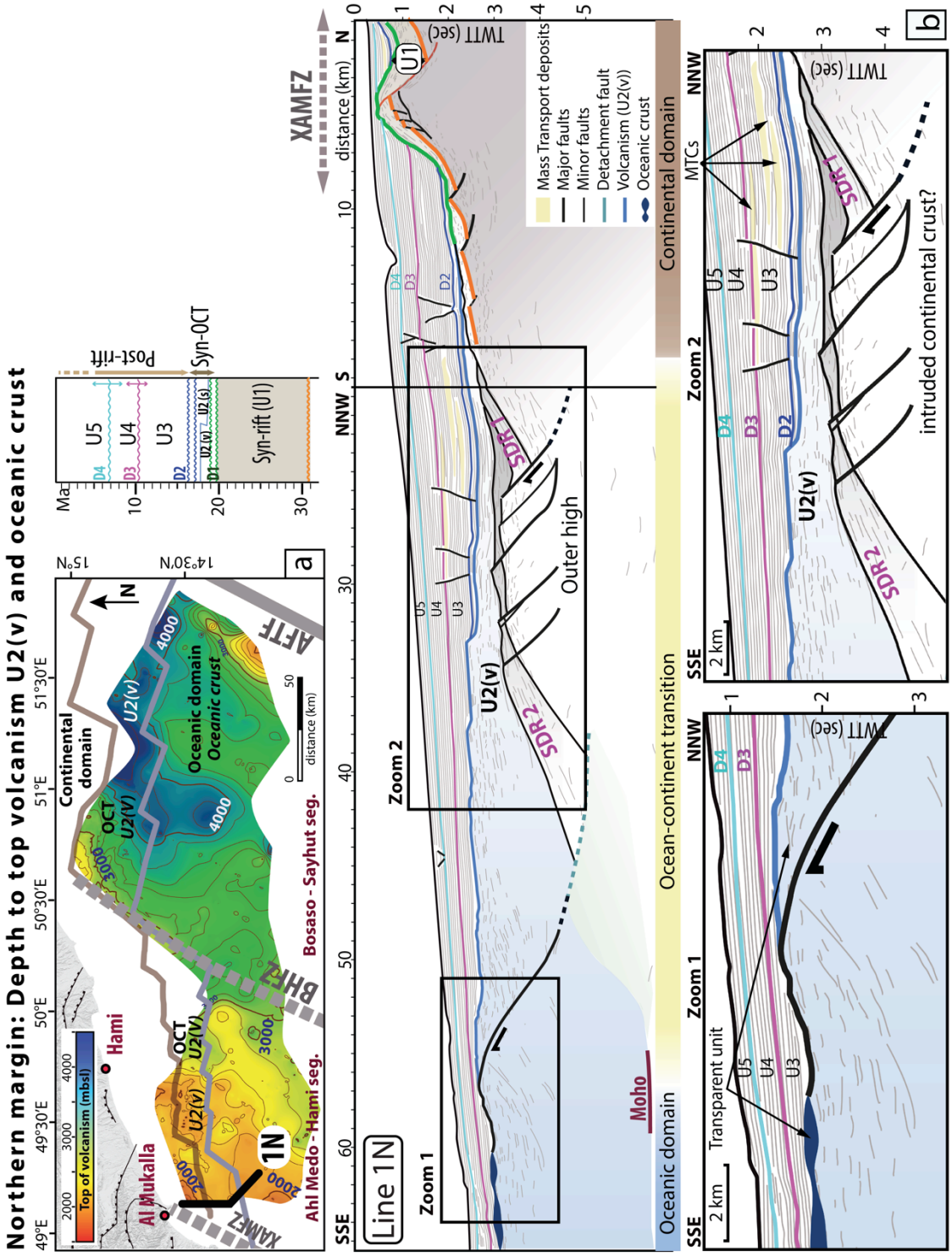


***Figure 11*** *- (a) Map of the depth to top of volcanic formations in the continental (U2(v)), transitional (U2(v)) and oceanic domains (Oceanic crust). Onshore topography is shaded (SRTM, Jarvis et al., 2008) and location of the seismic line 1N presented in b. (b) Interpreted line drawing of the seismic line 1N in the northern margin (near XAMFZ), with the different sedimentary sequences identified on the profiles and interpretation of crustal domains (vertical exaggeration ~1.8. Zoom 1: Close-up views of the line 1N showing the interpretations of the low-angle detachment fault in the oceanic crust. The top of the oceanic substratum exhibits a highly reflective uppermost reflector identified by its low frequency and high amplitude, showing a significant impedance contrast with the overlying post-rift sediments. A very specific transparent seismic unit marks the base of the post-rift sediments. Zoom 2: Close-up views of the line 1N showing the interpretations of the OCT near XAMFZ showing SDRs. In grey: the top of the pre-rift sequence (Cenozoic basement (CB1-2), Mesozoic and Neoproterozoic basements) and the upper crust. Upper right panel: simplified seismic stratigraphic column. OCT: Ocean-Continent Transition. AFTF: Alula Fartak Transform Fault. BHFZ: Bosaso Hami Fracture Zone. XAMFZ: Xiis Al Mukalla Fracture Zone.*

577 *4.1.4 Post-rift sequence*

578 The post-rift sequence (Fig. 3) covers a large part of the continental slope over continental, transitional and
579 oceanic crust and thickens oceanward (Figs. 4, 7 to 10, 11.b). On the northern margin, west and east of the
580 BHFZ, it attains a thickness of 2300 m and 4000 m (depth converted seismic profiles on Fig. 7). On the southern
581 margin, the post-rift sequence is up to 1 600 m thick (Fig. 10). The post-rift sequence lies between D2 and the
582 erosional seafloor. It comprises three main units that correlate in terms of timing with post-rift units of the
583 eastern Gulf of Aden (Autin et al., 2010a; Bache et al., 2011; Nonn et al., 2017): U3, U4 and U5 units separated
584 by the erosional unconformities D3 and D4 (Figs. 3, 4, 7 to 11; Tab. 1). U4 shows some occurrences of MTCs
585 (Mass Transport Complexes) on the proximal margins (zoom 2 on Fig. 11.b; Tab. 1). In the Ahl Medo-Hami
586 segment, U4 displays current-formed features corresponding to canyon indentation or contourites which also
587 distort the D4 unconformity at the Yemeni continental shelf break (Figs. 4.a, 7.a). In the Bosaso-Sayhut
588 segment, U4 is defined by large clinoforms (Fig. 9.a).
589
590 **4.2 Conjugate margins architecture**

591 Three major domains can be identified according to the geometry, bathymetry, sedimentation infill, gravimetry
592 and seismic facies (Figs. 3 to 12): (i) the continental domain is marked by a succession of basins and basement
593 highs; (ii) the steady-state oceanic crust is characterized by a rough top seismic basement; (iii) the ocean-
594 continent transition (OCT) is defined as a complex transitional domain between the continental and oceanic
595 domains (Figs. 3 to 12).
596
597 *4.2.1 Major features of acoustic basement morphology from offshore conjugate margins*

598 In the continental domains of the central Gulf of Aden conjugate margins, the depth to acoustic basement
599 maps (Figs. 5.a, b) corresponds to: (i) the top of the pre-rift sequences in the continental domain; (ii) the top of
600 the intermediated seismic basement in the OCT; and (iii) the top of the oceanic substratum in the oceanic
601 domain in agreement with previous studies in the eastern Gulf of Aden (Autin et al., 2010b; d'Acremont et al.,
602 2005; Nonn et al., 2017). The depth to basement maps represents the discontinuity between the upper-layered
603 sedimentary seismic facies and a lower more chaotic seismic facies of the seismic substratum (Tab. 1, Figs. 5.a,
604 b, 7 to 11).

The depth to basement map shows steep and narrow slopes all along the conjugate margins. The basement abruptly drops down from 0 mbsl near the coastlines to 5500 mbsl at the foot of the continental slope in the northern margin (Fig. 5.a) and to 4000 mbsl at the foot of the continental slope on the southern margin, over distance of less than 40 km (Figs. 5.a, b). The basement shows an eastward deepening in agreement with the eastward thickening of the sedimentary cover. On the overall morphology of the basement of conjugate margins, three main trends are observed (EW to N120°E, N70°E to N80°E and N30°E to N40°E; Figs. 5.a, b):

- **EW to N120°E-trending basins and highs*:*** On the northern margin, in the Ahl Medo-Hami segment and to the east of Al Mukalla city (Lat. 14°40'N, Long. 49°30'E; Fig. 5.a), EW escarpments cut the N70°E-trending relief. In the Bosaso-Sayhut segment, to the east of the Sayhut city (from Long. 51°30'E to Long. 52°E, Fig. 5.a, 9.a) a major basement high has a global N110°E trend toward the AFFZ. On the southern margin and in the Ahl Medo-Hami segment, a N80°E-trending basin reaches ~3000 mbsl of depth (Lat. 47°45'E to 47°45'E, Long. 11°15'N, Figs. 4.b, 5.b, 10.b). In the Southeastern prolongation of the BHFZ, N120°E-trending basin and high intersect the N40°E-trending structures (Long. 47°45'E to 48°15'E; Fig. 5.b). In the Bosaso-Sayhut segment, trends of basins and highs is N130°E at the North of Bosaso basin (Lat. 11°20'N and Long. 49°E; Fig. 5.b). This N120°E trend is also recorded in the northwest of Qandala city (Fig. 5.b).
- **N70°E to N80°E-trending basins and highs*:*** On the northern margin and in the Ahl Medo-Hami segment, a N70°E-trending basement high is parallel to the coastline of the Yemen margin and culminates at 1000 mbsl near Hami city (Lat. 14°30'N to 14°50'N, Long. 49°E to 50°15'E; Figs. 4.a, 5.a, 7.a). Farther south, at around 55 km south of Hami city, a N70°E-trending basement high culminates at a depth of 2300 mbsl (Fig. 5.a). Eastward in the Bosaso-Sayhut segment, a basement high (Lat. 14°50'N to 15°15'N) has a global N70°E direction from Long. 51°E up to Long. 51°30'E (Fig. 5.a). On the southern margin, in the Bosaso-Sayhut segment, trends of basins and highs is N70°E in the coastline (from Lat. 11°15'N to 11°30'N and from Long. 49°15'E to 49°45'E, Fig. 5.b).
- **N30°E-trending basin and highs** are recorded near Fracture zones in the Ahl Medo-Hami segment: On the Yemeni margin and southwestward of the Hami graben, the western border of the BHFZ is marked by a N30°E-trending basement high at 2000 mbsl depth (Fig. 5.a). On the southern margin, the eastern border of the XAMFZ is marked by a steep N40°E-trending basement high at 300 mbsl depth (from Lat. 11°N to 11°30'N at Long. 47°15'E; Figs. 5.b, 10.a). In the prolongation of the BHFZ, northeast of Las Khore city (Long. 47°45'E to 48°15'E, Fig. 5.b), N30°E to N40°E-trending elongate highs and basins vary in depth from 1500m to 4000 mbsl.

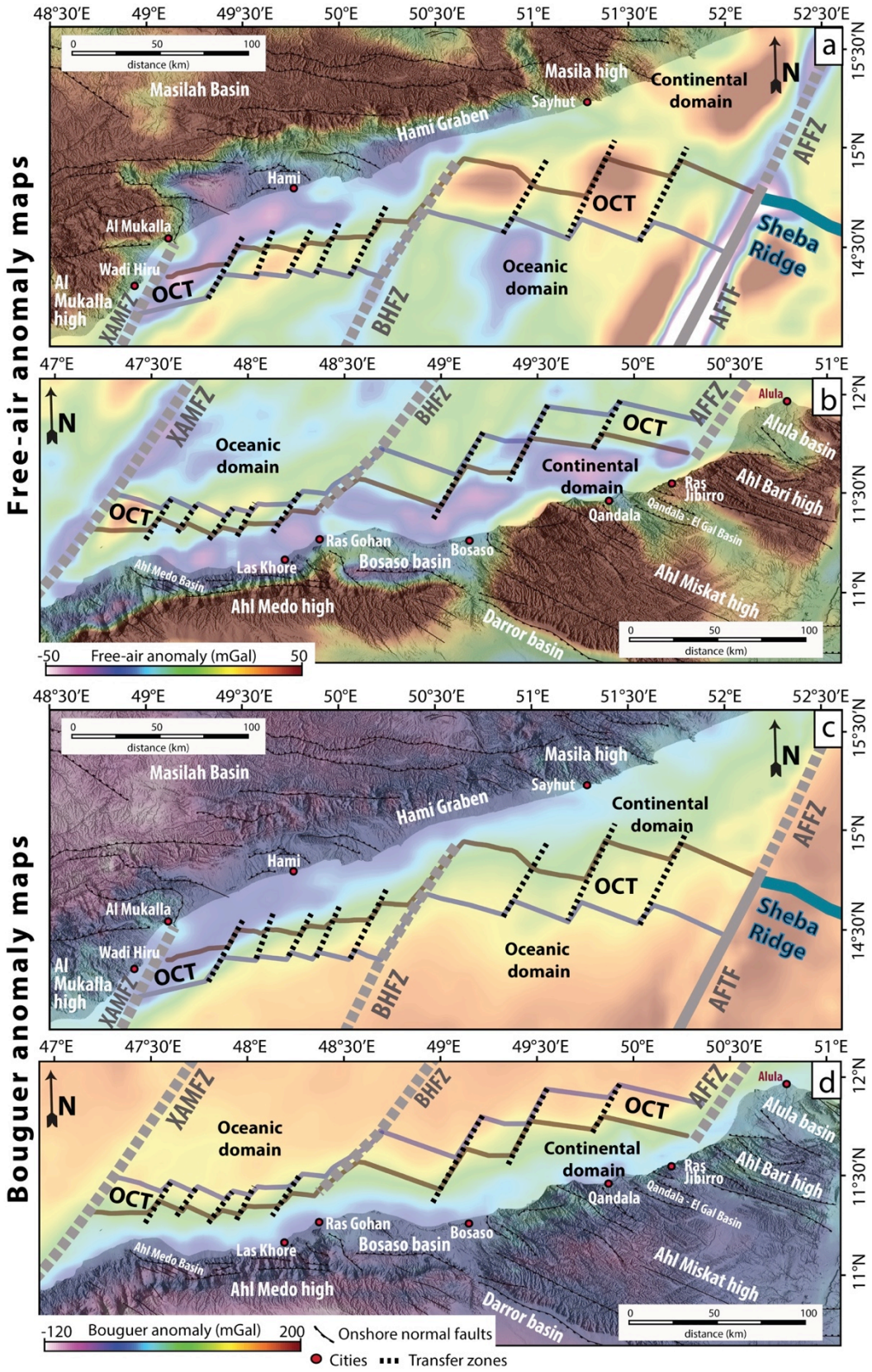


***Figure 12*** *- (a, b) Free-air anomaly and (c, d) Bouguer anomaly maps from the International Gravimetric Bureau (Drewes et al., 2012). Onshore topography is shaded (SRTM, Jarvis et al., 2008). The boundaries of crustal domains are drawn. OCT: Ocean-Continent Transition. AFFZ: Alula Fartak Fracture Zone. AFTF: Alula Fartak Transform Fault. BHFZ: Bosaso Hami Fracture Zone. XAMFZ: Xiis Al Mukalla Fracture Zone.*

640 *4.2.2 Continental domain*

641 The continental domain of conjugate margins presents a long-wavelength rough morphology at depths ranging
642 from 0 to 4500 mbsl (Figs. 5.c, d). The continental seismic basement is characterized by series of angular tilted
643 blocks bounded by normal faults (Fig. 5.c, d), completely buried under the sedimentary cover (Figs. 3.b, 4, 6 to
644 11). The top of the continental seismic basement is defined by the carbonates of the Cenozoic basement (e.g.
645 Figs. 3, 7), the Mesozoic or the Neoproterozoic basement (e.g. Figs. 3, 10) depending on the amount of erosion
646 of the pre-rift units. We define oceanward boundary of the continental domain at the place where no more
647 pre-rift basement is identified, on the distal margins (neither the Cenozoic basement, nor the Mesozoic
648 basement, nor the Neoproterozoic basement; Figs. 4.b, 5 to 10, 11.b, Tab. 1). However, some thick volcanic
649 formations and/or post-rift formations can mask reflections from the seismic basement on the distal margins (Figs.
650 4.b, 7.a, Zooms 1 and 2 on Fig. 8, Figs. 10, 11).

651 On the northern margin, most of the normal faults exhibit small offsets (~100 - 500 m of dip-slip motion, Figs.
652 4.a, 7, 8, 11.b). In the Ahl Medo-Hami segment, the faults dip toward the continent (Figs. 4.a, 7, 8, 11.b); In the
653 Bosaso-Sayhut segment, the faults are also mainly continentward-dipping (Fig. 9). On the southern margin, they
654 show greater dip-slip (from 1000 to 4000 m of vertical throw, Figs. 4.b, 10) than on the northern margin (from 100 to
655 400 m, e.g. Figs. 4.a, 7, 8, 11.b).

656 On the northern margin, the free-air (Fig. 12.a) and the Bouguer (Fig. 12.c) anomalies are negative and positive
657 west and east of BHFZ, respectively. On the southern margin, gravity data reveal large-amplitude, long-wavelength
658 negative free-air and Bouguer anomalies (Figs. 12.b, d).

659

660 *4.2.3 Ocean-continent transition*

661 The transitional domain corresponds to the distal part of the margin where: (i) the geological and geophysical
662 characteristics are typical neither of continental nor steady-state oceanic crust; (ii) a record of the U2 unit (Tab. 1),
663 deposited during the formation of the OCT (Autin et al., 2010; Leroy et al., 2010b), is identified. At the boundary with
664 the continental domain, the OCT domain begins with the disappearance of the clearly identified the Cenozoic,
665 Mesozoic or Neoproterozoic basements (Figs. 7.a, 8 to 10, 11.b; Tab. 1). The top of the transitional basement is
666 difficult to identify and less well defined than the oceanic or continental substratums. Chaotic reflectors characterize
667 the internal facies of the OCT basement (Figs. 7.a, 8). The mapped OCT mainly corresponds to an abrupt passage
668 from negative to positive free-air (up to ~40 mGal, Figs. 12.a, b) and Bouguer anomalies (~100 mGal, Figs. 12.c, d),

except in the OCT in the vicinity of the XAMFZ in the northern margin where the free-air (~-50 mGal in the OCT, Fig. 12.a) and Bouguer anomalies (~-10 mGal in the OCT, Fig. 12.a) are negative.

The OCT on the northern margin (Figs. 5.a, c, 6.a) is wider in the eastern segment (~23 - 45 km) than in the western segment (~17 – 33 km). On the southern margin, the OCT (Figs. 5.b, d, 6.b) is also wider in the Bosaso-Sayhut segment (~ 23 km) than in the Ahl-Medo-Hami segment (~10 – 20 km). The difference in width of the conjugate margins OCTs highlights the asymmetry of the Yemeni and Somalian margins.

The depth to basement maps (Figs. 5.a, b) reveals an eastward deepening of the transitional basement from ~3000 mbsl up to ~5200 mbsl in the eastern Bosaso-Sayhut segment on the northern margin. The conjugate margins OCTs are completely buried beneath syn-OCT to post-rift cover (Figs. 4.b, 7.a, 8 to 10, 11.b) and locally by the syn-rift units slided on the discontinuity L1 (Figs. 4.b, 6, 7.a, 8, 9.b, 10.b, c, d); U2 onlaps the top of the acoustic basement and on the allochthon syn-rift units on the OCT substratum (Figs. 4.b, 6, 7.a, 8, 9.b, 10.b, c, d). In both margins, U2(s) to U4 are affected by minor normal faults (with offsets of a few metres) and sealed by the discontinuity D3 (e.g. Figs. 11.b).

The transitional basement of the northern margin is defined by a flat (Fig. 9) or dome-shaped footwall on the edge of the continental domain (called OCT-ridges, Figs. 7.a, 8) capped by a detachment faults. This fault is low-angle and northward dipping under the continental domain (Figs. 7.a, 8). In the OCT on the northern margin, the detachment faults are oriented (i) N80°E in the western sub-segment near the XAMFZ (Fig. 5.c) and (ii) EW to N95°E in the other five sub-segments of the Ahl Medo-Hami segment at the west of the BHFZ (east of Long. 49°25'E; Figs. 5.c, d, 7, 8). West of the BHFZ, two detachment faults (DF1 and DF2) form two OCT-ridges (zooms 2, 3; Fig. 8.b): the upper basement DF1 is cut by a second detachment fault DF2 (45 – 49 km to the south). On the southern margin, the morphology of the acoustic basement indicates the presence of a basin at the foot of the continental slope (Figs. 5.b, 10).

Evidences of volcanism are identified in the OCT domain: (1) Near the XAMFZ, the northern margin OCT is characterized by SDRs (Zoom 2, Fig. 11.b). The SDR1 wedge overlies a continental block characterized by a domed-structure referred to here as the outer-high (Zoom 2, Fig. 11.b). The SDR2 and the outer-high are cut by several small offset normal faults (Fig. 11.b). (2) The southern margin OCT is affected by volcanism at the location of the XAMFZ (Fig. 10.a) and by a volcano that disturbs the overlaying syn-rift cover slided in the OCT (Fig. 10.b). (3) Near the BHFZ, the basement of the two OCT-ridges is rough and affected by volcanic additions (hummocky or chaotic, high-amplitude low-frequency reflectors; zooms 2, 3 on Fig. 8.b).

699 *4.2.4 Oceanic domain*

700 The oceanic domain is defined by a characteristic rough topography of the top of the seismic basement, mostly
701 found at ~2000 to 4000 mbsl (Figs. 8.a, 11.a), and entirely covered by post-rift units (Figs. 8, 11.b). The depth to
702 oceanic crust basement map (Fig. 11.a) reveals an eastward deepening of the top of the oceanic crust. Near the
703 XAMFZ, the oceanic crust is at a depth of 2000 mbsl and dips eastward to reach 3000 mbsl near the BHFZ. In the
704 Bosaso-Sayhut segment, the oceanic crust deepens towards the centre of the basin and reaches 4200 mbsl (Lat.
705 14°20'N, Long. 50°50'E, Fig. 11.a). We observe a locally a strong reflector that may be interpreted as the Moho (at
706 ~6.3 s TWTT, Fig. 11.b). It allows us to determine the limit of the steady-state oceanic crust (Figs. 11.a). The
707 oceanic domain displays characteristic free-air gravimetric anomalies, varying from -50 mGal on the oceanic
708 transform faults of XAMFZ, BHFZ and AFFZ to 50 mGal on either side of the AFFZ, with a mean value of -10 mGal in
709 the basin (Figs. 12.a, b). The Bouguer anomaly varies from 100 mGal to 200 mGal (Figs. 12.c, d). Low-angle
710 detachment fault in the oceanic basement (close-up view 1, Fig. 11.b) is associated with a large rotation and
711 exposure of the domal-shaped footwall of the fault over a short distance (~4 km in length).
712
713 **4.3 Conjugate margins segmentation**

714 Mapping of the structural domains and syn-rift thicknesses (Fig. 6) highlight NE-trending *en echelon* offsets of the
715 structures (Figs. 5.c, d). Two wavelengths of segmentation are mapped in the central Gulf of Aden. (i) The long-
716 wavelength type corresponds to the major dextral fracture zones (XAMFZ, BHFZ and AFFZ), trending ~N30°E on
717 the northern margin and ~N40°E on the southern margin (Figs. 5.c, d). (ii) In the Ahl Medo-Hami segment, six sub-
718 segments 10 - 30 km in length are subdivided by five ~N30°E-trending transfer zones corresponding to the short-
719 wavelength type (Figs. 5, 7). In the Bosaso-Sayhut segment, the sub-segments of 30 - 50 km in length are
720 delimited by three ~N30°E to N40°E -trending transfer zones (Fig. 5). These transfer zones are well correlated all
721 along both margins (Fig. 5). They show variable offsets (from 3 to 23 km) affecting the continental and the entire
722 OCT domains (Fig. 5), but have so far not developed on the proximal margins. Along the margin, the depth to
723 basement map (Figs. 5.a, b) and the along-strike seismic profiles (Fig. 7.b) display basement highs at the location
724 of transfer zones. These highs delimit the sub-basins corresponding to the syn-rift depocentres (Fig. 7.b).
725
726 **4.4 Decollement layer**

727 The syn-rift unit U1 depocentres (Fig. 6) are characterized by EW to N120°E, N70°E to N80°E and N30°E to N40°E
728 trends (Figs. 5.c, d). U1 depocentres seem to be controlled by the overall morphology of the basement (basins and

highs with EW to N120°E, N70°E to N80°E and N30°E to N40°E trends, Figs. 5.c, d, 7). Indeed, the syn-rift faults appear to be rooted on a common L1 surface on top of R1(a) (in red, Figs. 7, 8). In U1, the subunit R1(a) unit acts as a disharmonic layer (see brown unit, Figs. 7, 8, 9.a, 10.c). The syn-rift structures show various degrees of coupling between the rheologically distinct sedimentary cover and the basement (Figs. 7 to 10, 11.b). Hence, the faults can be restricted to the acoustic basement and to the syn-rift cover above R1(a) and the L1 unconformity (Figs. 4.a, 7, 8, 9.a, 10.c), or can affect the whole syn-rift sequence (including R1(a)) as well as the acoustic basement, e.g. Figs. 4.b, 9, 10.b, d). R1(a) depocentres controlled by the slope are slided into the distal part of the margin, towards the ocean. As such, undifferentiated syn-rift units slide locally on the OCT substratum owing to the decollement layer L1 (Figs. 6 to 10).

## 5. Discussion

The stratigraphic and structural study of our data set (Figs. 3 to 12) in the central Gulf of Aden conjugate margins enable us to discuss (i) the nature of the seismic basement in various crustal domains; (ii) the relationships between sedimentary deposits and volcanism in these hybrid-type conjugate margins; (iii) the tectono-sedimentary and magmatic evolution of the margins system. We compiled these observations on 3D synthetic diagram showing a reconstruction of the conjugate margins at the syn-OCT stage (Fig. 13)

### 5.1 Nature of the seismic basement and tectonic style

#### *5.1.1 Continental domain*

In agreement with previous studies in the eastern Gulf of Aden conjugate margins (d'Acremont et al., 2005; Leroy et al., 2010b; Nonn et al., 2017), we defined the continental domain in the offshore part of central Gulf of Aden conjugate margins based on the following observations: (i) it exhibits a slope morphology; (ii) it is characterized by a series of angular tilted blocks bounded by normal faults; (iii) it is buried beneath the syn- to post-rift sedimentary sequences and (iv) the top of the seismic basement corresponds to the pre-rift units.

On rifted margins, three main sub-domains are generally studied separately: (i) the weakly thinned proximal margin (~30-40 km thick); (ii) the necking zone of continental crust defined as an area of intense crustal thinning from ~30 to less than 10 km where the seismic Moho converge towards the top of the basement (e.g. the Norwegian margin, Péron-Pinvidic and Osmundsen, 2016; the Socotra margin, Ahmed et al., 2014) and (iii) the hyper-extended of continental crust that has been observed e.g. in Bay of Biscay-Pyrenees

(Lagabrielle et al., 2010; Teixell et al., 2016) or in the adjoining conjugate margins of the eastern Gulf of Aden (Autin et al., 2010b; Leroy et al., 2012; Nonn et al., 2017).

In the central Gulf of Aden, we suggest that the continental domain recognized in the offshore margins may correspond to the necking or hyper-extended domains. The ~40 km thick continental crust is thinned of 30-50% towards the ocean on the onshore conjugate margins up to 20 km thick near the coastline (Ali and Watts, 2013; Korostelev et al., 2016). Offshore, continental crust is thinned over very short distances, as the immerged continental domain do not exceed 60 km from the coastline to its distal boundary (Fig. 5). However, we are unable to determine the boundary between the necking and the hyper-extended domains due to a lack of deep penetration seismic data that could have allowed us to observe the Moho depths and deduce to the crustal thickness.

*5.1.2 Ocean-Continent Transition*

As proposed for the eastern Gulf of Aden conjugate margins (d'Acremont et al., 2005; Leroy et al., 2012; Nonn et al., 2017), we defined the location of the OCT based on the unreflective character of the seismic basement and the deposition of the syn-OCT units (U2(v) ou U2(s)) directly on the seismic basement (Figs. 7.a, 8 to 10, 11.b). Some SDRs may also cover directly the seismic basement (Fig. 11.b).

In the OCT domain of the northern margin, we identify two northward-dipping detachment faults on seismic line 5N (Fig. 8.b): the second detachment fault (DF2) is formed at the footwall of the first detachment fault (DF1) and leads to the exhumation of deeper units. This pattern of successive detachment faults is observed onshore in the continental crust on Tinos island (Brichau et al., 2007) and offshore on the distal part of the Australian-Antarctic margin (Direen et al., 2011; Gillard, 2015). On the southern margin, we identify that the acoustic basement forms a basin at the foot of the continental slope (Figs. 5.b, 10). We suppose that the southern tip of the basin may correspond to an oceanward low-angle large-offset fault (in green, Fig. 10) based on the observation of the detachment faults in the northern margin. The presence of detachment faults is reinforced by the dome-shaped footwall (OCT-ridges, Figs. 7, 8) bounding the northern margin OCT. This latter may be interpreted as exhumed subcontinental mantle (e.g. Boillot et al., 1980, 1989; Whitmarsh et al., 2001; Tucholke et al., 2007). Indeed, ridges of serpentinized peridotites display smooth-shaped basement highs as observed and drilled on the Iberian-Newfoundland margins (Beslier et al., 1996; Shillington et al., 2006; Whitmarsh et al., 2001) or observed on the eastern Gulf of Aden margins (Leroy et al., 2010b). Indeed, in the eastward adjacent Encens-Sheba segments, the OCT is composed, at least partially, of exhumed serpentinized

788 mantle (d'Acremont et al., 2006; Leroy et al., 2010b, 2012; Watremez et al., 2011). The unreflective character
789 of the upper seismic basement could be in agreement with the interpretation of exhumed serpentinized
790 mantle in distal margins (Pickup et al., 1996; Shillington et al., 2006).
791
792 *5.1.3 Narrowness, asymmetry and segmentation of the central Gulf of Aden conjugate margins*
793 In the eastern Gulf of Aden, (i.e. Encens-Sheba segment (d'Acremont et al., 2005; Leroy et al., 2012) and
794 Socotra-Sharbithat segment (Nonn et al., 2017)) similar data show narrowness, asymmetry and segmentation
795 of the conjugate margins. In the adjoining central Gulf of Aden, our data set reveals that the offshore part of
796 the continental domain is narrow (less than~ 150 km cumulated on both margins). The continental domain of
797 the southern margin is narrower (~20-40 km) than the northern one (~20–100 km). This narrowness and
798 asymmetry of the continental domain is also recorded in the OCT (less than ~50 km cumulated on both
799 margins, Fig. 5). The southern margin OCT is narrower (~10-20 km, Figs. 5.b, d) than the northern one (~20 – 40
800 km, Figs. 5.a, c, 12) but both widen eastward from ~10 to 40 km (Figs. 5, 12).
801 This asymmetry of the continental domain of the conjugate margins provides evidence for the activity of
802 lithospheric low-angle detachment faults during the formation of the OCTs as suggested in the eastern Gulf of
803 Aden (Nonn et al., 2017). The distinction between the hangingwall (upper plate) and the footwall (lower plate)
804 of the detachment fault (Lister et al., 1986) may be difficult as extension may involved the setting up of
805 numerous generations of detachment faults (e.g. Hayward and Ebinger, 1996; Sauter et al., 2013; Gillard et al.,
806 2015, 2016). Our study reveals a northward-dipping low-angle detachment fault (<30°, Figs. 7, 8) at the edge of
807 the Yemeni continental domain, corresponding to northward-dipping reflectors that argue strongly in favour of
808 a final northward dip of the final detachment fault. At the beginning of the exhumation phase, this northward-
809 dipping low-angle detachment fault is associated with the development of asymmetrical margins narrower in
810 the southern margin than in the northern one as proposed. However, the presence of multiple detachment
811 faults (DF1, DF2; Fig. 8.b) shows that this first detachment fault was not active during the whole rifting history
812 (e. g. Iberian-Newfoundland margins; Rosenbaum et al., 2008). Furthermore, the lack of data on the distal
813 margins prevents us from establishing a detailed architecture for the OCT on the Somalian margin. The
814 magmatism masks the OCT structures at the east of the BHFZ (Figs. 4.b, 10) and makes the interpretation of the
815 exhumation zone highly speculative.
816 The oblique rifting of the Gulf of Aden implies a significant segmentation of the conjugate margins. The long-
817 wavelength type of segmentation corresponds to the N30°E to N40°E-trending XAMFZ, BHFZ and AFFZ which

separate the ~ 180 km-long Ahl Medo-Hami and Bosaso-Sayhut segments and which seem to affect the proximal margin since the onset of rifting in the Gulf of Aden up to the OCT and are well correlated all along both margins (Figs. 5, 12). Between the major fracture zones, the N30°E to N40°E-trending transfer zones are also correlated all along the conjugate margins and affect the distal part of the continental domains, the OCTs and the oceanic domain (Figs. 5, 12). As the identified major fracture zones and the transfer zones shift the oceanic domain thanks to seismic interpretation (Fig. 2), gravity data (Fig. 12) and previous studies on magnetic data (Leroy et al., 2012), we suggest that they correspond to oceanic transform zones, at least at the beginning of the steady-state spreading of the oceanic crust (Burdigalian). Such a segmentation has been described and mapped in the eastern Gulf of Aden conjugate margins (d'Acremont et al., 2005; Leroy et al., 2012; Nonn et al., 2017). A classification of the segmentation proposed by Bellahsen et al. (2013b) distinguishes the oceanic fracture zones that are formed in the continuity of continental transform since the early rifting phase (Type 1-C) and other one formed at continental transfer zones since the syn-rift to early OCT phases (Type 1-T). In the central Gulf of Aden, the XAMFZ, BHFZ and AFFZ correspond to the Type 1-C and the transfer zones correspond to the type 1-T.

### 5.2 Stratigraphy, magmatism and vertical movements in hybrid-type margin

#### *5.2.1 Late syn-rift decoupling surfaces*

The central Gulf of Aden conjugate margins are subject to vertical movements associated with syn-rift decoupling surfaces especially in the Ahl-Medo Hami segment. The presence of layers of salt or clay is often necessary to act as decollement horizons. Studies on salt-influenced rift basins as in offshore Norway (Kane et al., 2010), Congo (Karner et al., 1997), Angola (Duval et al., 1992; Fort et al., 2004) and Morocco (Tari et al., 2000) have revealed a complex interplay between fault growth and salt movement which influences the evolution of syn-rift depocentres (e.g. Vendeville et al., 1995). When a ductile layer decouples the supra-salt cover from the basement, this leads to a diffusion of deformation in the basement and involves two separate fault populations: one in the cover and the other confined within the pre-salt basement (Richardson et al., 2005; Vendeville et al., 1995). The migration of this mechanically weak layer offsets the syn-rift depocentre and plays a fundamental role in controlling the size and distribution of the depocentre (e.g. Kane et al., 2010).

In the central Gulf of Aden, the R1(a) unit corresponds to the base of the Ghaydah Fm (Fig. 3) and represents an important weak layer that could act as a decoupling horizon during the extension (extensional faults affecting the R1(b) unit (in brown) are rooted on the discordance L1 (in red, Figs. 3, 4, 7 to 10). In the

wells, the Ghaydah Fm is characterized by sandstones, conglomerates, anhydrites and marls (Watchorn et al., 1998) providing evidence of a continental environment. According to Bott et al. (1992), the Ghaydah Fm is more evaporitic westward, in the Ahl Medo-Hami-segment. On the southern margins, the wells encounter anhydrites and shales of the Bandar-Harshau Fm (Bott et al., 1992; Ali and Watts, 2013). However, the wells are located on top of structural highs and the significant mobility of R1(a) at the base of Ghaydah confines the unit to the edge of these highs (i.e. 3 km south of the coastline for the northern margin, Fig. 3.a), thus preventing direct access to geological data. Nevertheless, in agreement with the significant ductile behaviour of R1(a) and the evaporitic nature of the Ghaydah and Bandar-Harshau Fms, we suggest that R1(a) could be a salt layer.

During the Aquitanian - Burdigalian, the rifting intensifies and the deepening increases is associated with margin subsidence. The syn-rift cover slides on a major decoupling layer R1(a) toward the distal margin. The sliding continues until the syn-OCT Phase (Burdigalian) as shown by the presence of syn-rift units in the OCT resting directly the transitional basement exhumed by the on the detachment fault, especially on the northern margin (Figs. 4.a, 7, 9.a). Such sliding of the sediment cover onto the exhumed OCT substratum is also observed in the Pyrenees (Lagabrielle et al., 2010).The onlapping post-rift units (Figs. 4.b, 7.a, 8, 9, 10.b, c, d) show that deformation does not continue during the post-rift phase.

This scenario is similar to that of the detachment tectonics involving decollement salt layers and the sliding of the mobile sedimentary cover on the exhumed mantle rocks described in the fossil Pyrenean margins (e.g. Lagabrielle et al., 2010; Masini et al., 2014; Tugend et al., 2014; Clerc et al., 2016). While stretching of syn-rift cover is observed on the proximal part of the margin, the glided syn-rift cover in the OCT does not display any evidence of shortening farther downslope, at the toe of the conjugate margin dips (Figs. 7.a, 8, 9.a, 10), as observed for example on the Angolan margin (Fort et al., 2004). To address the issue of spatial accommodation of the extension, Duval et al. (1992) proposed a conceptual model of gravity-driven deformation where allochthons can glide onto a newly formed domain without downslope shortening and with or without a frontal buttress (process of raft tectonics). In our study, we suggest that the Tertiary gravitational deformation of syn-rift units over R1(a) salt unit is accommodated on distal margins by the simultaneous creation of space during the emplacement of the OCT and the formation of detachment faults exhuming mantle rocks. That has been described on the southern Australian margin (Espurt et al., 2009, 2012) or in the Pyrenees (Jammes et al., 2010; Lagabrielle et al., 2010; Masini et al., 2014). The so-called OCT-Ridges (zooms 1, 3, Fig. 8.b) correspond to dome-shaped reliefs on the OCT basement that could act like buttresses along the margin (zoom 3 on Fig. 8.b) as slided syn-rift sediments onlap on their continentward slopes.

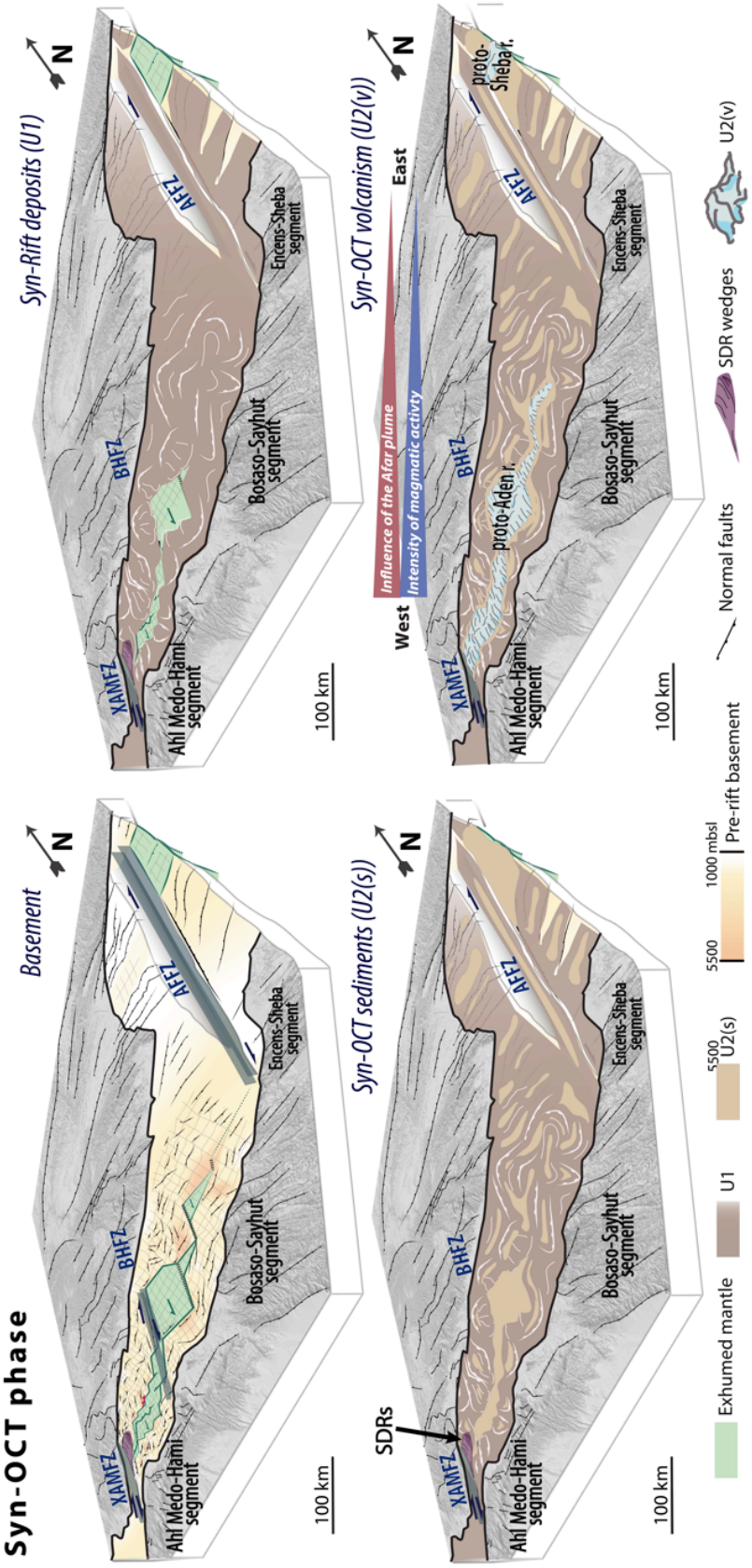


*Figure 13 – Synthetic 3D diagram at the syn-OCT phase (Burdigalian) showing the basement structures, syn-rift deposits (U1), syn-OCT sediments (U2(s)) and syn-OCT volcanism (U2(v)) arrangement. The Xiis Al Mukalla Fracture Zone (XAMFZ), Bosaso-Hami Fracture Zone (BHFZ) and Alula Fartak Fracture Zone (AFFZ) are developed in offshore part of the conjugate margins and bound on either side the Ahl Medo-Hami and Bosaso-Sayhut segments. Offshore margins are narrower on the Ahl Medo-Hami segment (~100 km wide) than on the Bosaso-Sayhut segment (~150 – 200 km wide). Upper left panel: In the east of the BHFZ, the exhumation zone in the OCT seems to be wider than the surrounding. However, the interpretation of this area is highly speculative since the OCT is entirely covered by the volcanic unit U2(v) (lower right panel) that masks the deeper structures and does not allow proper observation of the detachment fault. Onshore topography is shaded (SRTM, Jarvis et al., 2008).*

936 *5.2.2 Volcanic to non-volcanic margins transition*

937 The difference between magma-rich and magma-poor rifted margins depends on the timing and amount of
938 magma involved in relation to lithospheric extension, breakup and plate separation (Courtillot et al., 1999; Sengör
939 and Burke, 1978; White and McKenzie, 1989; Coffin and Eldholm, 1994). Since the two end-member types of
940 continental margins have been studied separately, the transition from volcanic to non-volcanic margins has
941 attracted less attention and is not yet well understood. Indeed, the distinction between magma-rich and magma-
942 poor is still problematic in view of the occurrence of hybrid margins (Reston and Manatschal, 2011).

943 In the central Gulf of Aden, we identify syn-rift and also syn-OCT volcanism in the west (SDR prisms and
944 U2(v), Figs. 4.b, 7.a, 8, 10.a, 11), whereas we observe less volcanism and more syn-OCT sediments onlapping the
945 syn-rift units toward the east (U2(s) on profiles; Figs.9, 10.d). This is associated with decreasing depth to the top of
946 volcanic structures away from the BHFZ (Fig. 11.a). The free-air and Bouguer anomaly maps are in agreement with
947 these observations by displaying negative and positive anomalies, respectively, to the west and east of the BHFZ
948 in the northern continental domain (Fig. 12.a) (Ali and Watts, 2013). Indeed, this mismatch between the gravity
949 anomalies and the mapping of the continental domain can be explained by a greater amount of volcanism (likely
950 combined with other alteration processes as e.g. metamorphism or hydratation) that may have changed the
951 physical properties and signal of the continental basement (e.g. in the Norwegian margin; Péron-Pinvidic et al.,
952 2016). While the southern margin is not so well defined due to lack of data in the distal parts, volcanism is also
953 more developed in the western part than in the eastern part of the margins (Fig. 13.a). These observations show
954 that the conjugate margins evolve gradually from a more magmatic near the XAMFZ, characterized by significant
955 volcanism (Fig. 10.a) and the development of SDRs in the OCT (Figs. 11) to magma-poor to the east of the BHFZ
956 (Figs. 7 to 9, 10.b, c, d). We propose then that the central Gulf of Aden is composed of hybrid margins, transitional
957 between magma-rich and magma-poor margins in the western and eastern parts of the Gulf of Aden,
958 respectively (e.g. Leroy et al., 2012). Offshore Aden city, the margins are typical volcanic margins with syn-rift
959 thick SDRs and underplated bodies in the west (Ahmed et al., 2013) whereas in the east volcanism occurred just
960 before the breakup (Lucazeau et al., 2009; Leroy et al., 2010b; Nonn et al., 2017). This hybrid-type margins has
961 also been described in West Greenland (Chalmers and Pulvertaft, 2001) or in the central domain of the
962 paleomargins of Pyrenean Cretaceous basin (at the transition between a cooler western domain and a hotter
963 eastern domain; Clerc and Lagabrielle, 2014).

964 Near XAMFZ, the SDR wedges (Figs. 11.b, d) shows that magmatic extrusions occurred during the thinning
965 of the continental crust and the development syn-extrusive growth detachments (Planke et al., 2000; Geoffroy

et al., 2015). The SDRs developed seaward on top of the intruded continental crust and migrated progressively toward the future oceanic spreading centre (Geoffroy, 2005). However, wedge-shape horizons of the U2(v) unit towards the OCT ridge (dipping continentward, zoom 2 Fig. 8) indicate that the volcanic units were deposited during the up doming of the OCT ridge. The wedge-shape U2(v) unit dipping continentward is strongly similar to the Continentward Dipping Reflectors (CDRs) described by Gillard et al. (2017) in the Gulf of Guinea. It suggests an increase of the extrusive magmatic supply during the formation of the OCT above the exhumed basement. In the Yemeni margins, two volcanic sub-units are recorded on U2(v) unit in the OCT (Fig. 8.a) and may be interpreted as two volcanic pulses in the OCT. These Our results show that the stage of mantle exhumation is accompanied or followed quickly by the establishment of volcanic activity (Fig. 13), as proposed in the Iberian-Newfoundland margins by Shillington et al., (2006) or in the Tyrrhenian basin by Prada et al., (2016) and in the eastern part of the Gulf of Aden by Autin et al., (2010a). Thus, we highlight a gradual eastward decline in the amount of volcanic activity and a diachronous emplacement of volcanism, which seem to appear later eastward along the hybrid conjugate margins of the central Gulf of Aden (Figs. 7 to 13). This assumption is in agreement with a greater influence of the Afar plume towards the west and the channelling of material coming from Afar plume along the main tectonic corridors (Leroy et al., 2010a, 2012) until a final lithospheric breakup.

A significant and localized volcanic supply in the OCT can contribute to focus the extension (e.g. Buck, 1991; Ebinger and Casey, 2001), while diffuse volcanic supply favours a distributed extension (e.g. Corti et al., 2003). Due to a higher thermal regime in the Ahl Medo-Hami segment than in the Bosaso-Sayhut segment, we suggest that the deformation is localized in the west and more diffuse in the east, leading to an early emplacement of the OCT in the west (Fig. 13). The higher thermal regime and the greater degree of rift localisation in the Ahl Medo-Hami segment are consistent with a greater influence of the Afar plume westward (Leroy et al., 2010a). It is also accompanied by (i) the more elevated topography of the basement on both margins (Fig. 9.b); (ii) the greater amount of volcanism in the continental, transitional and oceanic domains (as shown by the higher topography of the volcanic substratum westward (Figs. 4.b, 11.a) volcanic structures on seismic line 1S, Fig. 10.a) and (iii) by a narrower OCT to the west of the BHFZ (Figs. 5, 13).

*5.2.3 Syn-OCT uplift*

Ali and Watts (2013) have argued by wells backstripping and gravity modelling that the Yemeni margin was underplated by magmatic material during rifting of the Gulf of Aden and that an uplift event could have been

superimposed. During the OCT formation, the distal margins located near AFFZ record significant erosion (see red square, Fig. 9.b). Indeed, a significant block was individualized and rotated toward the ocean during the rifting process. During this period, the syn-rift units R1 and R2 deposited in the newly formed half-graben (Fig. 9.c). Later, the deposited units were affected by normal faults rooted on the units R1(a) and sealed by the discontinuity D1. The head of this block was eroded during the syn-OCT stage (Fig. 9.c) and is coeval with the filling of the basin with the syn-OCT unit U2. In the eastern Gulf of Aden a major regional uplift occurred at the end of the OCT formation (Leroy et al., 2012; Nonn et al., 2017).

We propose that this erosion also occurred in the central Gulf of Aden and may have eroded distal margins near the AFFZ, suggesting a shallow basement at the time of the OCT formation. The locally buoyant mantle (Bellahsen et al., 2013a) and the thinning of the crust could induce dynamic topography and uplift of the margin. These buoyancy forces may have been enhanced (i) by the crustal breakup (rift-induced decompression melting associated with the development of large-scale low-angle detachment faults exhuming subcontinental mantle in the OCT; White and McKenzie, 1989; Driscoll and Karner, 1998), (ii) by the rift dynamics and by the channelling of Afar plume material along the major transform zones as proposed by Leroy et al., (2010a) and/or (iii) by small-scale convection in the lower mantle induced by the lithosphere showing various ages and thicknesses on either side of transform fault zones (i.e. XAMFZ, BHFZ or AFFZ; Korostelev et al., 2015a, 2016). The onshore Cenozoic volcanism (Fantozzi, 1996; Leroy et al., 2010b) outcropping at the edge of the BHFZ and AFFZ (Fig. 2) is also compatible with the channelling of material coming from Afar plume along the main fracture zones.

### 5.3 Tectono-sedimentary evolution of hybrid-type margins

In this section, we propose a chronological interpretation of the sedimentary sequences on the deep margin is constructed using the onshore observations and dating results (Fig. 3).

During the stretching phase (Rupelian-Chattian, Fig. 3) the first syn-rift unit (R1 corresponding to Buwaysh Fm or Ghaydah Fm on the onshore and offshore Yemeni margin, respectively and to Scimi Fm or Lower Bandar-Harshau Fm. on the onshore and offshore Somalian margin, respectively; Fig. 3) is deposited in a continental environment under episodic hyper-saline conditions (Bott et al., 1992). During the thinning phase (Lavier and Manatschal, 2006) (Fig. 3), the R1(a) unit acts as a layer for the decoupling of syn-rift units over the basement (Figs. 4, 6 to 8, 9.a, 10.c). The Upper-Chattian – Aquitanian is marked by the accumulation of deep-marine deposits (R2 in this study; Fuwwah Fm (onshore), Hami Fm (offshore) on the Yemeni margins; Scusciuban or

Dubar Fm (onshore) and Bandar Harshau (offshore) on the Somalian margin; Fig. 3) within the syn-rift basins. Two tectonic subsidence events are recorded: (i) the deposition of R2(a) in N70°E-trending syn-rift basins (Fig. 5.c), mainly on the distal margins; (2) the increased deepening of the margins and the deposition of the R2(b) subunit all along the margins (e.g. Fig. 4). The eastward-dipping deposition profile which is acquired since the Jurassic (Figs. 5.a, b) (Luger et al., 1994) is a sedimentary pattern of the conjugate margins.

During the OCT formation, the conjugate margins are affected by late tilting and steepening of the margin slope, provoking erosion of the onshore domains which supplies sediments supply to the distal margins (Platel and Roger, 1989; Autin et al., 2010b; Razin et al., 2010; Leroy et al., 2012). Flat syn-OCT sediments (U2(s); Figs. 7 to 11) are deposited on both margins and onlap the OCT ridge on the northern margin (Figs. 7, 8).

The post-rift phase starts when an oceanic ridge is established in the asthenosphere, leading to steady-state oceanic spreading (Cannat et al., 2009). The post-rift sequence (U3 to U5, Figs. 3, 4, 7 to 10, 11.b) is thicker on the northern margin (up to 4000 m) than on the southern side (up to 1600 m). We argue that this difference may be due to tectonic factors (less subsidence on the southern margin) or environmental factors (poor drainage network in Somalian margin). According to (Watchorn et al., 1998), the post-rift sequence records at least three uplift pulses. We link first the uplift event to the end of the syn-OCT stage. Then the deposition of the U3 in distal parts of the margins occurred (Figs. 7.a, 8 to 10, 11.b), similar to the U3 unit recorded in the eastern Gulf of Aden (Autin et al., 2010b; d'Acremont et al., 2005; Bache et al., 2011; Leroy et al., 2012). If this event is synchronous throughout the Gulf of Aden, U3 could have been deposited between 17.6 and 10 Ma (Bache et al., 2011). However, U3 in the eastern Gulf of Aden displays more frequent occurrence of MTCs than the central margin unit. This discrepancy may be explained by increased subsidence and destabilization of the eastern margin (Leroy et al., 2012). Finally, the top of U3 is an erosional discontinuity (D3, Figs. 7.a, 8 to 10, 11.b) that we correlate to the second uplift recorded by Watchorn et al. (1998). A new subsidence phase (younger than 10 Ma) allows the deposition of U4 defined by the sudden occurrence of current-formed features that indicate an intensification of hydrodynamic regime. These features are consistent with a deep-sea domain and clearly imply the steepening of the margin slope as observed in the eastern Gulf of Aden (Ziegler, 2001; Bache et al., 2009; Baurion, 2012). The presence of significant progradations in the Bosaso-Sayhut segment (Fig. 9.a) suggests that deepening increases toward the east. U3 and U4 are tilted and faulted and the top of U4 is eroded, especially toward the continent (discontinuity D4, Figs. 7.a, 8, 9). This event can be correlated with the third uplift pulse recorded by sediments onlap (Watchorn et al., 1998). All these observations are interpreted as being related to a major uplift also recorded in the eastern Gulf of Aden

(Platel and Roger, 1989; Bache et al., 2011; Leroy et al., 2012; Nonn et al., 2017). Finally, U5 is characterized by sub-parallel deposits onlapping the eroded U4 and sealed at the surface by the present-day seabed (Figs.4, 7 to 11).

## 5. Conclusion

Our analysis of marine geophysical and geological data from the central Gulf of Aden contributes to a better understanding of the formation of hybrid margins system located at the transition between volcanic margins (offshore Aden city) and magma-poor margins in the east. We determine seismic stratigraphy and structural patterns and map the three main crustal domains (continental, Ocean-Continent Transition (OCT), oceanic domains) in order to propose a tectonic evolution of the Yemeni and Somalian conjugate margins. This study reveals that the conjugate margins formed during the oblique rifting of the central Gulf of Aden are narrow, asymmetrical (as the continental domain and the OCT of the southern margin is narrower than the northern one) and highly segmented. We highlight an eastward gradual decrease in intensity of magmatic activity and a diachronous set up of volcanic formations related to a strong influence of hot material coming probably from the Afar plume. At the western boundary of the studied zone near the XAMFZ, magmatic processes are predominant. The higher thermal regime is associated with the development of SDRs wedges from the late phase of the thinning of the continental crust (early Miocene-~21 Ma) up to the exhumation phase (Burdigalian-~18 Ma) that lead to the OCT development. Farther east, tectonic processes are predominant and evidence of volcanism appears later eastward, occurring during and shortly after the unroofing of sub-continental mantle along low-angle detachment faults (Burdigalian) in the OCT basement. The early syn-rift phase (Oligocene) is marked by the development of the main segmentation (XAMFZ, BHFZ and AFFZ). Between the XAMFZ and the BHFZ, the Ahl Medo-Hami segment (in the western part) experiences a greater influence of the Afar plume than the Bosaso-Sayhut segment between the BHFZ and the AFFZ (in the eastern part). The central Gulf of Aden is subject to a major uplift during the final syn-rift stage and up to OCT emplacement, associated with a major erosion in the east and gravitational deformation taking place on decoupling surfaces at the base of the syn-rift sequence (lower Ghaydah Fm) in the west.

## Acknowledgments

Partnership - TOTAL - UNIVERSITE PIERRE ET MARIE CURIE - CENTRE NATIONAL DE LA RECHERCHE SCIENTIFIQUE. This study is a contribution from Actions Marges (Total, CNRS-INSU, IFREMER and BRGM). We

are especially grateful to Total S.A. for their support during the project. We thank Thomas Maurin, Xavier du Bernard for valuable discussions. We are grateful to the editor Adam Bumby and the anonymous reviewer for their very helpful comments improving the manuscript. Dr M.S.N. Carpenter post-edited the English style and grammar.

**Bibliography**

Ahlbrandt, T.S., 2002. Madbi Amran/Qishn Total Petroleum System of the Ma'Rib-Al Jawf/Shabwah, and Masila-Jeza Basins, 1st ed. U.S. Geological Survey Bulletin.

Ahmed, A., Leroy, S., Keir, D., Korostelev, F., Khanbari, K., Rolandone, F., Stuart, G., Obrebski, M., 2014. Crustal structure of the Gulf of Aden southern margin: Evidence from receiver functions on Socotra Island (Yemen). Tectonophysics 637, 251–267. https://doi.org/10.1016/j.tecto.2014.10.014

Ahmed, A., Tiberi, C., Leroy, S., Stuart, G.W., Keir, D., Sholan, J., Khanbari, K., Al-Ganad, I., Basuyau, C., 2013. Crustal structure of the rifted volcanic margins and uplifted plateau of Western Yemen from receiver function analysis. Geophys. J. Int. 193, 1673–1690. https://doi.org/10.1093/gji/ggt072

Ali Kassim, M., 1991. Oligo-Miocene sedimentation in the Boosaaso and Qandala Basin, Gulf of Aden, NE Somalia. Geol. Basamento Ital. - Convegno Onore Tommaso Cocozza 87.

Ali, M.Y., 2015. Petroleum Geology and Hydrocarbon Potential of the Guban Basin, Northern Somaliland. J. Pet. Geol. 38, 433–457. https://doi.org/10.1111/jpg.12620

Ali, M.Y., Watts, A.B., 2016. Tectonic evolution of sedimentary basins of northern Somalia. Basin Res. 28, 340–364. https://doi.org/10.1111/bre.12113

Ali, M.Y., Watts, A.B., 2013. Subsidence history, crustal structure, and evolution of the Somaliland-Yemen conjugate margin. J. Geophys. Res. Solid Earth 118, 1638–1649. https://doi.org/10.1002/jgrb.50113

As-Saruri, M.A., Sorkhabi, R., Baraba, R., 2010. Sedimentary basins of Yemen: their tectonic development and lithostratigraphic cover. Arab. J. Geosci. 3, 515–527. https://doi.org/10.1007/s12517-010-0189-z

Autin, J., Bellahsen, N., Husson, L., Beslier, M.O., Leroy, S., d'Acremont, E., 2010a. Analog models of oblique rifting in a cold lithosphere. Tectonics 29, TC6016, doi:10.1029/2010TC002671.

Autin, J., Bellahsen, N., Leroy, S., Husson, L., Beslier, M.-O., d'Acremont, E., 2013. The role of structural inheritance in oblique rifting: Insights from analogue models and application to the Gulf of Aden. Tectonophysics, The Gulf of Aden rifted margins system : Special Issue dedicated to the YOCMAL project (Young Conjugate Margins Laboratory in the Gulf of Aden) 607, 51–64. https://doi.org/10.1016/j.tecto.2013.05.041

Autin, J., Leroy, S., Beslier, M.-O., D'Acremont, E., Razin, P., Ribodetti, A., Bellahsen, N., Robin, C., Al Toubi, K., 2010b. Continental break-up history of a deep magma-poor margin based on seismic reflection data (northeastern Gulf of Aden margin, offshore Oman). Geophys. J. Int. 180, 501–519. https://doi.org/10.1111/j.1365-246X.2009.04424.x

Azzaroli, A., 1958. L'oligocene e il Miocene della Somalia: stratigrafia, tettonica, paleontologia (macroforaminiferi, coralli, molluschi), Paleontolongia Italiana. Tipografia moderna, Pisa.

Bache, F., Leroy, S., Baurion, C., Robinet, J., Gorini, C., Lucazeau, F., Razin, P., d'Acremont, E., Al-Toubi, K., 2011. Post-rift uplift of the Dhofar margin (Gulf of Aden). Terra Nova 23, 11–18. https://doi.org/10.1111/j.1365-3121.2010.00975.x

Bache, F., Olivet, J.L., Gorini, C., Rabineau, M., Baztan, J., Aslanian, D., Suc, J.P., 2009. Messinian erosional and salinity crises: View from the Provence Basin (Gulf of Lions, Western Mediterranean). Earth Planet. Sci. Lett. 286, 139–157.

Baurion, C., 2012. Architecture sédimentaire et dynamique post-rift des marges conjuguées du Golfe d'Aden oriental. Université Pierre et Marie Curie (Paris VI), Paris.

Bellahsen, N., Husson, L., Autin, J., Leroy, S., d'Acremont, E., 2013a. The effect of thermal weakening and buoyancy forces on rift localization: Field evidences from the Gulf of Aden oblique rifting. Tectonophysics, The Gulf of Aden rifted margins system : Special Issue dedicated to the YOCMAL project (Young Conjugate Margins Laboratory in the Gulf of Aden) 607, 80–97. https://doi.org/10.1016/j.tecto.2013.05.042

Bellahsen, N., Leroy, S., Autin, J., Razin, P., d'Acremont, E., Sloan, H., Pik, R., Ahmed, A., Khanbari, K., 2013b. Pre-existing oblique transfer zones and transfer/transform relationships in continental margins: New insights from the southeastern Gulf of Aden, Socotra Island, Yemen. Tectonophysics, The Gulf of Aden rifted margins system : Special Issue dedicated to the YOCMAL project (Young Conjugate Margins Laboratory in the Gulf of Aden) 607, 32–50. https://doi.org/10.1016/j.tecto.2013.07.036

Beslier, M.-O., Cornen, G., Girardeau, J., 1996. Tectono-metamorphic evolution of peridotites from the ocean/continent transition of the Iberia Abyssal Plain margin. Proc. Ocean Drill. Program Sci. Results 149, 397–412. https://doi.org/10.2973/odp.proc.sr.149.218.1996

Beydoun, Z.R., 1997. Introduction to the revised Mesozoic stratigraphy and nomenclature for Yemen. Mar. Pet. Geol., Special Issue on Mesozoic Rift Basins of Yemen 14, 617–629. https://doi.org/10.1016/S0264-8172(96)00049-9

Beydoun, Z.R., 1970. Southern Arabia and Northern Somalia: Comparative Geology. Philos. Trans. R. Soc. Lond. Math. Phys. Eng. Sci. 267, 267–292. https://doi.org/10.1098/rsta.1970.0036

Beydoun, Z.R., As-Saruri, M.A.L., El-Nakhal, H., Al-Ganad, I.N., Baraba, R.S., Nani, A., Al-Aawah, M.H., 1998. International lexicon of stratigraphy : Republic of Yemen. 3, Asia, fasc 10 b 2. IUGS and Ministry of Oil and Mineral Resources, Republic of Yemen.

Beydoun, Z.R., As-Saruri, M.L., Baraba, R.S., 1996. Sedimentary Basins of the Republic of Yemen : Their Structural Evolution and Geological Characteristics. Oil Gas Sci. Technol. - Rev IFP 51, 763–775.

Birse, A.C.R., Bott, W.F., Morrison, J., Samuel, M.A., 1997. The Mesozoic and early tertiary tectonic evolution of the Socotra area, eastern Gulf of Aden, Yemen. Mar. Pet. Geol., Special Issue on Mesozoic Rift Basins of Yemen 14, 675–684. https://doi.org/10.1016/S0264-8172(96)00043-8

Boillot, G., Féraud, G., Recq, M., Girardeau, J., 1989. Undercrusting by serpentinite beneath rifted margins. Nature 6242.

Boillot, G., Grimaud, S., Mauffret, A., Mougenot, D., Kornprobst, J., Mergoil-Daniel, J., Torrent, G., 1980. Ocean-continent boundary off the Iberian margin: A serpentinite diapir west of the Galicia Bank. Earth Planet. Sci. Lett. 48, 23–34. https://doi.org/10.1016/0012-821X(80)90166-1

Bosence, D., Nichols, G., Al-Subbary, A.-K., Al-Thour, K.A., Reeder, M., 1996. Synrift continental to marine depositional sequences, Tertiary, Gulf of Aden, Yemen. J. Sediment. Res. 66, 766–777. https://doi.org/10.1306/D4268400-2B26-11D7-8648000102C1865D

Bosence, D.W.J., 1997. Mesozoic rift basins of Yemen. Mar. Pet. Geol., Special Issue on Mesozoic Rift Basins of Yemen 14, 611-IN6. https://doi.org/10.1016/S0264-8172(97)00039-1

Bosworth, W., Huchon, P., McClay, K., 2005. The Red Sea and Gulf of Aden Basins. J. Afr. Earth Sci. 43, 334–378. https://doi.org/:10.1016/j.jafrearsci.2005.07.020

Bott, W. f., Smith, B. a., Oakes, G., Sikander, A.H., Ibraham, A.I., 1992. The Tectonic Framework and Regional Hydrocarbon Prospectivity of the Gulf of Aden. J. Pet. Geol. 15, 211-243. https://doi.org/10.1111/j.1747-5457.1992.tb00963.x

Brannan, J., Gerdes, K.D., Newth, I.R., 1997. Tectono-stratigraphic development of the Qamar basin, eastern Yemen. Mar. Pet. Geol., Special Issue on Mesozoic Rift Basins of Yemen 14, 701-IN12. https://doi.org/10.1016/S0264-8172(96)00048-7

Brichau, S., Ring, U., Carter, A., Monié, P., Bolhar, R., Stockli, D., Brunel, M., 2007. Extensional faulting on Tinos Island, Aegean Sea, Greece: How many detachments? Tectonics 26, TC4009. https://doi.org/10.1029/2006TC001969

Buck, W.R., 1991. Modes of continental lithospheric extension. J. Geophys. Res. Solid Earth 96, 20,161-20,178. https://doi.org/10.1029/91JB01485

Cannat, M., Manatschal, G., Sauter, D., Péron-Pinvidic, G., 2009. Assessing the conditions of continental breakup at magma-poor rifted margins: What can we learn from slow spreading mid-ocean ridges? Comptes Rendus Geosci., Transition Océan-Continent 341, 406–427. https://doi.org/10.1016/j.crte.2009.01.005

Chalmers, J.A., Pulvertaft, T.C.R., 2001. Development of the continental margins of the Labrador Sea: a review. Geol. Soc. Lond. Spec. Publ. 187, 77–105. https://doi.org/10.1144/GSL.SP.2001.187.01.05

Clerc, C., Lagabrielle, Y., 2014. Thermal control on the modes of crustal thinning leading to mantle exhumation: Insights from the Cretaceous Pyrenean hot paleomargins. Tectonics 33, 2013TC003471. https://doi.org/10.1002/2013TC003471

Clerc, C., Lagabrielle, Y., Labaume, P., Ringenbach, J.-C., Vauchez, A., Nalpas, T., Bousquet, R., Ballard, J.-F., Lahfid, A., Fourcade, S., 2016. Basement – Cover decoupling and progressive exhumation of metamorphic sediments at hot rifted margin. Insights from the Northeastern Pyrenean analog. Tectonophysics 686, 82–97. https://doi.org/10.1016/j.tecto.2016.07.022

Coffin, M.F., Eldholm, O., 1994. Large igneous provinces: Crustal structure, dimensions, and external consequences. Rev. Geophys. 32, 1–36. https://doi.org/10.1029/93RG02508

Corti, G., Bonini, M., Conticelli, S., Innocenti, F., Manetti, P., Sokoutis, D., 2003. Analogue modelling of continental extension: a review focused on the relations between the patterns of deformation and the presence of magma. Earth-Sci. Rev. 63, 169–247. https://doi.org/10.1016/S0012-8252(03)00035-7

Courtillot, V., Jaupart, C., Manighetti, I., Tapponnier, P., Besse, J., 1999. On causal links between flood basalts and continental breakup. Earth Planet. Sci. Lett. 166, 177–195. https://doi.org/10.1016/S0012-821X(98)00282-9

d'Acremont, E., Leroy, S., Beslier, M.-O., Bellahsen, N., Fournier, M., Robin, C., Maia, M., Gente, P., 2005. Structure and evolution of the eastern Gulf of Aden conjugate margins from seismic reflection data. Geophys. J. Int. 160, 869–890. https://doi.org/10.1111/j.1365-246X.2005.02524.x

d'Acremont, E., Leroy, S., Maia, M., Gente, P., Autin, J., 2010. Volcanism, jump and propagation on the Sheba ridge, eastern Gulf of Aden: segmentation evolution and implications for oceanic accretion processes. Geophys. J. Int. 180, 535–551. https://doi.org/10.1111/j.1365-246X.2009.04448.x

d'Acremont, E., Leroy, S., Maia, M., Patriat, P., Beslier, M.-O., Bellahsen, N., Fournier, M., Gente, P., 2006. Structure and evolution of the eastern Gulf of Aden: insights from magnetic and gravity data (Encens-Sheba MD117 cruise). Geophys. J. Int. 165, 786–803. https://doi.org/10.1111/j.1365-246X.2006.02950.x

Direen, N.G., Stagg, H.M.J., Symonds, P.A., Colwell, J.B., 2011. Dominant symmetry of a conjugate southern Australian and East Antarctic magma-poor rifted margin segment. Geochem. Geophys. Geosystems 12, Q02006. https://doi.org/10.1029/2010GC003306

Dix, C.H., 1955. Seismic velocities from surface measurements. Geophysics 20, 68–86. https://doi.org/10.1190/1.1438126

Drewes, H., Hornik, H., Adams, J., Szabolcs, R., 2012. The International Gravimetric Bureau. In: "IAG Goedesist's handbook 2012." J. Geod., springer 86, 787–974. https://doi.org/10.1007/s00190-012-0584-1

Driscoll, N.W., Karner, G.D., 1998. Lower crustal extension across the Northern Carnarvon basin, Australia: Evidence for an eastward dipping detachment. J. Geophys. Res. Solid Earth 103, 4975–4991. https://doi.org/10.1029/97JB03295

Duval, B., Cramez, C., Jackson, M.P.A., 1992. Raft tectonics in the Kwanza Basin, Angola. Mar. Pet. Geol. 9, 389–404. https://doi.org/10.1016/0264-8172(92)90050-O

Ebinger, C.J., Casey, M., 2001. Continental breakup in magmatic provinces: An Ethiopian example. Geology 29, 527–530. https://doi.org/10.1130/0091-7613(2001)029<0527:CBIMPA>2.0.CO;2

Ellis, A.C., Kerr, H.M., Cornwell, C.P., Williams, D.O., 1996. A tectono-stratigraphic framework for Yemen and its implications for hydrocarbon potential. Pet. Geosci. 2, 29–42.

1225 Espurt, N., Callot, J.-P., Roure, F., Totterdell, J.M., Struckmeyer, H.I.M., Vially, R., 2012. Transition from
1226 symmetry to asymmetry during continental rifting: an example from the Bight Basin–Terre Adélie
1227 (Australian and Antarctic conjugate margins). Terra Nova 24, 167–180. https://doi.org/10.1111/j.1365-
1228 3121.2011.01055.x

1229 Espurt, N., Callot, J.-P., Totterdell, J., Struckmeyer, H., Vially, R., 2009. Interactions between continental
1230 breakup dynamics and large-scale delta system evolution: Insights from the Cretaceous Ceduna delta
1231 system, Bight Basin, Southern Australian margin. Tectonics 28, TC6002.
1232 https://doi.org/10.1029/2009TC002447

1233 Fantozzi, P.L., 1996. Transition from continental to oceanic rifting in the Gulf of Aden: structural evidence from
1234 field mapping in Somalia and Yemen. Tectonophysics 259, 285–311. https://doi.org/10.1016/0040-
1235 1951(95)00208-1

1236 Fantozzi, P.L., Ali-Kassim, M., 2002. Geological mapping in northeastern Somalia (Midjiurtinia region): Field
1237 evidence of the structural and paleogeographic evolution of the northern margin of the Somalian plate. J.
1238 Afr. Earth Sci., Horn of Africa 34, 21–55. https://doi.org/10.1016/S0899-5362(01)00100-2

1239 Fantozzi, P.L., Sgavetti, M., 1998. Tectonic and sedimentary evolution of the eastern Gulf of Aden continental
1240 margins: new structural and stratigraphic data from Somalia and Yemen, in: Purser, B., Bosence, D.J. (Eds.),
1241 Sedimentation and Tectonics in Rift Basins Red Sea:- Gulf of Aden. Springer Netherlands, pp. 56–76.

1242 Fort, X., Brun, J.-P., Chauvel, F., 2004. Salt tectonics on the Angolan margin, synsedimentary deformation
1243 processes. AAPG Bull. 88, 1523–1544. https://doi.org/10.1306/06010403012

1244 Fournier, M., Patriat, P., Leroy, S., 2001. Reappraisal of the Arabia-India-Somalia Triple Junction kinematics.
1245 Earth Planet Sci Lett 189, 103–114.

1246 Geoffroy, L., 2005. Volcanic passive margins. Comptes Rendus Geosci. 337, 1395–1408.
1247 https://doi.org/10.1016/j.crte.2005.10.006

1248 Geoffroy, L., Burov, E.B., Werner, P., 2015. Volcanic passive margins: another way to break up continents. Sci.
1249 Rep. 5. https://doi.org/10.1038/srep14828

1250 Gillard, M., 2015. Tectonomagmatic evolution of the final stages of rifting along the deep conjugate Australian-
1251 Antarctic magma-poor rifted margins: Constraints from seismic observations: Australian-Antarctic margins
1252 evolution. Tectonics 34. https://doi.org/10.1002/2015TC003850

1253 Gillard, M., Manatschal, G., Autin, J., 2016. How can asymmetric detachment faults generate symmetric Ocean
1254 Continent Transitions? Terra Nova 28, 27–34. https://doi.org/10.1111/ter.12183

1255 Gillard, M., Sauter, D., Tugend, J., Tomasi, S., Epin, M.-E., Manatschal, G., 2017. Birth of an oceanic spreading
1256 center at a magma-poor rift system. Sci. Rep. 7, 15072. https://doi.org/10.1038/s41598-017-15522-2

1257 Hakimi, M.H., Abdulah, W.H., Shalaby, M.R., 2010. Organic Geochemistry, Burial History and Hydrocarbon
1258 Generation Modelling of the Upper Jurassic Madbi Formation, Masila Basin, Yemen. J. Pet. Geol. 33, 299–
1259 318. https://doi.org/10.1111/j.1747-5457.2010.00481.x

1260 Hayward, N.J., Ebinger, C.J., 1996. Variations in the along-axis segmentation of the Afar Rift system. Tectonics
1261 15, 244–257. https://doi.org/10.1029/95TC02292

1262 Huchon, P., Khanbari, K., 2003. Rotation of the syn-rift stress field of the northern Gulf of Aden margin, Yemen.
1263 Tectonophysics 364, 147–166. https://doi.org/10.1016/S0040-1951(03)00056-8

1264 Hughes, G.W., Beydoun, Z.R., 1992. The Red Sea — Gulf of Aden: Biostratigraphy, Lithostratigraphy and
1265 Palaeoenvironments. J. Pet. Geol. 15, 135–156. https://doi.org/10.1111/j.1747-5457.1992.tb00959.x

1266 Jammes, S., Tiberi, C., Manatschal, G., 2010. 3D architecture of a complex transcurrent rift system: The
1267 example of the Bay of Biscay–Western Pyrenees. Tectonophysics 489, 210–226.
1268 https://doi.org/10.1016/j.tecto.2010.04.023

1269 Jarvis, A., Reuter, H.I., Nelson, A., Guevara, E., 2008. Hole-filled SRTM for the globe Version 4, available from
1270 the CGIAR-CSI SRTM 90m Database.

1271 Jestin, F., Huchon, P., Gaulier, J.M., 1994. The Somalia plate and the East African Rift System: present-day
1272 kinematics. Geophys. J. Int. 116, 637–654. https://doi.org/10.1111/j.1365-246X.1994.tb03286.x

Jolivet, L., Gorini, C., Smit, J., Leroy, S., 2015. Continental breakup and the dynamics of rifting in back-arc basins: The Gulf of Lion margin. Tectonics 34, 662–679. https://doi.org/10.1002/2014TC003570

Kane, K.E., Jackson, C.A.-L., Larsen, E., 2010. Normal fault growth and fault-related folding in a salt-influenced rift basin: South Viking Graben, offshore Norway. J. Struct. Geol. 32, 490–506. https://doi.org/10.1016/j.jsg.2010.02.005

Karner, G.D., Driscoll, N.W., McGinnis, J.P., Brumbaugh, W.D., Cameron, N.R., 1997. Tectonic significance of syn-rift sediment packages across the Gabon-Cabinda continental margin. Mar. Pet. Geol. 14, 973–1000. https://doi.org/10.1016/S0264-8172(97)00040-8

Korostelev, F., Leroy, S., Keir, D., Ahmed, A., Boschi, L., Rolandone, F., Stuart, G.W., Obrebski, M., Khanbari, K., El-Hussain, I., 2015. Upper mantle structure of the southern Arabian margin: Insights from teleseismic tomography. Geosphere 11, 1262–1278. https://doi.org/10.1130/GES01159.1

Korostelev, F., Leroy, S., Keir, D., Weemstra, C., Boschi, L., Molinari, I., Ahmed, A., Stuart, G.W., Rolandone, F., Khanbari, K., Al-Lazki, A., 2016. Magmatism at continental passive margins inferred from Ambient-Noise Phase-velocity in the Gulf of Aden. Terra Nova 28, 19–26. https://doi.org/10.1111/ter.12182

Kröner, A., Sassi, F.P., 1996. Evolution of the northern Somali basement: new constraints from zircon ages. J. Afr. Earth Sci. 22, 1–15. https://doi.org/10.1016/0899-5362(95)00121-2

Lagabrielle, Y., 2009. Mantle exhumation and lithospheric spreading: An historical perspective from investigations in the Oceans and in the Alps-Apennines ophiolites. Boll. Della Soc. Geol. Ital. 128, 279–293. https://doi.org/10.3301/IJG.2009.128.2.279

Lagabrielle, Y., Labaume, P., de Saint Blanquat, M., 2010. Mantle exhumation, crustal denudation, and gravity tectonics during Cretaceous rifting in the Pyrenean realm (SW Europe): Insights from the geological setting of the lherzolite bodies. Tectonics 29, TC4012. https://doi.org/10.1029/2009TC002588

Lavier, L.L., Manatschal, G., 2006. A mechanism to thin the continental lithosphere at magma-poor margins. Nature 440, 324–328. https://doi.org/10.1038/nature04608

Leroy, S., d'Acremont, E., Tiberi, C., Basuyau, C., Autin, J., Lucazeau, F., Sloan, H., 2010a. Recent off-axis volcanism in the eastern Gulf of Aden: Implications for plume–ridge interaction. Earth Planet. Sci. Lett., b 293, 140–153. https://doi.org/10.1016/j.epsl.2010.02.036

Leroy, S., Gente, P., Fournier, M., D'Acremont, E., Patriat, P., Beslier, M.-O., Bellahsen, N., Maia, M., Blais, A., Perrot, J., Al-Kathiri, A., Merkouriev, S., Fleury, J.-M., Ruellan, P.-Y., Lepvrier, C., Huchon, P., 2004. From rifting to spreading in the eastern Gulf of Aden: a geophysical survey of a young oceanic basin from margin to margin. Terra Nova 16, 185–192. https://doi.org/10.1111/j.1365-3121.2004.00550.x

Leroy, S., Lucazeau, F., d'Acremont, E., Watremez, L., Autin, J., Rouzo, S., Bellahsen, N., Tiberi, C., Ebinger, C., Beslier, M.-O., Perrot, J., Razin, P., Rolandone, F., Sloan, H., Stuart, G., Al-Lazki, A., Al-Toubi, K., Bache, F., Bonneville, A., Goutorbe, B., Huchon, P., Unternehr, P., Khanbari, K., 2010b. Contrasted styles of rifting in the eastern Gulf of Aden: A combined wide-angle, multichannel seismic, and heat flow survey. Geochem. Geophys. Geosystems 11, Q07004. https://doi.org/10.1029/2009GC002963

Leroy, S., Razin, P., Autin, J., Bache, F., d'Acremont, E., Watremez, L., Robinet, J., Baurion, C., Denèle, Y., Bellahsen, N., Lucazeau, F., Rolandone, F., Rouzo, S., Kiel, J.S., Robin, C., Guillocheau, F., Tiberi, C., Basuyau, C., Beslier, M.-O., Ebinger, C., Stuart, G., Ahmed, A., Khanbari, K., Al-Ganad, I., Clarens, P. de, Unternehr, P., Al-Toubi, K., Al-Lazki, A., 2012. From rifting to oceanic spreading in the Gulf of Aden: a synthesis. Arab. J. Geosci., Frontiers in Earth Sciences 5, 859–901. https://doi.org/10.1007/s12517-011-0476-3

Lister, G.S., Etheridge, M.A., Symonds, P.A., 1986. Detachment faulting and the evolution of passive continental margins. Geology 14, 246–250. https://doi.org/10.1130/0091-7613(1986)14<246:DFATEO>2.0.CO;2

Lucazeau, F., Leroy, S., Autin, J., Bonneville, A., Goutorbe, B., Watremez, L., D'Acremont, E., Düsünur, D., Rolandone, F., Huchon, P., Bellahsen, N., Tuchais, P., 2009. Post-rift volcanism and high heat-flow at the ocean-continent transition of the eastern Gulf of Aden. Terra Nova 21, 285–292. https://doi.org/10.1111/j.1365-3121.2009.00883.x

Luger, P., Gröschke, M., Bussmann, M., Dina, A., Mette, W., Uhmann, A., Kallenbach, H., 1994. Comparison of the Jurassic and Cretaceous sedimentary cycles of Somalia and Madagascar: implications for the Gondwana breakup. Geol. Rundsch. 83, 711–727. https://doi.org/10.1007/BF00251070

Masini, E., Manatschal, G., Tugend, J., Mohn, G., Flament, J.-M., 2014. The tectono-sedimentary evolution of a hyper-extended rift basin: the example of the Arzacq–Mauléon rift system (Western Pyrenees, SW France). Int. J. Earth Sci. 103, 1569–1596. https://doi.org/10.1007/s00531-014-1023-8

Menzies, M., Al-Kadasi, M., Al-Khirbash, S., A.K, A.-S., Baker, J., Blakey, S., Bosence, D., Davison, I., Dart, C., Owen, L., McClay, K.R., Nichols, G., Yelland, A., 1994. Geology of the Republic of Yemen. In: McCombe, D.A., Fernette, G.L., and Alawi, A.J. (compilers). The geological and mineral resources of Yemen. Ministry of Oil and Mineral Resources, Geology and Minerals Exploration Board,Yemen Mineral Sector Project, World Bank Technical Report.

Menzies, M., Baker, J., Bosence, D., Dart, C., Davison, I., Hurford, A., Al'Kadasi, M., McClay, K., Nichols, G., Al'Subbary, A., Yelland, A., 1992. The timing of magmatism, uplift and crustal extension: preliminary observations from Yemen. Geol. Soc. Lond. Spec. Publ. 68, 293–304. https://doi.org/10.1144/GSL.SP.1992.068.01.18

Menzies, M., Gallagher, K., Yelland, A., Hurford, A.J., 1997. Volcanic and nonvolcanic rifted margins of the Red Sea and Gulf of Aden: Crustal cooling and margin evolution in Yemen. Geochim. Cosmochim. Acta 61, 2511–2527.

Nichols, G., Watchorn, F., 1998. Climatic and geomorphic controls on rift sedimentation: Oligo-Miocene syn-rift facies in the Gulf of Aden, Yemen. Mar. Pet. Geol. 15, 505–518. https://doi.org/10.1016/S0264-8172(98)80001-9

Nonn, C., Leroy, S., Khanbari, K., Ahmed, A., 2017. Tectono-sedimentary evolution of the eastern Gulf of Aden conjugate passive margins: Narrowness and asymmetry in oblique rifting context. Tectonophysics 721, 322–348. https://doi.org/10.1016/j.tecto.2017.09.024

Péron-Pinvidic, G., Manatschal, G., Osmundsen, P.T., 2013. Structural comparison of archetypal Atlantic rifted margins: A review of observations and concepts. Mar. Pet. Geol. 43, 21–47. https://doi.org/10.1016/j.marpetgeo.2013.02.002

Péron-Pinvidic, G., Osmundsen, P.T., 2016. Architecture of the distal and outer domains of the Mid-Norwegian rifted margin: Insights from the Rån-Gjallar ridges system. Mar. Pet. Geol. 77, 280–299. https://doi.org/10.1016/j.marpetgeo.2016.06.014

Péron-Pinvidic, G., Osmundsen, P.T., Ebbing, J., 2016. Mismatch of geophysical datasets in distal rifted margin studies. Terra Nova 28, 340–347. https://doi.org/10.1111/ter.12226

Pickup, S.L.B., Whitmarsh, R.B., Fowler, C.M.R., Reston, T.J., 1996. Insight into the nature of the ocean-continent transition off West Iberia from a deep multichannel seismic reflection profile. Geology 24, 1079–1082. https://doi.org/10.1130/0091-7613(1996)024<1079:IITNOT>2.3.CO;2

Pik, R., Bellahsen, N., Leroy, S., Denèle, Y., Razin, P., Ahmed, A., Khanbari, K., 2013. Structural control of basement denudation during rifting revealed by low-temperature (U–Th–Sm)/He thermochronology of the Socotra Island basement—Southern Gulf of Aden margin. Tectonophysics, The Gulf of Aden rifted margins system : Special Issue dedicated to the YOCMAL project (Young Conjugate Margins Laboratory in the Gulf of Aden) 607, 17–31. https://doi.org/10.1016/j.tecto.2013.07.038

Planke, S., Symonds, P.A., Alvestad, E., Skogseid, J., 2000. Seismic volcanostratigraphy of large-volume basaltic extrusive complexes on rifted margins. J. Geophys. Res. Solid Earth 105, 19335–19351. https://doi.org/10.1029/1999JB900005

Platel, J.P., Roger, J., 1989. Evolution géodynamique du Dhofar (sultanat d'Oman) pendant le Crétace et le Tertiaire en relation avec l'ouverture du golfe d'Aden. Bull. Soc. Geol. Fr. V, 253–263. https://doi.org/10.2113/gssgfbull.V.2.253

Prada, M., Ranero, C.R., Sallarès, V., Zitellini, N., Grevemeyer, I., 2016. Mantle exhumation and sequence of magmatic events in the Magnaghi–Vavilov Basin (Central Tyrrhenian, Italy): New constraints from geological and geophysical observations. Tectonophysics. https://doi.org/10.1016/j.tecto.2016.01.041

Razin, P., Leroy, S., Robin, C., Robinet, J., Serra Kiel, J., Bellahsen, N., Grelaud, C., 2010. Dispositifs tecto-sédimentaires syn-rift et post-rift oligo-miocènes sur la marge sud du golfe d'Aden-Ile de Socotra (Yémen).

Redfern, P., Jones, J.A., 1995. The interior rifts of the Yemen - analysis of basin structure and stratigraphy in a regional plate tectonic context. Basin Res. 7, 337–356. https://doi.org/10.1111/j.1365-2117.1995.tb00121.x

Reston, T., Manatschal, G., 2011. Rifted margins: building blocks of later collision, in: Arc-Continent Collision, Frontiers in Earth Sciences. Springer Berlin Heidelberg, pp. 3–21. https://doi.org/10.1007/978-3-540-88558-0_1

Richardson, N.J., Underhill, J.R., Lewis, G., 2005. The role of evaporite mobility in modifying subsidence patterns during normal fault growth and linkage, Halten Terrace, Mid-Norway. Basin Res. 17, 203–223. https://doi.org/10.1111/j.1365-2117.2005.00250.x

Robinet, J., Razin, P., Serra-Kiel, J., Gallardo-Garcia, A., Leroy, S., Roger, J., Grelaud, C., 2013. The Paleogene pre-rift to syn-rift succession in the Dhofar margin (northeastern Gulf of Aden): Stratigraphy and depositional environments. Tectonophysics, The Gulf of Aden rifted margins system : Special Issue dedicated to the YOCMAL project (Young Conjugate Margins Laboratory in the Gulf of Aden) 607, 1–16. https://doi.org/10.1016/j.tecto.2013.04.017

Roger, J., Platel, J.P., Cavelier, C., Bourdillon-de-Grissac, C., 1989. Donnees nouvelles sur la stratigraphie et l'histoire geologique du Dhofar (sultanat d'Oman). Bull. Soc. Geol. Fr. V, 265–277. https://doi.org/10.2113/gssgfbull.V.2.265

Rosenbaum, G., Weinberg, R.F., Regenauer-Lieb, K., 2008. The geodynamics of lithospheric extension. Tectonophysics, Geodynamics of Lithospheric Extension 458, 1–8. https://doi.org/10.1016/j.tecto.2008.07.016

Sauter, D., Cannat, M., Rouméjon, S., Andreani, M., Birot, D., Bronner, A., Brunelli, D., Carlut, J., Delacour, A., Guyader, V., MacLeod, C.J., Manatschal, G., Mendel, V., Ménez, B., Pasini, V., Ruellan, E., Searle, R., 2013. Continuous exhumation of mantle-derived rocks at the Southwest Indian Ridge for 11 million years. Nat. Geosci. 6, 314–320. https://doi.org/10.1038/ngeo1771

Sengör, A.M.C., Burke, K., 1978. Relative timing of rifting and volcanism on Earth and its tectonic implications. Geophys. Res. Lett. 5, 419–421. https://doi.org/10.1029/GL005i006p00419

Shillington, D.J., Holbrook, W.S., Van Avendonk, H.J.A., Tucholke, B.E., Hopper, J.R., Louden, K.E., Larsen, H.C., Nunes, G.T., 2006. Evidence for asymmetric nonvolcanic rifting and slow incipient oceanic accretion from seismic reflection data on the Newfoundland margin. J. Geophys. Res. Solid Earth 111, B09402. https://doi.org/10.1029/2005JB003981

Stab, M., Bellahsen, N., Pik, R., Quidelleur, X., Ayalew, D., Leroy, S., 2016. Modes of rifting in magma-rich settings: Tectono-magmatic evolution of Central Afar. Tectonics 2015TC003893. https://doi.org/10.1002/2015TC003893

Tard, F., Masse, P., Walgenwitz, F., Gruneisen, P., 1991. The volcanic passive margin in the vicinity of Aden, Yemen. Bull. Cent. Rech. Explor.-Prod. Elf Aquitaine 15, 1–9.

Tari, G., Molnar, J., Ashton, P., Hedley, R., 2000. Salt tectonics in the Atlantic margin of Morocco. Lead. Edge 19, 1074–1078. https://doi.org/10.1190/1.1438481

Teixell, A., Labaume, P., Lagabrielle, Y., 2016. The crustal evolution of the west-central Pyrenees revisited: Inferences from a new kinematic scenario. Comptes Rendus Geosci., From rifting to mountain building: the Pyrenean Belt 348, 257–267. https://doi.org/10.1016/j.crte.2015.10.010

Tucholke, B.E., Sawyer, D.S., Sibuet, J.-C., 2007. Breakup of the Newfoundland Iberia rift. Geol. Soc. Lond. Spec. Publ. 282, 9–46. https://doi.org/10.1144/SP282.2

Tugend, J., Manatschal, G., Kusznir, N.J., Masini, E., Mohn, G., Thinon, I., 2014. Formation and deformation of hyperextended rift systems: Insights from rift domain mapping in the Bay of Biscay-Pyrenees. Tectonics 33, 2014TC003529. https://doi.org/10.1002/2014TC003529

Vendeville, B.C., Ge, H., Jackson, M.P.A., 1995. Scale models of salt tectonics during basement-involved extension. Pet. Geosci. 1, 179–183. https://doi.org/10.1144/petgeo.1.2.179

1417 Warden, A.J., Horkel, A.D., 1984. The geological evolution of the NE-branch of the Mozambique Belt (Kenya,
1418 Somalia, Ethiopia). Mitteilungen Osterreichischen Geol. Ges. 77, 161–184.

1419 Watchorn, F., Nichols, G.J., Bosence, D. W. J., 1998. Rift-related sedimentation and stratigraphy, southern
1420 Yemen (Gulf of Aden), in: Purser, B.H., Bosence, Dan W. J. (Eds.), Sedimentation and Tectonics in Rift Basins
1421 Red Sea:- Gulf of Aden. Springer Netherlands, pp. 165–189.

1422 Watremez, L., Leroy, S., Rouzo, S., d'Acremont, E., Unternehr, P., Ebinger, C., Lucazeau, F., Al-Lazki, A., 2011.
1423 The crustal structure of the north-eastern Gulf of Aden continental margin: insights from wide-angle seismic
1424 data. Geophys. J. Int. 184, 575–594. https://doi.org/10.1111/j.1365-246X.2010.04881.x

1425 White, R., McKenzie, D., 1989. Magmatism at rift zones: The generation of volcanic continental margins and
1426 flood basalts. J. Geophys. Res. Solid Earth 94, 7685–7729. https://doi.org/10.1029/JB094iB06p07685

1427 Whitmarsh, R.B., Manatschal, G., Minshull, T.A., 2001. Evolution of magma-poor continental margins from
1428 rifting to seafloor spreading. Nature 413, 150–154. https://doi.org/10.1038/35093085

1429 Ziegler, M.A., 2001. Late Permian to Holocene Paleofacies Evolution of the Arabian Plate and its Hydrocarbon
1430 Occurrences, in: GeoArabia. GulfPetroLink, pp. 445–504.

1431

# Central Gulf of Aden conjugate margins (Yemen-Somalia): tectono-sedimentary and magmatism evolution in hybrid-type margins

Chloé NONN [1], Sylvie LEROY [1], Marc LESCANNE [2], Raymi CASTILLA[2]

*1* - Sorbonne Université, CNRS-INSU, Institut des Sciences de la Terre Paris, ISTeP UMR 7193, F-75005 Paris, France.

*2 - Total, CSTJF, Research & Development, Av Larribau Pau, France.*

Magma-rich and magma-poor passive margins are generally studied separately. Yet, the spatial evolution from one type to another is not well understood. Central Gulf of Aden margins are at the transition between these two types of margins. Based on new seismic data, published wells and gravity data, we determine seismic stratigraphy and structural patterns. We map the distinct crustal domains (continental, Ocean-Continent Transition (OCT), oceanic domains) and propose a tectonic evolution of the Yemeni and Somalian conjugate margins in an oblique rifting context. The most striking results are the significant segmentation, narrowness and asymmetry of conjugate margins, as well as the gradual eastward decrease in the intensity of magmatic activity of these hybrid-type margins. West of Bosaso-Hami Fracture Zone (BHFZ), the Hami-Ahl Medo segment presents magmatic-type margin features in the distal Yemeni margin related to the strong influence from the Afar plume: Seaward dipping reflectors develop since the late syn-rift stage (~21 - 18 Ma) near the Xiis-Al Mukalla Fracture Zone. Conversely, east of BHFZ, the Bosaso-Sayhut margins segment is characterized by magma-poor margins for which the exhumation stage is characterized by the unroofing of mantle along multiple detachment faults in the OCT and shortly followed by diachronous volcanism (~18 Ma). The central Gulf of Aden is affected by a major uplift during the final syn-rift stage and up to OCT formation. This event is associated with the formation of erosional surfaces in the east and with gravitational deformation taking place on decoupling surfaces at the base of the syn-rift sequence (lower Ghaydah Fm) that lead to the sliding of syn-rift units on top of the exhumed mantle rocks in the OCT.

***Key words:*** *hybrid margins, Gulf of Aden, crustal domains, tectono-stratigraphic evolution, asymmetry, magmatism.*

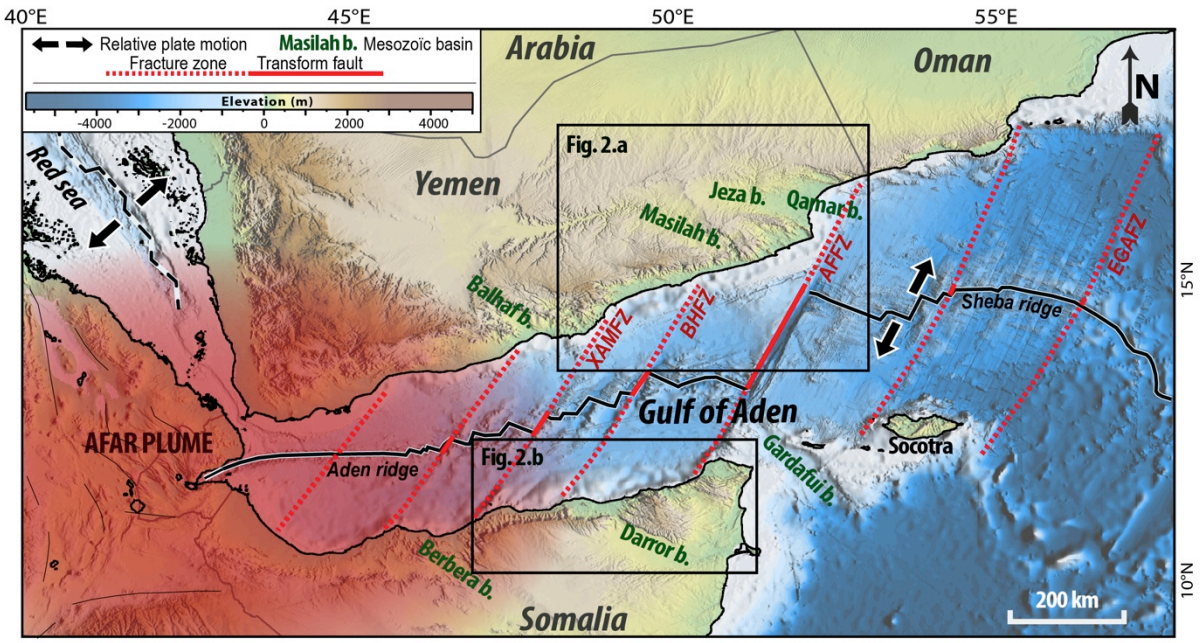


*Figure 1- Topographic and bathymetric map of the Gulf of Aden (modified from Nonn et al., 2017) showing the first-order fracture zones. Black arrows represent the relative plate motion; the studied area is framed in black in the central Gulf of Aden, between the Xiis Al Mukalla Fracture Zone (XAMFZ) and the Alula Fartak Fracture Zone (AFFZ). The Mesozoic basins correspond to: (i) the Balhaf, the Masilah, the Jeza and the Qamar basins (b.) in Yemen; (ii) the Berbera, the Darror and the Gardafui basins (b.) in Somalia. BHFZ: Bosaso-Hami Fracture Zone. EGAFZ: Eastern Gulf of Aden Fracture Zone.*

## 1. Introduction

To improve our understanding of how the deformation localized in distal part of the margins, towards the future area of lithospheric breakup, we need to better figure out the actual architecture of crustal domains in present-day passive margins. Despite of variable tectonic and magmatic processes involved during their formation, magma-poor and magma-rich rifted margins present major crustal domains displaying structural similarities at first-order (Péron-Pinvidic et al., 2013). The continental domain is characterized by unequivocal continental crust that is progressively thinned in distal parts of the margins. The Ocean-Continent Transition (OCT) corresponds to the gradual transition from the thinned continental domain to the stable oceanic crust. The rifting process is driven by lithospheric mantle dynamic until the OCT formation (Lagabrielle, 2009; Jolivet et al., 2015; Péron-Pinvidic and Osmundsen, 2016). Subsequently, the formation of steady-state oceanic crust is driven by asthenospheric mantle dynamic. The geological and geophysical attributes of the OCT contrast from one margin to another, as does the amount of volcanic supply (Péron-Pinvidic and Osmundsen, 2016; Stab et al., 2016).

During and after rifting, magmatism is an essential process in the formation of continental passive margins. The question of whether conjugate passives margins are magma-poor or magma-rich, and the along strike variation from one to another, are significant issues for the understanding of rift systems with lateral

52 changes in thermal state. The distinction between margins that are magma-rich (related to large volumes of
53 magma) or magma-poor (related to lithospheric detachment faulting) is based on the timing and degree of
54 mantle melting associated with lithospheric thinning as well as with crustal and lithospheric break-up (White
55 and McKenzie, 1989; Coffin and Eldholm, 1994; Courtillot et al., 1999; Geoffroy et al., 2015). However, the
56 occurrence of hybrid margins, for which the volume of volcanic products varies along strike from magma-poor
57 to magma-rich settings (Reston and Manatschal, 2011), show that these definitions are still ambiguous. In any
58 case, significant and localized magma supply can contribute to focusing the extension (e.g. Buck, 1991; Ebinger
59 and Casey, 2001; Péron-Pinvidic et al., 2013), while diffuse volcanic supply can lead to a wider distribution of
60 the extensional stress (Corti et al., 2003).
61 In the present study, we focus on the type of stratigraphic, structural and magmatic architectures that
62 can develop on a hybrid continental margin. We focus on the central Gulf of Aden located between the Xiis-Al
63 Mukalla (XAMFZ) and Alula Fartak (AFFZ) Fracture Zones (area Framed in black, Fig. 1). In this oceanic basin, the
64 Somalia-Yemen conjugate margins were formed by a polyphase and oblique divergence of the Arabian and
65 African plates during the Mesozoic and Cenozoic. The little-known studied area is located between magma-rich
66 margins in the western part (influenced by the Afar plume; Tard et al., 1991; Beydoun et al., 1998; Leroy et al.,
67 2012; Stab et al., 2016) and magma-poor margins in the eastern part (Leroy et al., 2004, 2012, d'Acremont et
68 al., 2005, 2006; Autin et al., 2010b; Watremez et al., 2011; Nonn et al., 2017). The aim of this paper is to
69 explore the Cenozoic syn- to post-rift tectonic history of the central Gulf of Aden conjugate margins. Based on
70 interpretations of a dense grid of seismic profiles combined with wells, bathymetric, gravimetric data, we
71 correlate the onshore and offshore stratigraphy; we map the structures and the crustal domains in order to
72 correlate the conjugate margin and constrain their spatial evolution. We attempt to address questions on the
73 nature of the seismic basement in various crustal domains and on the relationships between the tectono-
74 stratigraphic and magmatic evolution of the conjugate margins in an area of along strike transition from
75 volcanic to non-volcanic margins. The mapping of crustal domains shows the narrowness and the asymmetrical
76 style of these hybrid-type margins. The observation of the sedimentary sequences reveals the activity of
77 decoupling surface at the base of the syn-rift sequence from the late syn-rift period to the syn-OCT period. We
78 observed that the period of formation of the OCT is marked by a phase of significant uplift of the whole
79 margins also recorded by significant erosion in the central Gulf of Aden distal margins.
80
81 **2. Geological setting**

### 2.1 Kinematic context

The continental rifting of Gulf of Aden started 34 Ma ago between the Arabian and Somalian plates (Figs. 1, 2) with a direction of extension (N20°E) oblique to the trend of the rift (N70°E) (Roger et al., 1989; Watchorn et al., 1998; Leroy et al., 2012; Pik et al., 2013; Robinet et al., 2013). The obliquity led to a significant segmentation characterized by various fault sets including several major fracture zones parallel to the divergence such as the XAMFZ, the AFFZ and the Bosaso Hami Fracture Zone (BHFZ) (in grey, Figs. 1, 2). None inherited zones of weakness trending ~N70°E parallel to the Gulf is reactivated (Autin et al., 2010a, 2013; Bellahsen et al., 2013a). Oceanic seafloor spreading started during the Burdigalian at ~17 Ma in the Gulf of Aden (e.g. Leroy et al., 2004; d'Acremont et al., 2006, 2010; Leroy et al., 2010; Nonn et al., 2017). The oceanic spreading rate increases from the west (13 mm yr-1 along N35°E) towards the eastern Sheba-Ridge (18 mm yr-1 along N25°E, Jestin et al., 1994; Fournier et al., 2001) (Fig. 2). Extension resulted in magma-rich margins in the western part near the Afar plume (Tard et al., 1991; Beydoun et al., 1998; Leroy et al., 2012; Stab et al., 2016) and magma-poor margins in the eastern Gulf of Aden, leading to mantle exhumation from the AFFZ to the EGAFZ (Leroy et al., 2004, 2010a; d'Acremont et al., 2005, 2006; Autin et al., 2010b; Watremez et al., 2011; Leroy et al., 2012; Nonn et al., 2017) (Fig. 1).

### 2.2 Structural framework onland and crustal thickness

In the central Gulf of Aden, significant outcrops of Cenozoic pre-rift units (in orange, Figs. 2, 3.a) occur in series of grabens and horsts on the conjugate margins. On the Yemeni margin, the EW to N110°E-trending Masilah basin is bounded to the southwest by the Mukalla High, to the northeast by the Fartak High and to the north by the Hadramaut Arch (Fig. 2.a). Along the coastline, the Hami graben is limited to the north by the highest relief of the Yemeni margin that reaches an elevation of ~2000 m and trends EW (Lat. 15°N, Long. 50°E, Fig. 2.a). Basins, plateaus and mountains also form the morphology of the onshore Somalian margin (Fig. 2.b). In the western part, the EW trending Ahl Medo High (2000 m of elevation) borders the Ahl Medo and Bosaso basins (Lat. 11°10'N, Long. 49°E, Fig. 2.b). In the eastern part, the Ahl Miskat and the Ahl Bari highs border the major WNW-ESE Darror (10°30'N, 49°30'E, Fig. 2.b), the Qandala El Gal and Alula basins (Lat. 11°25'N, Long. 50°10'E and Lat. 11°50'N, Long. 50°50'E, Fig. 2.b).

On the onshore conjugate margins, the continental crust is thinned of ~30-50% towards the ocean (Fig. 2): Moho depths range from 20 km near the coastline to 35 km at a distance of ~75 km from the coastline to 42 km in the outer parts of the rift system (Ali and Watts, 2013; Korostelev et al., 2016).

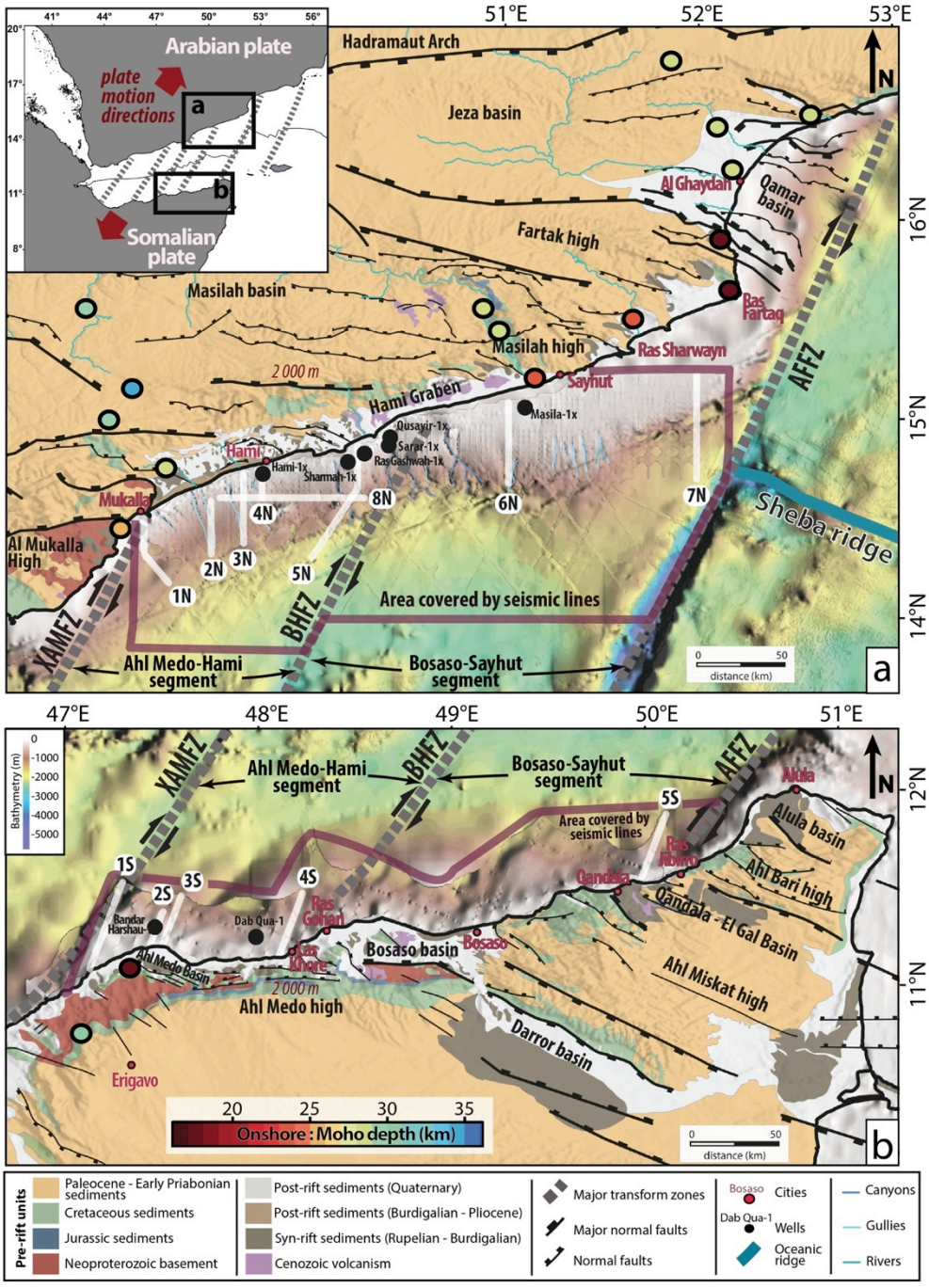


***Figure 2*** *- Simplified geological map of the Central Gulf of Aden conjugate margins (Ellis et al., 1996; Birse et al., 1997; Beydoun, 1970; Bott et al., 1992; Bosence, 1997; Brannan et al., 1997; Fantozzi and Sgavetti, 1998; Nichols and Watchorn, 1998; Watchorn et al., 1998; Fantozzi and Ali-Kassim, 2002; Leroy et al., 2012; Ali, 2015) (location on Figure 1) showing bathymetry from GEBCO 30 arc-second global grid (2014) and interpretation of seismic data, with topographic map in background, for the northern (a) and southern (b) margins. The offshore areas covered by seismic profiles are surrounded by the dark purple lines and the conjugate coastlines (represented in black). The colour coding of the geological map is the same as on Figure 3: in red, the Neoproterozoic crystalline basement (metamorphic and igneous rocks (e.g. Menzies et al., 1992, 1994, 1997; Redfern and Jones, 1995) crops out with a global EW structural trend (e.g. Fantozzi and Ali-Kassim, 2002) near the Mukalla High in Yemen (Bosence et al., 1996; Watchorn et al., 1998), near Erigavo and Bosaso cities in Somalia (Warden and Horkel, 1984; Kröner and Sassi, 1996). In blue, Jurassic basement; in green, Cretaceous basement; in light orange, Cenozoic pre-rift units (Palaeocene – Eocene); in dark brown, syn- rift units (Priabonian – Burdigalian); in light brown, post-rift units (Burdigalian – Pliocene); in white, Quaternary units; in violet, Oligo-Miocene volcanic formations. Colourful circles: Onshore crustal thicknesses (a) from receiver function analysis (Korostelev et al., 2016) and (b) derived from gravity and flexure modelling (Ali and Watts, 2013). The hydrological network is inferred from sea bottom observations. The location of wells is derived from Ahlbrandt (2002), Ali and Watts (2013) and Bott et al. (1992) and other references therein. Top-left inset: simplified regional map indicating the relative motions of the Arabian and Somalian plates (red arrows), the fracture zones (in dashed grey) and the location of Figures a and b. AFFZ: Alula Fartak Fracture Zone. XAMFZ: Xiis Al Mukalla Fracture Zone. BHFZ: Bosaso Hami Fracture Zone.*

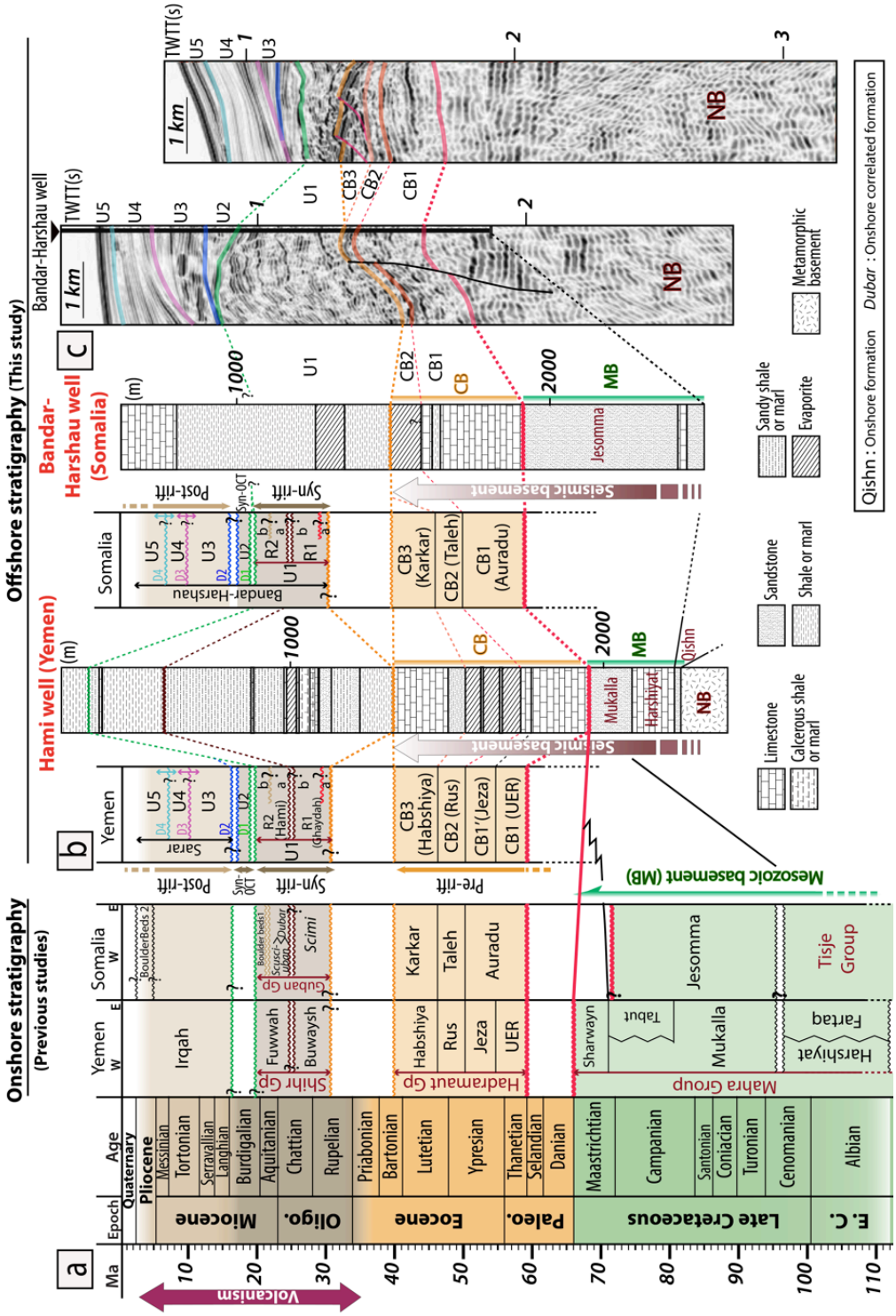


*Figure 3 - Synthesis of onshore stratigraphy and correlation with various units proposed for the stratigraphy of offshore profiles. (a) Synthesis of onland stratigraphy of the central Gulf of Aden conjugate margins taking into account the spatial distribution (Azzaroli, 1958; Menzies et al., 1992, 1997; Ali Kassim, 1991; Bott et al., 1992; Redfern and Jones, 1995; Kröner and Sassi, 1996; Bosence et al., 1996; Beydoun et al., 1996, 1998; Beydoun, 1997; Bosence, 1997; Fantozzi and Sgavetti, 1998; Fantozzi and Ali-Kassim, 2002; Nichols and Watchorn, 1998; Watchorn et al., 1998; Ahlbrandt, 2002; Bosworth et al., 2005; Hakimi et al., 2010; Ali and Watts, 2013; Ali, 2015) (b) Summary of different units in Yemen and Somalia suggested as correlating with the offshore stratigraphy. Correlation with Hami well (Yemen) (Bott et al., 1992) and Bandar-Harshau well (Somalia) (Ali, 2015; Bott et al., 1992). (c) Correlation with segment of seismic line in Somalia published by (Ali and Watts, 2013; Ali, 2015) showing the seismic facies and various units mentioned here. The working correlation is based on well data, seismic facies, sediment geometries and location of sedimentary units in the stratigraphic column in accordance with the tectono-sedimentary evolution of the Gulf of Aden. See text for explanation. CB: Cenozoic basement. Gp: Group. MB: Mesozoic basement. NB: Neoproterozoic basement. UER: Umm Er Radhuma.*

### 2.3 Tectono-stratigraphic record: previous works in the central Gulf of Aden

Previous field works and well studies show the relationships between the sedimentary record and tectonic events of the central segment of the Gulf of Aden, along the conjugate margins bordering Yemen (e.g. Brannan et al., 1997; Huchon and Khanbari, 2003) and Somalia (e.g. Fantozzi and Ali-Kassim, 2002; Ali and Watts, 2016) (Fig. 3). Note that the terms 'pre-rift', 'syn-rift', and 'post-rift' are used here with respect to the Oligo-Miocene rifting of the Gulf of Aden. In this work, the Mesozoic series are included in the pre-rift sequence.

#### *2.3.1 Pre-rift sequence: Mesozoic and Cenozoic sequences*

The Cenozoic pre-rift succession, which is widely exposed in the central Gulf of Aden segment (Fig. 2), lies unconformably on the Mesozoic basement. Its eastward thickening expresses the eastward increase of subsidence (Beydoun, 1970, 1997; Brannan et al., 1997; Ali and Watts, 2013). In Yemen, the Hadramaut Group represents the Palaeocene to Eocene sequence and is composed of the Umm Er Radhuma (UER), Jeza, Rus and Habshiya Fms (in orange, Figs. 2, 3.a, b) (Beydoun, 1997; Bosence, 1997; Brannan et al., 1997; Watchorn et al., 1998).

A first major transgression is recorded by the shallow marine reefal carbonates of the UER (Thanetian – Ypresian) and marly carbonates of the Jeza Fms (Ypresian) in Yemen (Beydoun et al., 1998) correlated to the limestone of the Auradu Fm (Thanetian – Ypresian) in Somalia (Figs. 3.a, b) (Beydoun, 1970; Fantozzi and Ali-Kassim, 2002). A second period of regression (middle Ypresian – early Lutetian) is associated with the evaporites of the Rus Fm in Yemen and Taleh Fm in Somalia (Beydoun, 1970; Brannan et al., 1997; Beydoun et al., 1998) (Figs. 3.a, b). The latest transgression (Lutetian) led to the accumulation of the Habshiya Fm in Yemen and Karkar Fm in Somalia (Figs. 3.a, b), which are made up of shallow marine reefal carbonates (Beydoun, 1970; Fantozzi and Ali-Kassim, 2002). The Eocene is characterized by a major uplift of the conjugate margins recorded by broad erosion at the top of the carbonates of the Habshiya and Karkar Fms (Brannan et al., 1997; Leroy et al., 2012) (Figs. 3.a, b).

#### *2.3.2 Syn-rift sequence*

On the northern margin, the onshore syn-rift succession (Shihr Group, Upper-Priabonian – Burdigalian, Fig. 3.a) (Watchorn et al., 1998; Beydoun et al., 1998; Ahlbrandt, 2002) crops out along the coast to the East of Al Mukalla city (Fig. 2). On the southern margin, the syn-rift sequence (Guban Group and lower Bandar-Harshau

193 Fms, Fig. 3.a) (Azzaroli, 1958; Fantozzi and Ali-Kassim, 2002) is restricted to the Darror basin and along the
194 coastline east of Qandala city (Lat. 11°N, Long. 49°E, Fig. 2).

195 During the Oligocene, the rifting is characterized by a phase of tectonic subsidence as shown by a
196 transition from clastic to carbonate deposits on the conjugate margins. In onshore Yemen, the Buwaysh Fm is
197 composed of alternating shales, sandstones, conglomerates and anhydrites (Beydoun et al., 1998; Ahlbrandt,
198 2002) (Fig. 3.a). Offshore Yemen, the Ghaydah Fm (Rupelian – Early Chattian) is characterized by sandstones
199 and conglomerates in the lower part and anhydrites and marls in the upper part (Fig. 3. b); this unit is more
200 evaporitic towards the west and mainly carbonate-bearing towards the east (Beydoun, 1970; Bott et al., 1992;
201 Bosence et al., 1996; Beydoun et al., 1998; Watchorn et al., 1998). In Somalia, the base of the syn-rift sequence
202 seen onshore is composed of sandstones and conglomerates correlated with the Scimi Fm (e.g. Fantozzi and
203 Ali-Kassim, 2002; Bosworth et al., 2005; Ali and Watts, 2016) (Fig. 3.a). Offshore Somalia, the lower part of
204 Bandar-Harshau Fm comprises anhydrites and shales recorded in the Bandar-Harshau-1 (Bott et al., 1992; Ali
205 and Watts, 2013) (Fig. 3.b).

206 During the Chattian – Burdigalian, rifting intensified and is associated with the development of major
207 faults (Leroy et al., 2012). Onshore Yemen, carbonate marls and conglomerates form the base and a carbonate
208 platform forms the top of the Fuwwah Fm (Beydoun et al., 1998; Ahlbrandt, 2002) (Fig. 3.a). Offshore Yemen,
209 this sequence is equivalent to the Hami Fm defined by alternations of carbonate marls and sandstones passing
210 up into limestones (Beydoun, 1970; Bott et al., 1992; Bosence et al., 1996; Beydoun et al., 1998; Watchorn et
211 al., 1998) (Fig. 3.b). The onshore Somalia succession corresponds to reefal carbonates (correlated with the
212 Dubar Fm) which passes laterally into lagoon and fluvial facies (correlated with the Scusciuban Fm) (Azzaroli,
213 1958; Ali Kassim, 1991; Bott et al., 1992; Fantozzi and Sgavetti, 1998; Fantozzi and Ali-Kassim, 2002; Bosworth
214 et al., 2005; Ali and Watts, 2016) (Fig. 3.a). Offshore Somalia, the Bandar-Harshau Fm corresponds to deep-
215 marine deposits (Hughes and Beydoun, 1992) (Figs. 3.b, c).

216

217 *2.3.3 Syn-OCT development sequence*

218 The end of rifting is characterized by a regional uplift and late-stage tilting of the conjugate margins (Leroy et
219 al., 2012). On the Somalian margin, the upper part of the syn-rift sequence displays regressive facies overlain
220 by syn-tectonic conglomeratic deposits of the Boulder beds 1 Fm (Fig. 3.a) near the coast of Somalia with
221 alluvial fan deposits along normal faults (Fantozzi and Ali-Kassim, 2002).

222

223 *2.3.4 Post-rift sequence*

224 On the emerged Yemen margin, the middle Miocene-Pliocene post-rift sequence (Beydoun et al., 1998)
225 unconformably overlies the Shihr Group (Fig. 3) and is composed of marine sandstones, conglomerates and
226 siltstones of the Irqah Fm (Bosence et al., 1996; Nichols and Watchorn, 1998; As-Saruri et al., 2010). However,
227 this unit is restricted to the coastline and is poorly documented onshore (Fig. 2.a). The post-rift sequence
228 records at least three uplift pulses (Watchorn et al., 1998). Offshore Yemen, the Sarar Fm (Figs. 2.a, 3.a)
229 consists of various lithologies including turbidite sands, shales and marls (Bott et al., 1992). On the emerged
230 Somalian margin, the post-rift sequence is recorded on the coastline and in the Darror basin (Figs. 2.b, 3). It is
231 composed of a conglomeratic unit, named Boulder beds 2 Fm, dated as probably Pliocene (Fantozzi and Ali-
232 Kassim, 2002) (Fig. 3.b). Offshore Somalia, the upper part of the Bandar-Harshau Fm (Figs. 2, 3.b, c) is
233 characterized by shale, carbonates and evaporites observed in the Dab-Qua-1 and Bandar-Harshau-1 wells
234 (Bott et al., 1992; Ali and Watts, 2013). Plio-Quaternary volcanic formations dated from ~3 - 6 Ma to present,
235 are recorded in the Hami graben (Yemeni, Fig. 2.a), in the Bosaso and the Qandala basins (Somalia, Fig. 2.b) and
236 are located in the prolongation of the BHFZ and AFFZ (Bott et al., 1992; Fantozzi and Sgavetti, 1998; Watchorn
237 et al., 1998; Leroy et al., 2010b).
238
239 **3. Data of the central Gulf of Aden conjugate margins**

240 This study is based on investigations of oil industry data including deep reflection seismic surveys and
241 published information on wells (Bott et al., 1992; Ahlbrandt, 2002; Ali and Watts, 2013; Ali, 2015) (Fig. 2). This
242 analysis benefits from access to a large number of seismic reflection profiles across and along the conjugate
243 central margins of the Gulf of Aden (see area covered by seismic profiles, Fig. 2). The offshore seismic data
244 were acquired during a large-scale and dense seismic survey carried out in the 1980s. Unfortunately, we are
245 not able to show the seismic profiles. Further control on this interpretation is obtained through well data (Figs.
246 3.b, c, 4) and field observations of onshore stratigraphy derived from literature (Bott et al., 1992; Fantozzi,
247 1996; Bosence et al., 1996; Beydoun et al., 1996; Beydoun, 1997; Beydoun et al., 1998; Watchorn et al., 1998;
248 Fantozzi and Sgavetti, 1998; Nichols and Watchorn, 1998; Fantozzi and Ali-Kassim, 2002; Bosworth et al., 2005;
249 Ali and Watts, 2013; Ali, 2015). The depth to basement and thickness maps are compiled from interpretations
250 of all densely spaced seismic data available in the area. The Sismage® software was used to perform grids
251 obtained by interpolating interpreted horizons with a spacing of 10 to 15 km. The depth conversions for the
252 maps and seismic interpretations are carried out according to estimated P-waves velocities from processing

253 stack velocities (Dix formula; Dix, 1955) (1500 m.s-1 for the water and surface sediments, 1800 to 2200 m.s-1
254 for post-rift and syn-OCT units, 2500 m.s-1 for the syn-rift sequence, 5500 m.s-1 for the continental basement,
255 6500 m.s-1 for the transitional basement and 7000 m.s-1 for the whole oceanic crust).
256
257 **4. Results from seismic stratigraphy and crustal domains mapping of the central Gulf of Aden conjugate**
258 **margins**
259 For both the northern and southern margins of the central Gulf of Aden segment, we describe the offshore
260 seismic stratigraphy using the seismic units and major discontinuities based on a compilation of seismic and
261 well data (Figs. 3, 4) correlated with the offshore and previous onshore geological studies (e.g. Bott et al., 1992;
262 Fantozzi and Ali-Kassim, 2002; Bosworth et al., 2005). We summarize the seismic units patterns (boundaries,
263 geometries, continuity, amplitude, frequency and ages), and the onshore-offshore correlations in Figure 3 and
264 Table 1. In a second section, we describe the major features of acoustic basement morphology of offshore
265 conjugate margins thanks to the depth to basement maps (Figs. 5.a, b).
266
267 **4.1 Seismic stratigraphy**
268 *4.1.1 Pre-rift sequence*
269 At the top of the tilted blocks in the continental domains, we identify three main sequences (Figs. 2, 3, 4; Tab.
270 1): the Neoproterozoic crystalline basement, the Mesozoic basement and the Cenozoic basement (CB1 to CB3).
271 In the Cenozoic basement, the CB1 subunit can be correlated to carbonates of the Umm Er Radhuma and Jeza
272 Fms on the Yemeni margin and to the Auradu Fm on the Somalian margin using the well data (Figs. 3.c, d).
273 Wells data show that CB2 corresponds to the evaporitic Rus Fm on the northern margin and the Taleh Fm on
274 the southern margin (Fig. 3). CB3 is composed of double reflectors that are very remarkable, deposited
275 unconformably above the eroded CB2 subunit (Fig. 3.c; Tab. 1), and locally cut by small-offset normal faults
276 that are rooted at a common decollement layer on CB2 (Right segment of seismic line, Fig. 3.c). According to
277 the wells considered, CB3 corresponds to the carbonates of the Habshiya and the Karkar Fms in offshore
278 Yemen and Somalia, respectively (Figs. 3.b, c, 4.a).

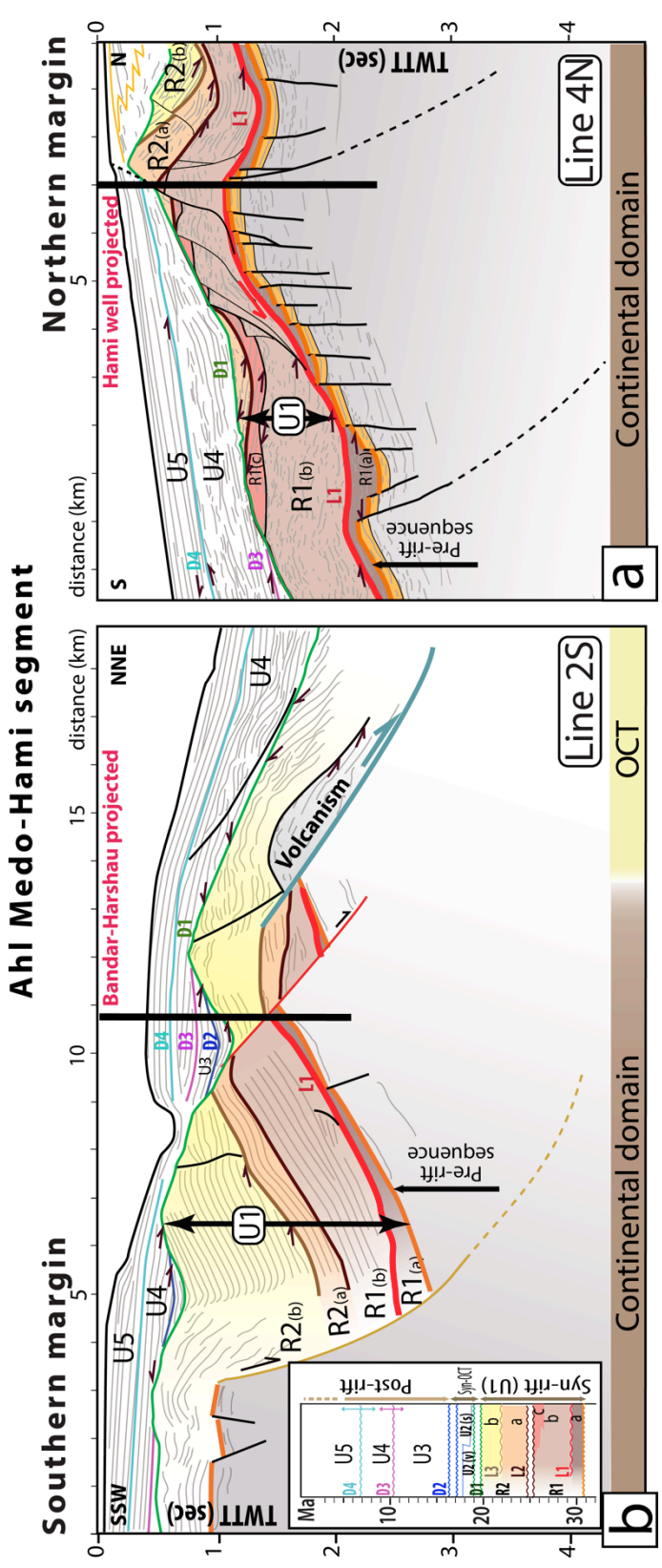


***Figure 4*** *- Interpreted line drawing of (a) the northern part of the seismic line 5N in the northern margin (Location on Figure 2.a) (b) the seismic line 2S in the southern margin (in the Ahl Medo-Hami segment) with the different sedimentary sequences identified on the seismic profiles in the continental domain and Ocean-Continent Transition (OCT) (vertical exaggeration ~1.8) and the projected Hami well and Bandar-Harshau well. The pre-rift sequence (CB1-2 and the Mesozoic basement) and the upper crust are represented in grey and the top of the pre-rift sequence is represented in orange (CB3).*

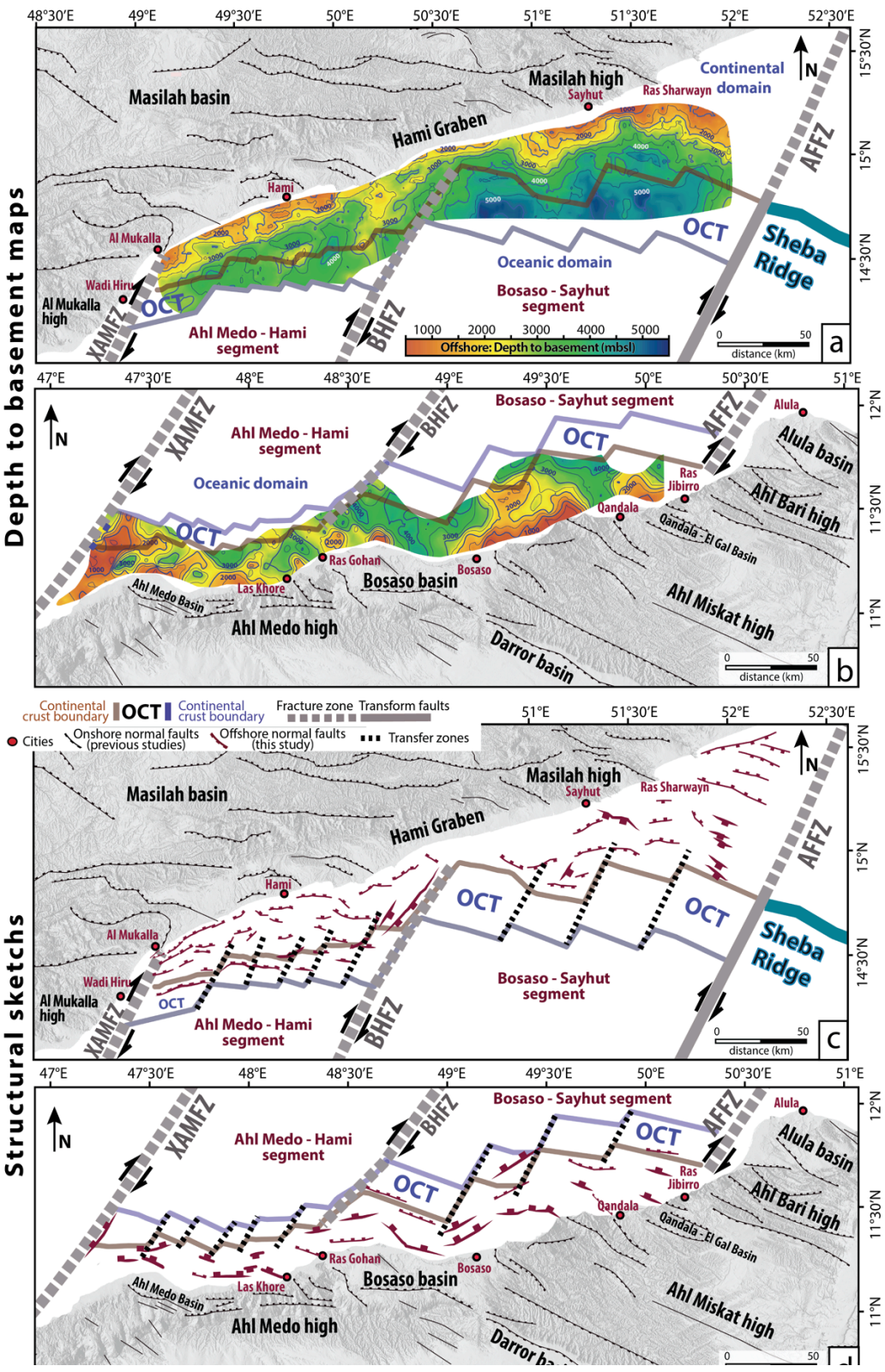


***Figure 5*** *– Upper panels: Depth to seismic basement maps of (a) the Yemeni and (b) Somalian margins established from seismic reflection data. Onshore first-order structures (after Beydoun, 1970; Bott et al., 1992; Bosence, 1997; Brannan et al., 1997; Fantozzi and Sgavetti, 1998; Nichols and Watchorn, 1998; Watchorn et al., 1998; Fantozzi and Ali-Kassim, 2002; Leroy et al., 2012; Ali, 2015) and other references therein. Lower panels: Structural sketches of the northern (c) and southern (d) margins with different crustal domains and major structures that affect the continental and transitional seismic basements. Thicker lines represent major faults. Note that structures are drawn at the foot of the faults. OCT: Ocean-Continent Transition. AFFZ: Alula Fartak Fracture Zone. BHFZ: Bosaso Hami Fracture Zone. XAMFZ: Xiis Al Mukalla Fracture Zone. Shaded topography is shown onshore (SRTM, Jarvis et al., 2008).*

| Seismic units | Reflection characteristics | | | | | Ages |
|---|---|---|---|---|---|---|
| | Boundaries | Geometry | Continuity | Amplitude | Frequency | |
| **Post-rift units (U3 to U5)** | | | | | | |
| **U5** | Top: toplaps, erosional truncations at the seafloor<br>Base: onlaps on D4 | Draping, parallel, locally prograding | Continuous | Low to middle | High | ~7 Ma |
| **U4** | Top: toplaps, truncations on D4 (channels)<br>Base: onlaps on D3 | Parallel, prograding, hummocky, chaotic | Continuous to chaotic | Low to middle | Middle to high | ~10 - 7 Ma |
| **U3** | Top: toplaps on D3<br>Base: onlaps on D2 | Draping, parallel | Continuous | Middle to high | Middle | ~17 - 10 Ma |
| **Syn-OCT units (U2)** | | | | | | |
| **U2(s)** | Top: toplaps on D2<br>Base: onlaps, downlaps on D1, SDR<br>or on the surface of the transitional basement | Draping, parallel | Continuous to chaotic | Low to high, locally transparent | Low to middle | ~20 – 17.6 Ma |
| **U2(v)** | | Parallel, divergent To chaotic | Continuous to chaotic | High | Low to middle | |
| **SDR** | Top: conformable on U2(v)<br>Base: onlaps, dowlaps on the surface of the transitional basement | Divergent | Continuous to chaotic | High | Low | |
| **Syn-rift units (U1)** | | | | | | |
| **R2(b)** | Top: toplaps on D1<br>Base: onlaps, downlaps on L2 and L3 | Divergent | Continuous | Middle to high | Low to middle | Burdigalian >20 Ma |
| **R2(a)** | Top: toplaps, concordant on L3<br>Base: onlaps or downlaps on L2 | Divergent | Continuous or discontinuous | Low to high, locally transparent | Low to middle | Mid. Chattian? - Low. Burdigalian? |
| **R1(c)** | Top: toplaps on L2<br>Base: onlaps at the top of R1(b) | Parallel to slightly divergent | Discontinuous | Low, transparent | Middle | Middle Chattian? |
| **R1(b)** | Top: toplaps on L2<br>or at the base of R1(c)<br>Base: onlaps on L1 | Slightly divergent | Discontinuous | Low to middle<br>Transparent at the top | Low to middle | Mid. Rupelian? – Low. Chattian? |
| **R1(a)** | Top: toplaps on L1<br>Base: downlaps on CB | Parallel to slightly divergent | Discontinuous | Low, transparent | Low | Middle Rupelian |
| **Cenozoic basement (CB)** | | | | | | |
| **CB3** | Top: conformable or toplaps<br>Base: conformable or onlaps | Parallel | Continuous | Very high | Middle | Lutetian - Barthonian |
| **CB2** | Top: conformable<br>Base: conformable | Parallel | Discontinuous | Low to middle | Middle | Upper Ypresian - Lutetian |
| **CB1** | Top: conformable<br>Base: onlaps, downlaps on MB | Parallel | Discontinuous | Middle to high | Low to middle | Thanetian - Ypresian |
| **Mesozoic basement (MB) and Neoproterozoic basement (NB)** | | | | | | |
| **MB** | Top: toplaps on CB<br>Base: onlaps on NB | Parallel to chaotic | Continuous to discontinuous | Low to high | Low | Mesozoic |
| **NB** | Top: angular unconformity | Chaotic | Chaotic | Low | Low | Neoproterozoic |

D4
D3
D2
D1
L3
L2
L1

***Table 1*** *- Summary of key observations of the seismic units, with their reflection characteristics and ages.*

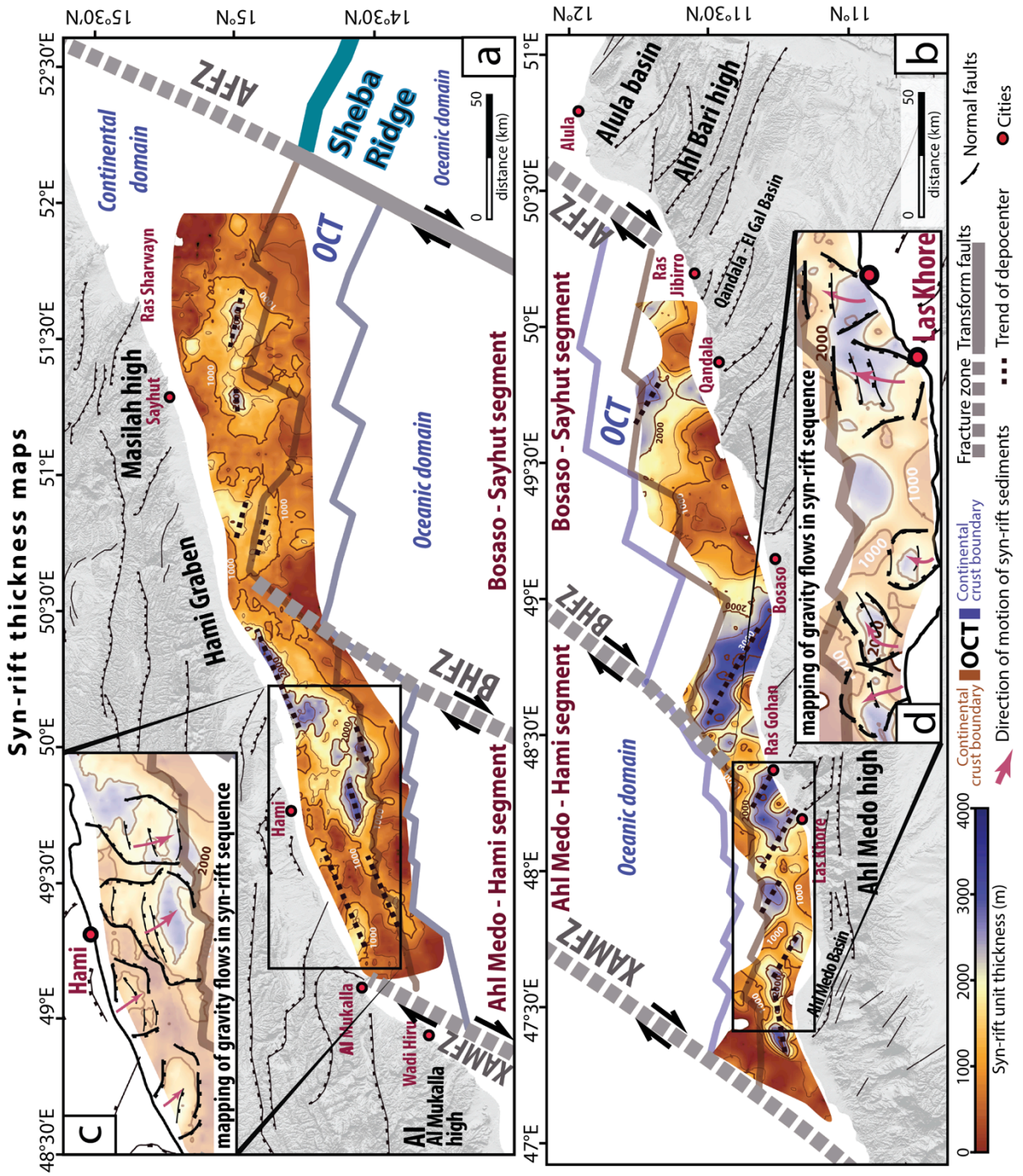


***Figure 6*** *- Isopach map of the syn-rift unit (U1) inferred from our interpretation of the datasets for (a) the Yemeni margin and (b) the Somalian margin. In black insets: mapping of gravity flows in the syn-rift sequence U1 and direction of motion; major normal faults are represented by thick lines and no evidence of reverse faults is observed. OCT: Ocean-Continent Transition. AFFZ: Alula Fartak Fracture Zone. BHFZ: Bosaso Hami Fracture Zone. XAMFZ: Xiis Al Mukalla Fracture Zone. Onshore topography is shaded (SRTM, Jarvis et al., 2008).*

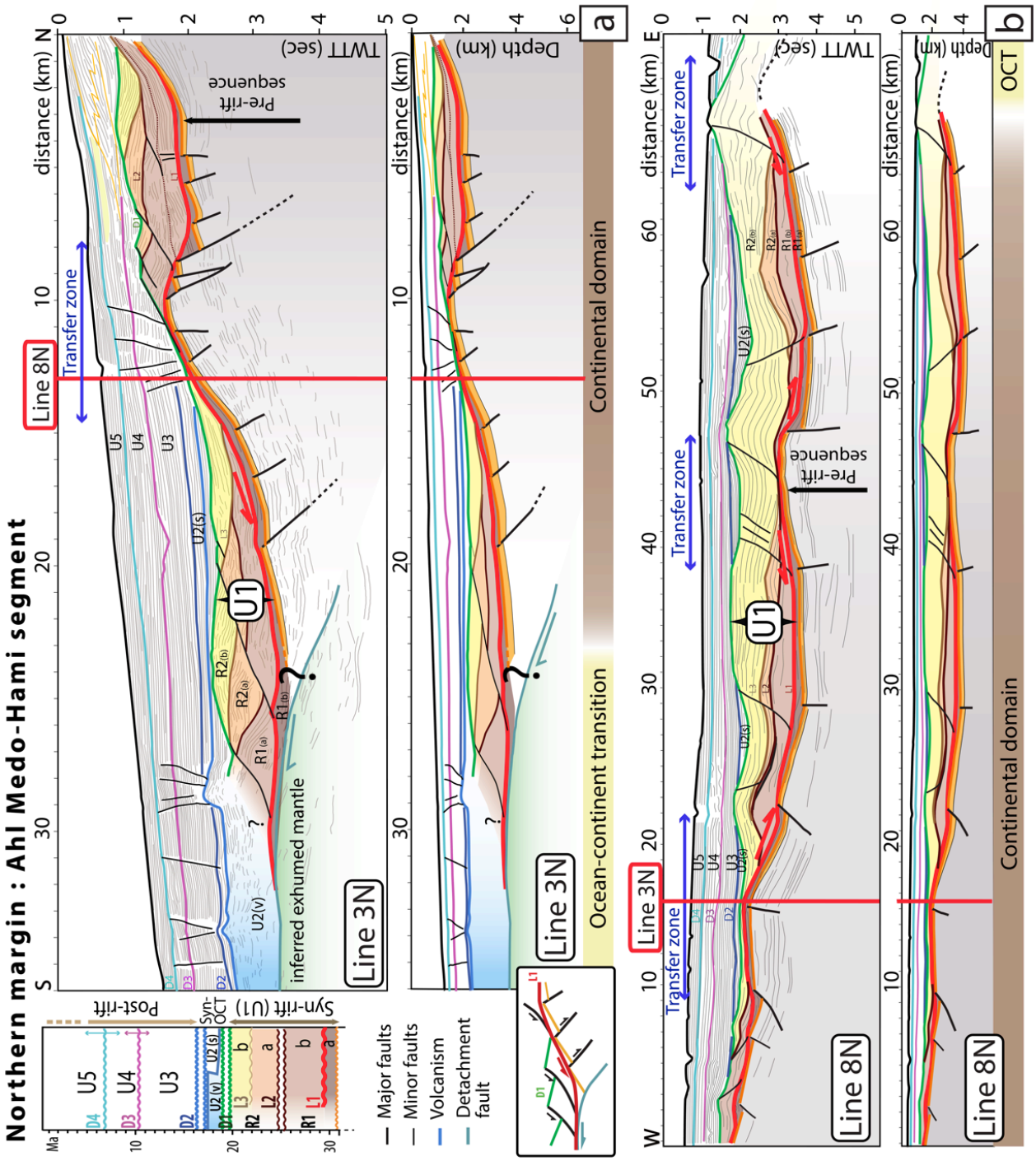


*Figure 7 - Interpreted line drawing of (a) the seismic profiles 4N and (b) the along-strike seismic line 9N in the northern margin (in the Ahl Medo-Hami segment) with the different sedimentary sequences identified on the profiles and interpretation of crustal domains (vertical exaggeration ~1.8). See location on Figure 2.a. (a) Seismic profiles 4N: Some intra-R1(b) decollement layers are recorded. Lower pannel: depth converted seismic line and its interpretation, with no vertical exaggeration. (b) seismic line 9N: the transfer zones are characterized by positive relief delimiting syn-rift basins. Lower panel: depth converted seismic line 9N and its interpretation, with no vertical exaggeration. In grey under the orange unit (CB3), the top of the pre-rift sequence CB1-2 and the Mesozoic basement (~2 km of thickness, characterized by sub-parallel to chaotic reflections), the Neoproterozoic basement and the upper crust are in contact with the exhumed mantle in distal part of the margin (at a distance of 16 – 25 km from the North of the cross-section). Inset: Sketch of the line 4N showing the geometry of the faults and their chronology. Left panel: Simplified seismic stratigraphic column.*

*4.1.2 Syn-rift sequence*

The syn-rift sequence U1 in the central Gulf of Aden is dated as Oligo-Miocene (Fig. 3) and composed of a clastic to carbonate deposits in the Hami well (Yemen, Figs. 3.b, 4.a) and Bandar-Harshau well (Somalia, Figs. 3.b**,** 4.b). The thickness of U1 varies from 0 to 3500 m in the continental domain (Figs. 6 to 10) and decrease westwards from the Ahl Medo-Hami (Figs. 6 to 8, 10.a, b, c) to the Bosaso-Sayhut segment (Figs. 6, 9, 10.d). U1 is thinner on the northern margin (reaching 2500 m, Figs. 6.a) in interpreted profiles 2N to 8N (Figs. 4.a, 7 to 9), than on the southern margin (reaching 3500 m, Fig. 6.b) in interpreted profiles 1S to 5S (Figs. 4.b, 10).

The deformation of U1 is decoupled from the basement structures (Figs. 3.c, 4.a, 6.c, d, 7 to 9). U1 is mainly recorded in the centre of the syn-rift sub-basins (that trend N70°E to N80°E, EW to N120°E; Figs. 6.a, b) and between the areas of positive topography corresponding to and N30°E to N40°E transfer fault zones (Figs. 5, 7):

- **N70°E to N80°E-trending depocenter:** On the Yemeni margin in the Ahl Medo-Hami segment, U1 displays N70°E-trending depocenter and is up to 2500 m thick (Figs. 6.a, 7, 8). Four main submarine landslides are mapped with a global SE direction of flow (orthogonal to the depressions along a N70°E-axis parallel to the coastline; Fig. 6.c). On the Somalian margin, U1 displays a N80°E-elongate depocenter east of the XAMFZ (Fig. 6.b).
- **EW to N120°E-trending depocenter:** On the Yemeni margin in the Bosaso-Sayhut segment, U1 fills *en echelon* N110°E-elongated basins and reaches up to ~2000 m (e.g. South of Ras Sharwayn, Figs. 6.a, 9.b). On the Somalian margin, from north of the Ahl Medo basin to the northwest of the Bosaso city, several *en echelon* sedimentary packages (up to ~3200 m thick, Fig. 6.b) trending N120°E are obvious (Figs. 10.a, b, c). Five main submarine landslides are observed with global NE direction of flow (orthogonal to depressions along a EW to N120°E-axis; Fig. 6.d).
- **N30°E to N40°E-trending highs:** On the Yemeni margin, U1 is 1500 m thick with a N30°E-trend southwest of the Hami graben and along the western border of the BHFZ (Fig. 6.a). On the Somalian margin, U1 is less than 500 m thick in N40°E-trending zones northeast of Bosaso city (Fig. 6.b). U1 reaches less than 100 m and is eroded with a N40°E-trend at the eastern border of the XAMFZ in the eroded basement high (Figs. 6.b, 10.a).

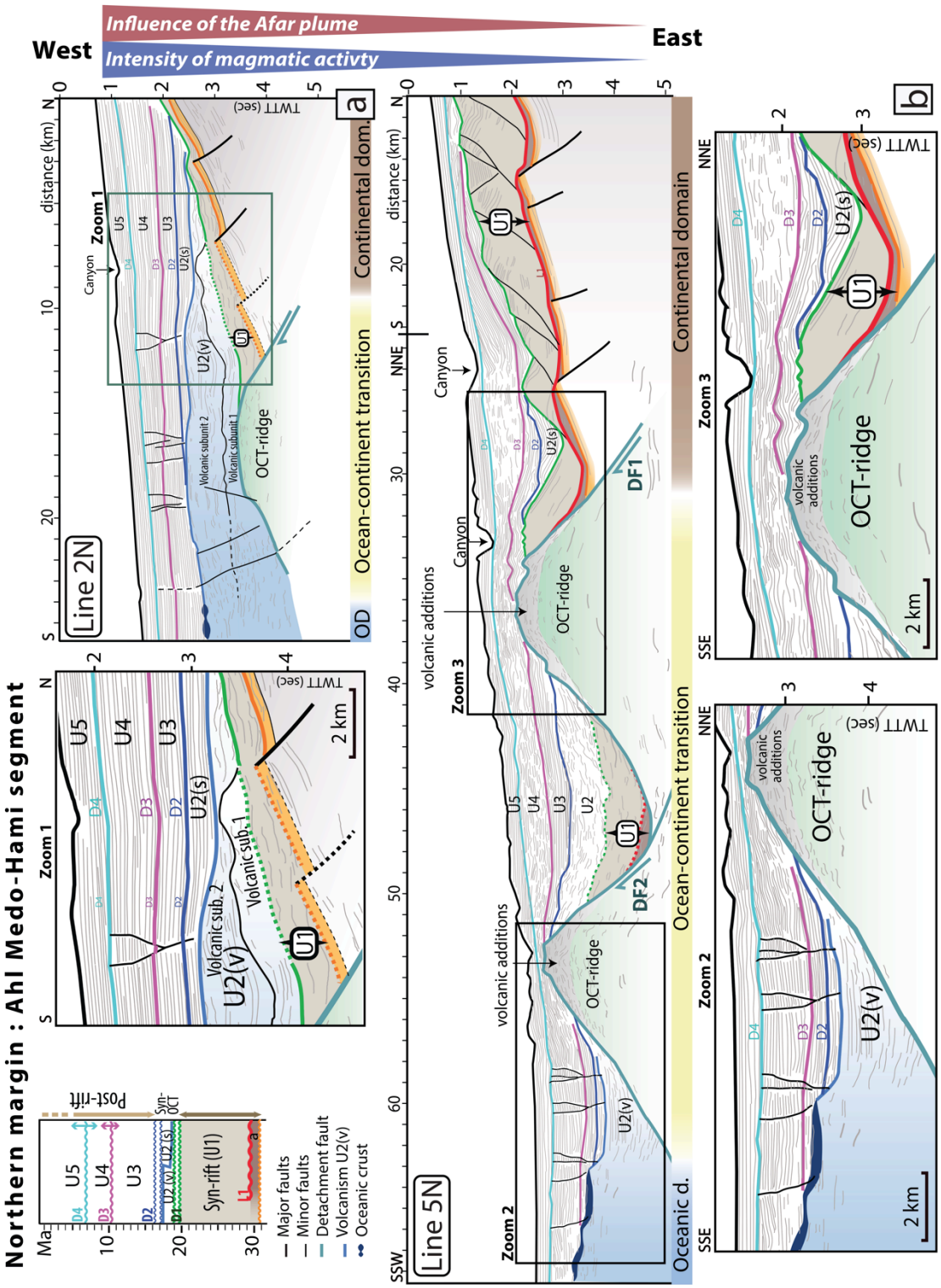


*Figure 8 - Interpreted line drawing of the seismic profiles (a) 2N and (b) 5N in the Ahl Medo-Hami segment in the northern margin with the different sedimentary sequences identified on the seismic profiles and interpretation of crustal domains in the Ahl Medo-Hami segment (vertical exaggeration ~1.8). See location on Figure 2.a. (a) Zoom 1: Close-up view of line 2N showing the interpretation of basement structures, volcanic and sedimentary units in the OCT. (b) Zoom 2: Close-up view of line 5N showing the interpretation of an OCT-ridge and associated volcanic formations. Zoom 3: Close-up view of line 5N showing the interpretation of an OCT-ridge and structural relation between the pre- and syn-rift units in the continental domain and OCT domain. Left panel: simplified seismic stratigraphic column. OD: Oceanic domain.*

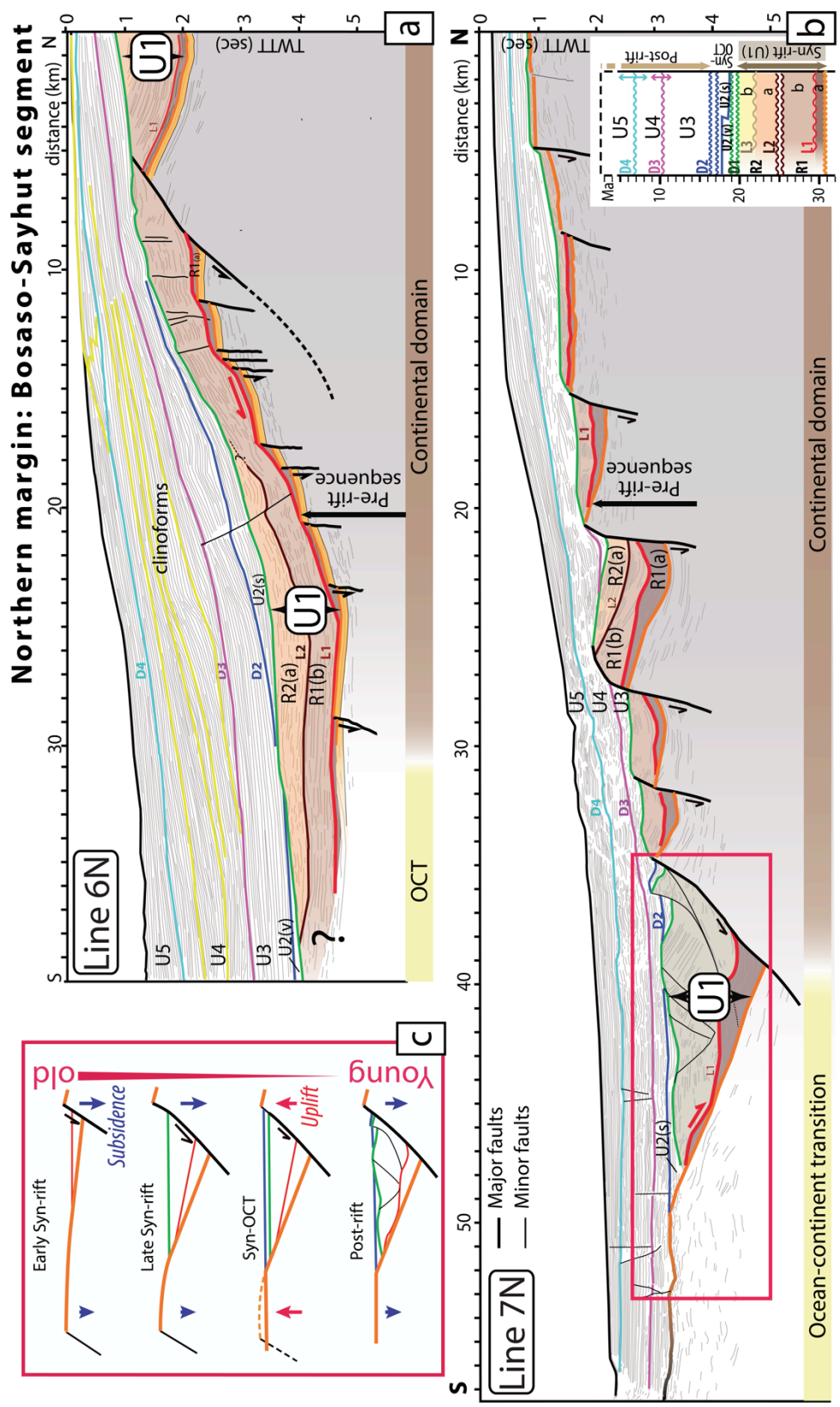


***Figure 9*** *- Interpreted line drawing (a) of the seismic line 6N and (b) of the seismic line 7N in the northern margin (in the Bosaso-Sayhut segment) with the different sedimentary sequences identified on the profiles and our interpretation of crustal domains (vertical exaggeration ~1.8). Upper left inset: sketch of OCT evolution from the syn-rift (at top) to post-rift phases (at bottom). Bottom right panel: simplified seismic stratigraphic column. In grey: the top of the pre-rift sequence (CB1-3 and the Mesozoic basement for the seismic line 6N and CB1-CB2 and the Mesozoic basement for the seismic line 7N) and the upper crust.*

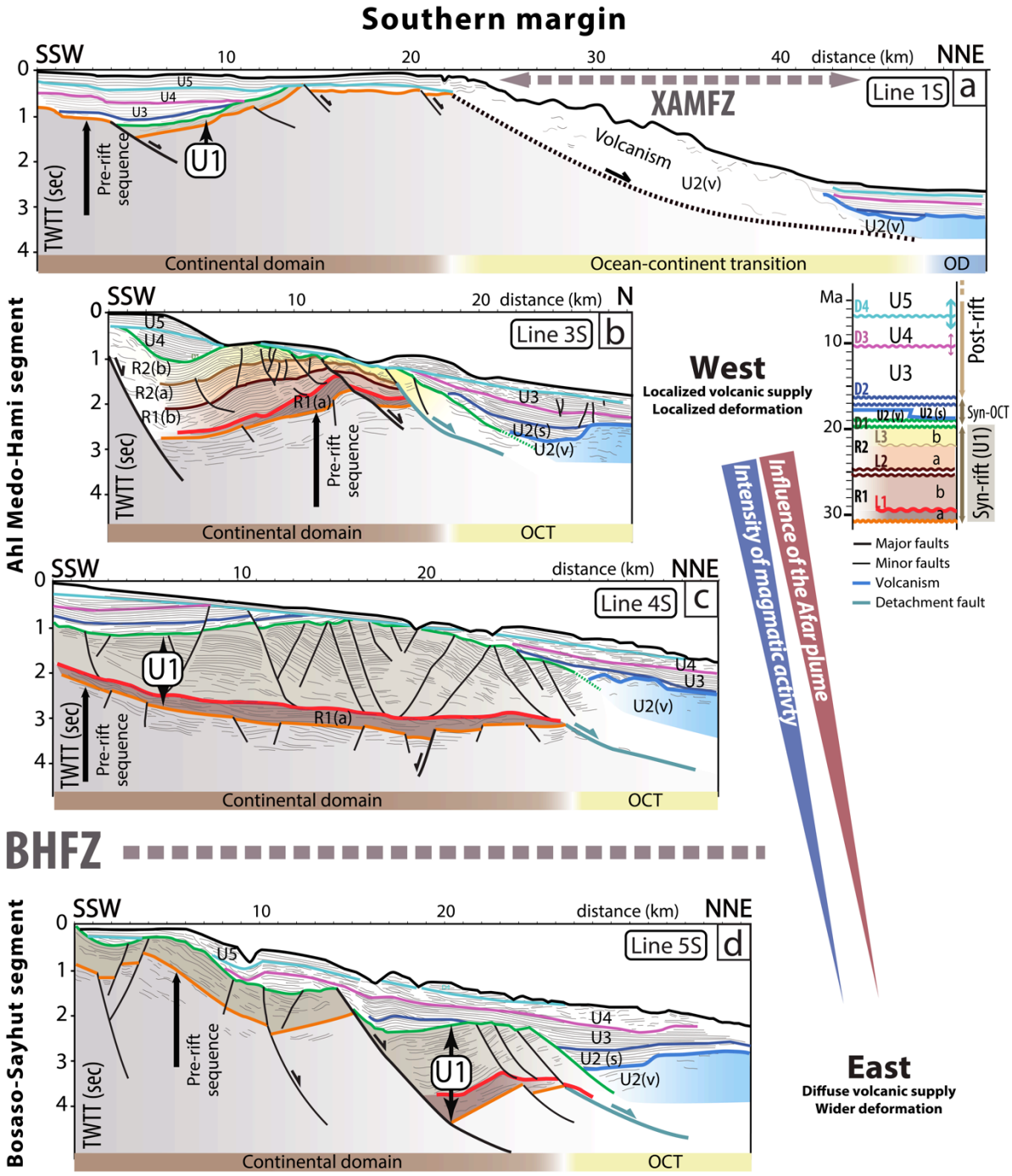


*Figure 10 - (a) to (d) Interpreted line drawing of the seismic profiles 1S, 3S, 4S and 5S in the southern margin, with the different sedimentary sequences identified on the profiles and our interpretation of crustal domains (vertical exaggeration ~1.8). Location of seismic profiles on Figure 2.b. OD: Oceanic Domain. OCT: Ocean Continent Transition. Right panel: simplified seismic stratigraphic column. In grey: the top of the pre-rift sequence (CB1-2 and the Mesozoic basement) and the upper crust.*

U1 is composed of two units (R1 and R2, Fig. 3, Tab. 1) and subunits mainly recorded in the Ahl Medo-Hami segment, on the Yemeni (Figs. 4.a, 7) and Somalian margins (Figs. 4.b, 10.b), and in the Bosaso-Sayhut segment on the Yemeni margin (Figs. 9, 3.b, c). The seismic horizons of U1 are in general parallel and do not display significant fan-shape as expected for deposits contemporaneous with fault activity (Fig. 4).

In the Ahl Medo-Hami segment, unit R1 corresponds to the Ghaydah Fm on the northern margin (Hami well; Figs. 3.b, 4.a; Tab. 1) and to the base of the Bandar-Harshau Fm on the southern margin (Bandar-Harshau well; Figs. 3.b, c, 4.b). The unit R1 is composed of three distinct subunits named R1(a), R1(b) and R1(c) (Figs. 3.a, 4; Tab. 1). The L1 discontinuity delimits the onlaps at the base of the R1(b) subunit and the toplaps of R1(a) subunit (Fig. 4, Tab. 1). On the northern margin, some intra-R1(b) decollement layers are recorded on Line 3N (Fig. 7.a). South of Hami city, the R1(c) subunit is locally observed and onlaps onto the top of R1(b) on a local boundary under the L2 discontinuity (in black, Fig. 7.a; Tab. 1). Extensional faults affecting the R1(b) unit are rooted on L1, L2 discontinuities and/or attenuated in R1(a) and R1(c) (Fig. 4.a). R2 is composed of the R2(a) and R2(b) subunits delimited by the L3 discontinuity (Figs. 3, 4). The whole syn-rift sequence (U1) is affected by normal faults (in black, Figs. 4, 7, 8.b line 5N, zoom 3, 9.a, 10.b, c, d) and rooted on the L1 discontinuity at the base of U1.

*4.1.3 Syn-OCT sequence*

The syn-OCT sequence (U2) was deposited during a period of complex transition between the end of the syn-rift phase and the onset of the steady-state oceanic spreading (~17 Ma; Leroy et al., 2010a; Nonn et al., 2017) (Fig. 3, Tab. 1). U2 is characterized by onlaps that directly cover the OCT basement and the pre- and syn-rift sediments in the continental domain (see dark blue horizon for top of U2, Figs. 3.c, 7 to 10, 11.b). U2 is absent on the steady-state oceanic crust (Figs. 8, 11.a, zoom 1 on Fig. 11.b). The syn-OCT sequence may correspond to the sedimentary subunit U2(s) (Figs. 3.c, 7 to 10; Tab. 1) and/or to the volcanic deposits of U2(v) (Fig. 7, zoom 1 on Fig. 8.a, zoom 2 on Fig. 8.b, Figs. 10, 11; Tab. 1). U2(v) onlaps on top of exhumed basement and displays wedge-shape horizons towards the OCT ridge in the western part (zoom 2, Fig. 8.b). In the Yemeni margins on the Ahl Medo-Hami segment, two volcanic subunits are recorded on U2(v) (zoom 1, Fig. 8.a). U2(s) onlaps, in some place, on top of U2(v) at the end of the syn-OCT period (Figs. 7, 8, 10, zoom 2 on Fig. 11). Near the XAMFZ, the U2 is more complex and composed of seaward dipping reflectors (SDR1 and SDR2; Fig. zoom 2 on 11.b) emplaced during the deformation of highly intruded continental crust. The SDR1 and SDR2 display fan-shape growth structures controlled by low-angle normal faults, dipping toward the continent with high-amplitude/low-frequency facies. The top of U2(s) correspond to the erosional discontinuity D2 (Figs. 3, 7, 8, 10.b, 11).

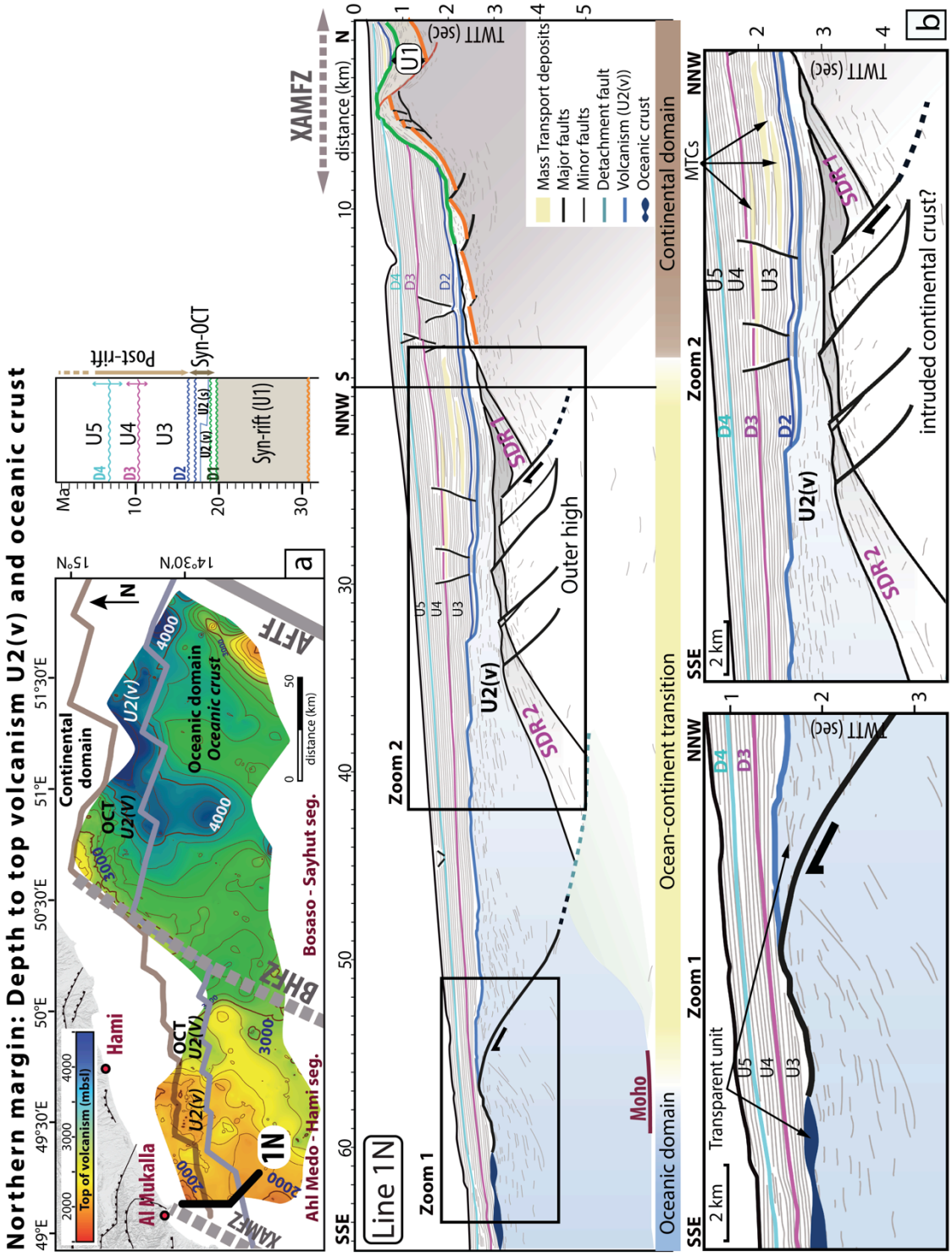


***Figure 11*** *- (a) Map of the depth to top of volcanic formations in the continental (U2(v)), transitional (U2(v)) and oceanic domains (Oceanic crust). Onshore topography is shaded (SRTM, Jarvis et al., 2008) and location of the seismic line 1N presented in b. (b) Interpreted line drawing of the seismic line 1N in the northern margin (near XAMFZ), with the different sedimentary sequences identified on the profiles and interpretation of crustal domains (vertical exaggeration ~1.8. Zoom 1: Close-up views of the line 1N showing the interpretations of the low-angle detachment fault in the oceanic crust. The top of the oceanic substratum exhibits a highly reflective uppermost reflector identified by its low frequency and high amplitude, showing a significant impedance contrast with the overlying post-rift sediments. A very specific transparent seismic unit marks the base of the post-rift sediments. Zoom 2: Close-up views of the line 1N showing the interpretations of the OCT near XAMFZ showing SDRs. In grey: the top of the pre-rift sequence (Cenozoic basement (CB1-2), Mesozoic and Neoproterozoic basements) and the upper crust. Upper right panel: simplified seismic stratigraphic column. OCT: Ocean-Continent Transition. AFTF: Alula Fartak Transform Fault. BHFZ: Bosaso Hami Fracture Zone. XAMFZ: Xiis Al Mukalla Fracture Zone.*

577 *4.1.4 Post-rift sequence*

578 The post-rift sequence (Fig. 3) covers a large part of the continental slope over continental, transitional and
579 oceanic crust and thickens oceanward (Figs. 4, 7 to 10, 11.b). On the northern margin, west and east of the
580 BHFZ, it attains a thickness of 2300 m and 4000 m (depth converted seismic profiles on Fig. 7). On the southern
581 margin, the post-rift sequence is up to 1 600 m thick (Fig. 10). The post-rift sequence lies between D2 and the
582 erosional seafloor. It comprises three main units that correlate in terms of timing with post-rift units of the
583 eastern Gulf of Aden (Autin et al., 2010a; Bache et al., 2011; Nonn et al., 2017): U3, U4 and U5 units separated
584 by the erosional unconformities D3 and D4 (Figs. 3, 4, 7 to 11; Tab. 1). U4 shows some occurrences of MTCs
585 (Mass Transport Complexes) on the proximal margins (zoom 2 on Fig. 11.b; Tab. 1). In the Ahl Medo-Hami
586 segment, U4 displays current-formed features corresponding to canyon indentation or contourites which also
587 distort the D4 unconformity at the Yemeni continental shelf break (Figs. 4.a, 7.a). In the Bosaso-Sayhut
588 segment, U4 is defined by large clinoforms (Fig. 9.a).

589

590 **4.2 Conjugate margins architecture**

591 Three major domains can be identified according to the geometry, bathymetry, sedimentation infill, gravimetry
592 and seismic facies (Figs. 3 to 12): (i) the continental domain is marked by a succession of basins and basement
593 highs; (ii) the steady-state oceanic crust is characterized by a rough top seismic basement; (iii) the ocean-
594 continent transition (OCT) is defined as a complex transitional domain between the continental and oceanic
595 domains (Figs. 3 to 12).

596

597 *4.2.1 Major features of acoustic basement morphology from offshore conjugate margins*

598 In the continental domains of the central Gulf of Aden conjugate margins, the depth to acoustic basement
599 maps (Figs. 5.a, b) corresponds to: (i) the top of the pre-rift sequences in the continental domain; (ii) the top of
600 the intermediated seismic basement in the OCT; and (iii) the top of the oceanic substratum in the oceanic
601 domain in agreement with previous studies in the eastern Gulf of Aden (Autin et al., 2010b; d'Acremont et al.,
602 2005; Nonn et al., 2017). The depth to basement maps represents the discontinuity between the upper-layered
603 sedimentary seismic facies and a lower more chaotic seismic facies of the seismic substratum (Tab. 1, Figs. 5.a,
604 b, 7 to 11).

The depth to basement map shows steep and narrow slopes all along the conjugate margins. The basement abruptly drops down from 0 mbsl near the coastlines to 5500 mbsl at the foot of the continental slope in the northern margin (Fig. 5.a) and to 4000 mbsl at the foot of the continental slope on the southern margin, over distance of less than 40 km (Figs. 5.a, b). The basement shows an eastward deepening in agreement with the eastward thickening of the sedimentary cover. On the overall morphology of the basement of conjugate margins, three main trends are observed (EW to N120°E, N70°E to N80°E and N30°E to N40°E; Figs. 5.a, b):

- **EW to N120°E-trending basins and highs*:*** On the northern margin, in the Ahl Medo-Hami segment and to the east of Al Mukalla city (Lat. 14°40'N, Long. 49°30'E; Fig. 5.a), EW escarpments cut the N70°E-trending relief. In the Bosaso-Sayhut segment, to the east of the Sayhut city (from Long. 51°30'E to Long. 52°E, Fig. 5.a, 9.a) a major basement high has a global N110°E trend toward the AFFZ. On the southern margin and in the Ahl Medo-Hami segment, a N80°E-trending basin reaches ~3000 mbsl of depth (Lat. 47°45'E to 47°45'E, Long. 11°15'N, Figs. 4.b, 5.b, 10.b). In the Southeastern prolongation of the BHFZ, N120°E-trending basin and high intersect the N40°E-trending structures (Long. 47°45'E to 48°15'E; Fig. 5.b). In the Bosaso-Sayhut segment, trends of basins and highs is N130°E at the North of Bosaso basin (Lat. 11°20'N and Long. 49°E; Fig. 5.b). This N120°E trend is also recorded in the northwest of Qandala city (Fig. 5.b).
- **N70°E to N80°E-trending basins and highs*:*** On the northern margin and in the Ahl Medo-Hami segment, a N70°E-trending basement high is parallel to the coastline of the Yemen margin and culminates at 1000 mbsl near Hami city (Lat. 14°30'N to 14°50'N, Long. 49°E to 50°15'E; Figs. 4.a, 5.a, 7.a). Farther south, at around 55 km south of Hami city, a N70°E-trending basement high culminates at a depth of 2300 mbsl (Fig. 5.a). Eastward in the Bosaso-Sayhut segment, a basement high (Lat. 14°50'N to 15°15'N) has a global N70°E direction from Long. 51°E up to Long. 51°30'E (Fig. 5.a). On the southern margin, in the Bosaso-Sayhut segment, trends of basins and highs is N70°E in the coastline (from Lat. 11°15'N to 11°30'N and from Long. 49°15'E to 49°45'E, Fig. 5.b).
- **N30°E-trending basin and highs** are recorded near Fracture zones in the Ahl Medo-Hami segment: On the Yemeni margin and southwestward of the Hami graben, the western border of the BHFZ is marked by a N30°E-trending basement high at 2000 mbsl depth (Fig. 5.a). On the southern margin, the eastern border of the XAMFZ is marked by a steep N40°E-trending basement high at 300 mbsl depth (from Lat. 11°N to 11°30'N at Long. 47°15'E; Figs. 5.b, 10.a). In the prolongation of the BHFZ, northeast of Las Khore city (Long. 47°45'E to 48°15'E, Fig. 5.b), N30°E to N40°E-trending elongate highs and basins vary in depth from 1500m to 4000 mbsl.

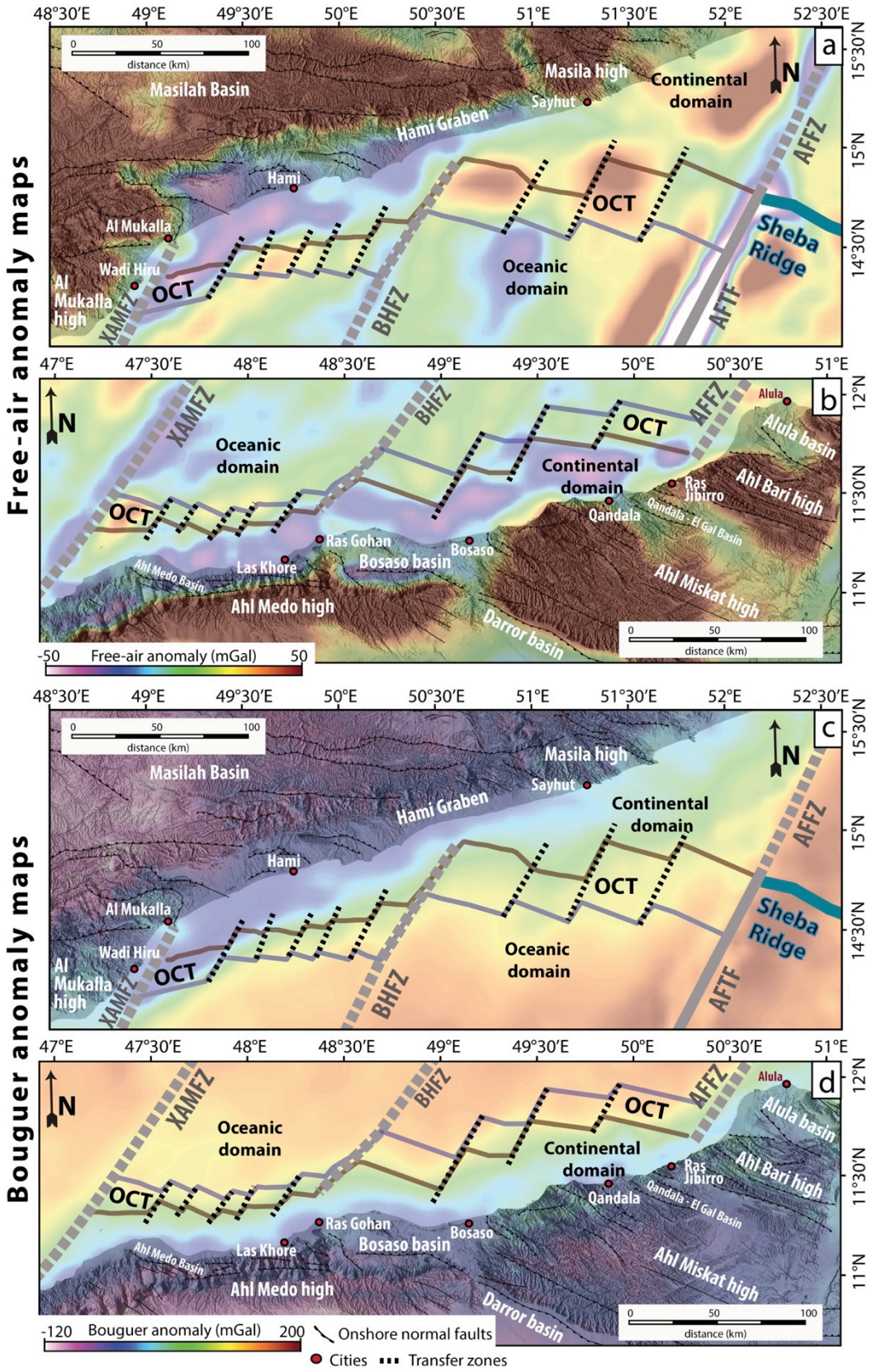


***Figure 12*** *- (a, b) Free-air anomaly and (c, d) Bouguer anomaly maps from the International Gravimetric Bureau (Drewes et al., 2012). Onshore topography is shaded (SRTM, Jarvis et al., 2008). The boundaries of crustal domains are drawn. OCT: Ocean-Continent Transition. AFFZ: Alula Fartak Fracture Zone. AFTF: Alula Fartak Transform Fault. BHFZ: Bosaso Hami Fracture Zone. XAMFZ: Xiis Al Mukalla Fracture Zone.*

640 *4.2.2 Continental domain*

641 The continental domain of conjugate margins presents a long-wavelength rough morphology at depths ranging
642 from 0 to 4500 mbsl (Figs. 5.c, d). The continental seismic basement is characterized by series of angular tilted
643 blocks bounded by normal faults (Fig. 5.c, d), completely buried under the sedimentary cover (Figs. 3.b, 4, 6 to
644 11). The top of the continental seismic basement is defined by the carbonates of the Cenozoic basement (e.g.
645 Figs. 3, 7), the Mesozoic or the Neoproterozoic basement (e.g. Figs. 3, 10) depending on the amount of erosion
646 of the pre-rift units. We define oceanward boundary of the continental domain at the place where no more
647 pre-rift basement is identified, on the distal margins (neither the Cenozoic basement, nor the Mesozoic
648 basement, nor the Neoproterozoic basement; Figs. 4.b, 5 to 10, 11.b, Tab. 1). However, some thick volcanic
649 formations and/or post-rift formations can mask reflections from the seismic basement on the distal margins (Figs.
650 4.b, 7.a, Zooms 1 and 2 on Fig. 8, Figs. 10, 11).

651 On the northern margin, most of the normal faults exhibit small offsets (~100 - 500 m of dip-slip motion, Figs.
652 4.a, 7, 8, 11.b). In the Ahl Medo-Hami segment, the faults dip toward the continent (Figs. 4.a, 7, 8, 11.b); In the
653 Bosaso-Sayhut segment, the faults are also mainly continentward-dipping (Fig. 9). On the southern margin, they
654 show greater dip-slip (from 1000 to 4000 m of vertical throw, Figs. 4.b, 10) than on the northern margin (from 100 to
655 400 m, e.g. Figs. 4.a, 7, 8, 11.b).

656 On the northern margin, the free-air (Fig. 12.a) and the Bouguer (Fig. 12.c) anomalies are negative and positive
657 west and east of BHFZ, respectively. On the southern margin, gravity data reveal large-amplitude, long-wavelength
658 negative free-air and Bouguer anomalies (Figs. 12.b, d).

659

660 *4.2.3 Ocean-continent transition*

661 The transitional domain corresponds to the distal part of the margin where: (i) the geological and geophysical
662 characteristics are typical neither of continental nor steady-state oceanic crust; (ii) a record of the U2 unit (Tab. 1),
663 deposited during the formation of the OCT (Autin et al., 2010; Leroy et al., 2010b), is identified. At the boundary with
664 the continental domain, the OCT domain begins with the disappearance of the clearly identified the Cenozoic,
665 Mesozoic or Neoproterozoic basements (Figs. 7.a, 8 to 10, 11.b; Tab. 1). The top of the transitional basement is
666 difficult to identify and less well defined than the oceanic or continental substratums. Chaotic reflectors characterize
667 the internal facies of the OCT basement (Figs. 7.a, 8). The mapped OCT mainly corresponds to an abrupt passage
668 from negative to positive free-air (up to ~40 mGal, Figs. 12.a, b) and Bouguer anomalies (~100 mGal, Figs. 12.c, d),

except in the OCT in the vicinity of the XAMFZ in the northern margin where the free-air (~-50 mGal in the OCT, Fig. 12.a) and Bouguer anomalies (~-10 mGal in the OCT, Fig. 12.a) are negative.

The OCT on the northern margin (Figs. 5.a, c, 6.a) is wider in the eastern segment (~23 - 45 km) than in the western segment (~17 – 33 km). On the southern margin, the OCT (Figs. 5.b, d, 6.b) is also wider in the Bosaso-Sayhut segment (~ 23 km) than in the Ahl-Medo-Hami segment (~10 – 20 km). The difference in width of the conjugate margins OCTs highlights the asymmetry of the Yemeni and Somalian margins.

The depth to basement maps (Figs. 5.a, b) reveals an eastward deepening of the transitional basement from ~3000 mbsl up to ~5200 mbsl in the eastern Bosaso-Sayhut segment on the northern margin. The conjugate margins OCTs are completely buried beneath syn-OCT to post-rift cover (Figs. 4.b, 7.a, 8 to 10, 11.b) and locally by the syn-rift units slided on the discontinuity L1 (Figs. 4.b, 6, 7.a, 8, 9.b, 10.b, c, d); U2 onlaps the top of the acoustic basement and on the allochthon syn-rift units on the OCT substratum (Figs. 4.b, 6, 7.a, 8, 9.b, 10.b, c, d). In both margins, U2(s) to U4 are affected by minor normal faults (with offsets of a few metres) and sealed by the discontinuity D3 (e.g. Figs. 11.b).

The transitional basement of the northern margin is defined by a flat (Fig. 9) or dome-shaped footwall on the edge of the continental domain (called OCT-ridges, Figs. 7.a, 8) capped by a detachment faults. This fault is low-angle and northward dipping under the continental domain (Figs. 7.a, 8). In the OCT on the northern margin, the detachment faults are oriented (i) N80°E in the western sub-segment near the XAMFZ (Fig. 5.c) and (ii) EW to N95°E in the other five sub-segments of the Ahl Medo-Hami segment at the west of the BHFZ (east of Long. 49°25'E; Figs. 5.c, d, 7, 8). West of the BHFZ, two detachment faults (DF1 and DF2) form two OCT-ridges (zooms 2, 3; Fig. 8.b): the upper basement DF1 is cut by a second detachment fault DF2 (45 – 49 km to the south). On the southern margin, the morphology of the acoustic basement indicates the presence of a basin at the foot of the continental slope (Figs. 5.b, 10).

Evidences of volcanism are identified in the OCT domain: (1) Near the XAMFZ, the northern margin OCT is characterized by SDRs (Zoom 2, Fig. 11.b). The SDR1 wedge overlies a continental block characterized by a domed-structure referred to here as the outer-high (Zoom 2, Fig. 11.b). The SDR2 and the outer-high are cut by several small offset normal faults (Fig. 11.b). (2) The southern margin OCT is affected by volcanism at the location of the XAMFZ (Fig. 10.a) and by a volcano that disturbs the overlaying syn-rift cover slided in the OCT (Fig. 10.b). (3) Near the BHFZ, the basement of the two OCT-ridges is rough and affected by volcanic additions (hummocky or chaotic, high-amplitude low-frequency reflectors; zooms 2, 3 on Fig. 8.b).

699 *4.2.4 Oceanic domain*

700 The oceanic domain is defined by a characteristic rough topography of the top of the seismic basement, mostly
701 found at ~2000 to 4000 mbsl (Figs. 8.a, 11.a), and entirely covered by post-rift units (Figs. 8, 11.b). The depth to
702 oceanic crust basement map (Fig. 11.a) reveals an eastward deepening of the top of the oceanic crust. Near the
703 XAMFZ, the oceanic crust is at a depth of 2000 mbsl and dips eastward to reach 3000 mbsl near the BHFZ. In the
704 Bosaso-Sayhut segment, the oceanic crust deepens towards the centre of the basin and reaches 4200 mbsl (Lat.
705 14°20'N, Long. 50°50'E, Fig. 11.a). We observe a locally a strong reflector that may be interpreted as the Moho (at
706 ~6.3 s TWTT, Fig. 11.b). It allows us to determine the limit of the steady-state oceanic crust (Figs. 11.a). The
707 oceanic domain displays characteristic free-air gravimetric anomalies, varying from -50 mGal on the oceanic
708 transform faults of XAMFZ, BHFZ and AFFZ to 50 mGal on either side of the AFFZ, with a mean value of -10 mGal in
709 the basin (Figs. 12.a, b). The Bouguer anomaly varies from 100 mGal to 200 mGal (Figs. 12.c, d). Low-angle
710 detachment fault in the oceanic basement (close-up view 1, Fig. 11.b) is associated with a large rotation and
711 exposure of the domal-shaped footwall of the fault over a short distance (~4 km in length).
712
713 **4.3 Conjugate margins segmentation**

714 Mapping of the structural domains and syn-rift thicknesses (Fig. 6) highlight NE-trending *en echelon* offsets of the
715 structures (Figs. 5.c, d). Two wavelengths of segmentation are mapped in the central Gulf of Aden. (i) The long-
716 wavelength type corresponds to the major dextral fracture zones (XAMFZ, BHFZ and AFFZ), trending ~N30°E on
717 the northern margin and ~N40°E on the southern margin (Figs. 5.c, d). (ii) In the Ahl Medo-Hami segment, six sub-
718 segments 10 - 30 km in length are subdivided by five ~N30°E-trending transfer zones corresponding to the short-
719 wavelength type (Figs. 5, 7). In the Bosaso-Sayhut segment, the sub-segments of 30 - 50 km in length are
720 delimited by three ~N30°E to N40°E -trending transfer zones (Fig. 5). These transfer zones are well correlated all
721 along both margins (Fig. 5). They show variable offsets (from 3 to 23 km) affecting the continental and the entire
722 OCT domains (Fig. 5), but have so far not developed on the proximal margins. Along the margin, the depth to
723 basement map (Figs. 5.a, b) and the along-strike seismic profiles (Fig. 7.b) display basement highs at the location
724 of transfer zones. These highs delimit the sub-basins corresponding to the syn-rift depocentres (Fig. 7.b).
725
726 **4.4 Decollement layer**

727 The syn-rift unit U1 depocentres (Fig. 6) are characterized by EW to N120°E, N70°E to N80°E and N30°E to N40°E
728 trends (Figs. 5.c, d). U1 depocentres seem to be controlled by the overall morphology of the basement (basins and

highs with EW to N120°E, N70°E to N80°E and N30°E to N40°E trends, Figs. 5.c, d, 7). Indeed, the syn-rift faults appear to be rooted on a common L1 surface on top of R1(a) (in red, Figs. 7, 8). In U1, the subunit R1(a) unit acts as a disharmonic layer (see brown unit, Figs. 7, 8, 9.a, 10.c). The syn-rift structures show various degrees of coupling between the rheologically distinct sedimentary cover and the basement (Figs. 7 to 10, 11.b). Hence, the faults can be restricted to the acoustic basement and to the syn-rift cover above R1(a) and the L1 unconformity (Figs. 4.a, 7, 8, 9.a, 10.c), or can affect the whole syn-rift sequence (including R1(a)) as well as the acoustic basement, e.g. Figs. 4.b, 9, 10.b, d). R1(a) depocentres controlled by the slope are slided into the distal part of the margin, towards the ocean. As such, undifferentiated syn-rift units slide locally on the OCT substratum owing to the decollement layer L1 (Figs. 6 to 10).

## 5. Discussion

The stratigraphic and structural study of our data set (Figs. 3 to 12) in the central Gulf of Aden conjugate margins enable us to discuss (i) the nature of the seismic basement in various crustal domains; (ii) the relationships between sedimentary deposits and volcanism in these hybrid-type conjugate margins; (iii) the tectono-sedimentary and magmatic evolution of the margins system. We compiled these observations on 3D synthetic diagram showing a reconstruction of the conjugate margins at the syn-OCT stage (Fig. 13)

### 5.1 Nature of the seismic basement and tectonic style

#### *5.1.1 Continental domain*

In agreement with previous studies in the eastern Gulf of Aden conjugate margins (d'Acremont et al., 2005; Leroy et al., 2010b; Nonn et al., 2017), we defined the continental domain in the offshore part of central Gulf of Aden conjugate margins based on the following observations: (i) it exhibits a slope morphology; (ii) it is characterized by a series of angular tilted blocks bounded by normal faults; (iii) it is buried beneath the syn- to post-rift sedimentary sequences and (iv) the top of the seismic basement corresponds to the pre-rift units.

On rifted margins, three main sub-domains are generally studied separately: (i) the weakly thinned proximal margin (~30-40 km thick); (ii) the necking zone of continental crust defined as an area of intense crustal thinning from ~30 to less than 10 km where the seismic Moho converge towards the top of the basement (e.g. the Norwegian margin, Péron-Pinvidic and Osmundsen, 2016; the Socotra margin, Ahmed et al., 2014) and (iii) the hyper-extended of continental crust that has been observed e.g. in Bay of Biscay-Pyrenees

(Lagabrielle et al., 2010; Teixell et al., 2016) or in the adjoining conjugate margins of the eastern Gulf of Aden (Autin et al., 2010b; Leroy et al., 2012; Nonn et al., 2017).

In the central Gulf of Aden, we suggest that the continental domain recognized in the offshore margins may correspond to the necking or hyper-extended domains. The ~40 km thick continental crust is thinned of 30-50% towards the ocean on the onshore conjugate margins up to 20 km thick near the coastline (Ali and Watts, 2013; Korostelev et al., 2016). Offshore, continental crust is thinned over very short distances, as the immerged continental domain do not exceed 60 km from the coastline to its distal boundary (Fig. 5). However, we are unable to determine the boundary between the necking and the hyper-extended domains due to a lack of deep penetration seismic data that could have allowed us to observe the Moho depths and deduce to the crustal thickness.

*5.1.2 Ocean-Continent Transition*

As proposed for the eastern Gulf of Aden conjugate margins (d'Acremont et al., 2005; Leroy et al., 2012; Nonn et al., 2017), we defined the location of the OCT based on the unreflective character of the seismic basement and the deposition of the syn-OCT units (U2(v) ou U2(s)) directly on the seismic basement (Figs. 7.a, 8 to 10, 11.b). Some SDRs may also cover directly the seismic basement (Fig. 11.b).

In the OCT domain of the northern margin, we identify two northward-dipping detachment faults on seismic line 5N (Fig. 8.b): the second detachment fault (DF2) is formed at the footwall of the first detachment fault (DF1) and leads to the exhumation of deeper units. This pattern of successive detachment faults is observed onshore in the continental crust on Tinos island (Brichau et al., 2007) and offshore on the distal part of the Australian-Antarctic margin (Direen et al., 2011; Gillard, 2015). On the southern margin, we identify that the acoustic basement forms a basin at the foot of the continental slope (Figs. 5.b, 10). We suppose that the southern tip of the basin may correspond to an oceanward low-angle large-offset fault (in green, Fig. 10) based on the observation of the detachment faults in the northern margin. The presence of detachment faults is reinforced by the dome-shaped footwall (OCT-ridges, Figs. 7, 8) bounding the northern margin OCT. This latter may be interpreted as exhumed subcontinental mantle (e.g. Boillot et al., 1980, 1989; Whitmarsh et al., 2001; Tucholke et al., 2007). Indeed, ridges of serpentinized peridotites display smooth-shaped basement highs as observed and drilled on the Iberian-Newfoundland margins (Beslier et al., 1996; Shillington et al., 2006; Whitmarsh et al., 2001) or observed on the eastern Gulf of Aden margins (Leroy et al., 2010b). Indeed, in the eastward adjacent Encens-Sheba segments, the OCT is composed, at least partially, of exhumed serpentinized

788 mantle (d'Acremont et al., 2006; Leroy et al., 2010b, 2012; Watremez et al., 2011). The unreflective character
789 of the upper seismic basement could be in agreement with the interpretation of exhumed serpentinized
790 mantle in distal margins (Pickup et al., 1996; Shillington et al., 2006).
791
792 *5.1.3 Narrowness, asymmetry and segmentation of the central Gulf of Aden conjugate margins*
793 In the eastern Gulf of Aden, (i.e. Encens-Sheba segment (d'Acremont et al., 2005; Leroy et al., 2012) and
794 Socotra-Sharbithat segment (Nonn et al., 2017)) similar data show narrowness, asymmetry and segmentation
795 of the conjugate margins. In the adjoining central Gulf of Aden, our data set reveals that the offshore part of
796 the continental domain is narrow (less than~ 150 km cumulated on both margins). The continental domain of
797 the southern margin is narrower (~20-40 km) than the northern one (~20–100 km). This narrowness and
798 asymmetry of the continental domain is also recorded in the OCT (less than ~50 km cumulated on both
799 margins, Fig. 5). The southern margin OCT is narrower (~10-20 km, Figs. 5.b, d) than the northern one (~20 – 40
800 km, Figs. 5.a, c, 12) but both widen eastward from ~10 to 40 km (Figs. 5, 12).
801 This asymmetry of the continental domain of the conjugate margins provides evidence for the activity of
802 lithospheric low-angle detachment faults during the formation of the OCTs as suggested in the eastern Gulf of
803 Aden (Nonn et al., 2017). The distinction between the hangingwall (upper plate) and the footwall (lower plate)
804 of the detachment fault (Lister et al., 1986) may be difficult as extension may involved the setting up of
805 numerous generations of detachment faults (e.g. Hayward and Ebinger, 1996; Sauter et al., 2013; Gillard et al.,
806 2015, 2016). Our study reveals a northward-dipping low-angle detachment fault (<30°, Figs. 7, 8) at the edge of
807 the Yemeni continental domain, corresponding to northward-dipping reflectors that argue strongly in favour of
808 a final northward dip of the final detachment fault. At the beginning of the exhumation phase, this northward-
809 dipping low-angle detachment fault is associated with the development of asymmetrical margins narrower in
810 the southern margin than in the northern one as proposed. However, the presence of multiple detachment
811 faults (DF1, DF2; Fig. 8.b) shows that this first detachment fault was not active during the whole rifting history
812 (e. g. Iberian-Newfoundland margins; Rosenbaum et al., 2008). Furthermore, the lack of data on the distal
813 margins prevents us from establishing a detailed architecture for the OCT on the Somalian margin. The
814 magmatism masks the OCT structures at the east of the BHFZ (Figs. 4.b, 10) and makes the interpretation of the
815 exhumation zone highly speculative.
816 The oblique rifting of the Gulf of Aden implies a significant segmentation of the conjugate margins. The long-
817 wavelength type of segmentation corresponds to the N30°E to N40°E-trending XAMFZ, BHFZ and AFFZ which

separate the ~ 180 km-long Ahl Medo-Hami and Bosaso-Sayhut segments and which seem to affect the proximal margin since the onset of rifting in the Gulf of Aden up to the OCT and are well correlated all along both margins (Figs. 5, 12). Between the major fracture zones, the N30°E to N40°E-trending transfer zones are also correlated all along the conjugate margins and affect the distal part of the continental domains, the OCTs and the oceanic domain (Figs. 5, 12). As the identified major fracture zones and the transfer zones shift the oceanic domain thanks to seismic interpretation (Fig. 2), gravity data (Fig. 12) and previous studies on magnetic data (Leroy et al., 2012), we suggest that they correspond to oceanic transform zones, at least at the beginning of the steady-state spreading of the oceanic crust (Burdigalian). Such a segmentation has been described and mapped in the eastern Gulf of Aden conjugate margins (d'Acremont et al., 2005; Leroy et al., 2012; Nonn et al., 2017). A classification of the segmentation proposed by Bellahsen et al. (2013b) distinguishes the oceanic fracture zones that are formed in the continuity of continental transform since the early rifting phase (Type 1-C) and other one formed at continental transfer zones since the syn-rift to early OCT phases (Type 1-T). In the central Gulf of Aden, the XAMFZ, BHFZ and AFFZ correspond to the Type 1-C and the transfer zones correspond to the type 1-T.

### 5.2 Stratigraphy, magmatism and vertical movements in hybrid-type margin

#### *5.2.1 Late syn-rift decoupling surfaces*

The central Gulf of Aden conjugate margins are subject to vertical movements associated with syn-rift decoupling surfaces especially in the Ahl-Medo Hami segment. The presence of layers of salt or clay is often necessary to act as decollement horizons. Studies on salt-influenced rift basins as in offshore Norway (Kane et al., 2010), Congo (Karner et al., 1997), Angola (Duval et al., 1992; Fort et al., 2004) and Morocco (Tari et al., 2000) have revealed a complex interplay between fault growth and salt movement which influences the evolution of syn-rift depocentres (e.g. Vendeville et al., 1995). When a ductile layer decouples the supra-salt cover from the basement, this leads to a diffusion of deformation in the basement and involves two separate fault populations: one in the cover and the other confined within the pre-salt basement (Richardson et al., 2005; Vendeville et al., 1995). The migration of this mechanically weak layer offsets the syn-rift depocentre and plays a fundamental role in controlling the size and distribution of the depocentre (e.g. Kane et al., 2010).

In the central Gulf of Aden, the R1(a) unit corresponds to the base of the Ghaydah Fm (Fig. 3) and represents an important weak layer that could act as a decoupling horizon during the extension (extensional faults affecting the R1(b) unit (in brown) are rooted on the discordance L1 (in red, Figs. 3, 4, 7 to 10). In the

wells, the Ghaydah Fm is characterized by sandstones, conglomerates, anhydrites and marls (Watchorn et al., 1998) providing evidence of a continental environment. According to Bott et al. (1992), the Ghaydah Fm is more evaporitic westward, in the Ahl Medo-Hami-segment. On the southern margins, the wells encounter anhydrites and shales of the Bandar-Harshau Fm (Bott et al., 1992; Ali and Watts, 2013). However, the wells are located on top of structural highs and the significant mobility of R1(a) at the base of Ghaydah confines the unit to the edge of these highs (i.e. 3 km south of the coastline for the northern margin, Fig. 3.a), thus preventing direct access to geological data. Nevertheless, in agreement with the significant ductile behaviour of R1(a) and the evaporitic nature of the Ghaydah and Bandar-Harshau Fms, we suggest that R1(a) could be a salt layer.

During the Aquitanian - Burdigalian, the rifting intensifies and the deepening increases is associated with margin subsidence. The syn-rift cover slides on a major decoupling layer R1(a) toward the distal margin. The sliding continues until the syn-OCT Phase (Burdigalian) as shown by the presence of syn-rift units in the OCT resting directly the transitional basement exhumed by the on the detachment fault, especially on the northern margin (Figs. 4.a, 7, 9.a). Such sliding of the sediment cover onto the exhumed OCT substratum is also observed in the Pyrenees (Lagabrielle et al., 2010).The onlapping post-rift units (Figs. 4.b, 7.a, 8, 9, 10.b, c, d) show that deformation does not continue during the post-rift phase.

This scenario is similar to that of the detachment tectonics involving decollement salt layers and the sliding of the mobile sedimentary cover on the exhumed mantle rocks described in the fossil Pyrenean margins (e.g. Lagabrielle et al., 2010; Masini et al., 2014; Tugend et al., 2014; Clerc et al., 2016). While stretching of syn-rift cover is observed on the proximal part of the margin, the glided syn-rift cover in the OCT does not display any evidence of shortening farther downslope, at the toe of the conjugate margin dips (Figs. 7.a, 8, 9.a, 10), as observed for example on the Angolan margin (Fort et al., 2004). To address the issue of spatial accommodation of the extension, Duval et al. (1992) proposed a conceptual model of gravity-driven deformation where allochthons can glide onto a newly formed domain without downslope shortening and with or without a frontal buttress (process of raft tectonics). In our study, we suggest that the Tertiary gravitational deformation of syn-rift units over R1(a) salt unit is accommodated on distal margins by the simultaneous creation of space during the emplacement of the OCT and the formation of detachment faults exhuming mantle rocks. That has been described on the southern Australian margin (Espurt et al., 2009, 2012) or in the Pyrenees (Jammes et al., 2010; Lagabrielle et al., 2010; Masini et al., 2014). The so-called OCT-Ridges (zooms 1, 3, Fig. 8.b) correspond to dome-shaped reliefs on the OCT basement that could act like buttresses along the margin (zoom 3 on Fig. 8.b) as slided syn-rift sediments onlap on their continentward slopes.

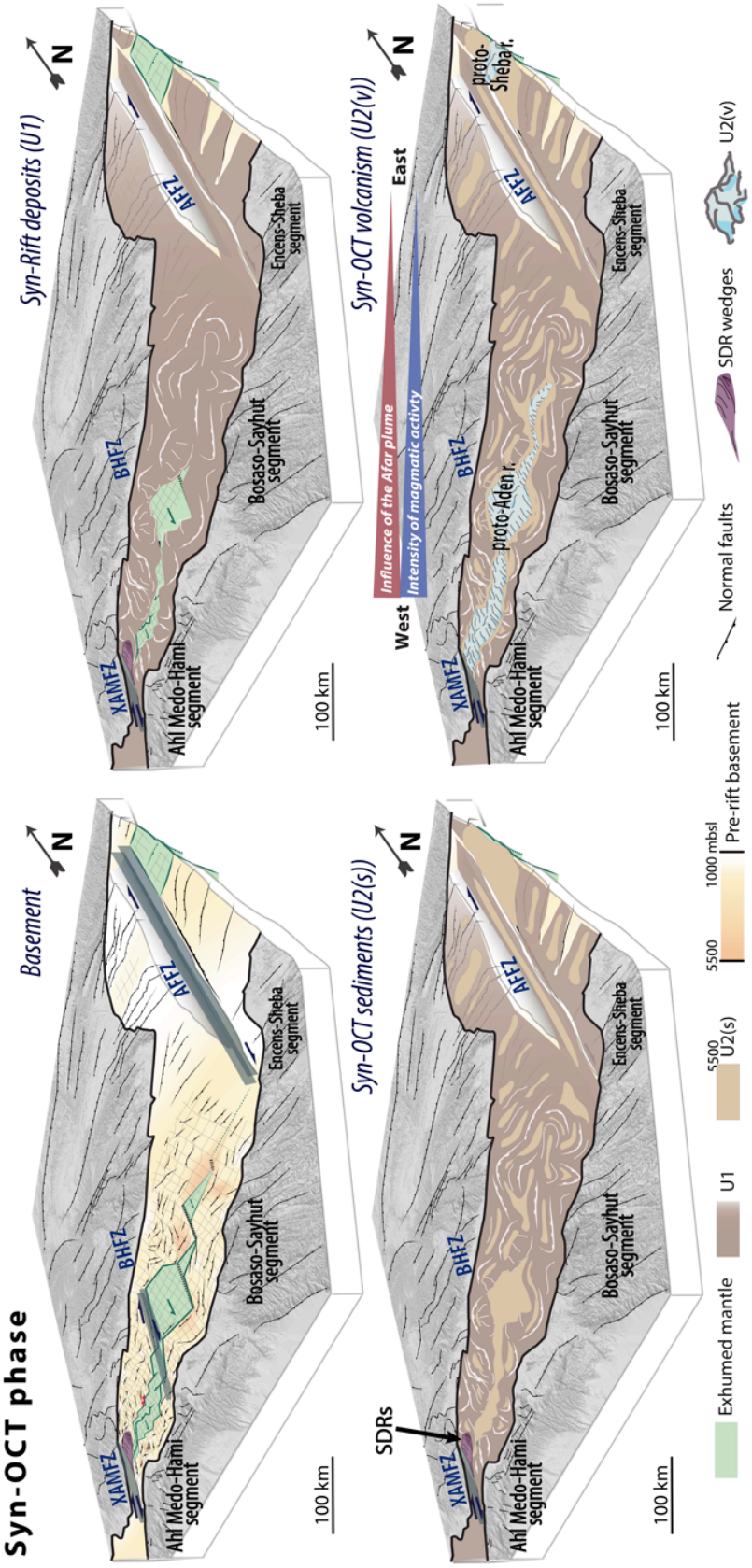


*Figure 13 – Synthetic 3D diagram at the syn-OCT phase (Burdigalian) showing the basement structures, syn-rift deposits (U1), syn-OCT sediments (U2(s)) and syn-OCT volcanism (U2(v)) arrangement. The Xiis Al Mukalla Fracture Zone (XAMFZ), Bosaso-Hami Fracture Zone (BHFZ) and Alula Fartak Fracture Zone (AFFZ) are developed in offshore part of the conjugate margins and bound on either side the Ahl Medo-Hami and Bosaso-Sayhut segments. Offshore margins are narrower on the Ahl Medo-Hami segment (~100 km wide) than on the Bosaso-Sayhut segment (~150 – 200 km wide). Upper left panel: In the east of the BHFZ, the exhumation zone in the OCT seems to be wider than the surrounding. However, the interpretation of this area is highly speculative since the OCT is entirely covered by the volcanic unit U2(v) (lower right panel) that masks the deeper structures and does not allow proper observation of the detachment fault. Onshore topography is shaded (SRTM, Jarvis et al., 2008).*

936 *5.2.2 Volcanic to non-volcanic margins transition*

937 The difference between magma-rich and magma-poor rifted margins depends on the timing and amount of
938 magma involved in relation to lithospheric extension, breakup and plate separation (Courtillot et al., 1999; Sengör
939 and Burke, 1978; White and McKenzie, 1989; Coffin and Eldholm, 1994). Since the two end-member types of
940 continental margins have been studied separately, the transition from volcanic to non-volcanic margins has
941 attracted less attention and is not yet well understood. Indeed, the distinction between magma-rich and magma-
942 poor is still problematic in view of the occurrence of hybrid margins (Reston and Manatschal, 2011).

943 In the central Gulf of Aden, we identify syn-rift and also syn-OCT volcanism in the west (SDR prisms and
944 U2(v), Figs. 4.b, 7.a, 8, 10.a, 11), whereas we observe less volcanism and more syn-OCT sediments onlapping the
945 syn-rift units toward the east (U2(s) on profiles; Figs.9, 10.d). This is associated with decreasing depth to the top of
946 volcanic structures away from the BHFZ (Fig. 11.a). The free-air and Bouguer anomaly maps are in agreement with
947 these observations by displaying negative and positive anomalies, respectively, to the west and east of the BHFZ
948 in the northern continental domain (Fig. 12.a) (Ali and Watts, 2013). Indeed, this mismatch between the gravity
949 anomalies and the mapping of the continental domain can be explained by a greater amount of volcanism (likely
950 combined with other alteration processes as e.g. metamorphism or hydratation) that may have changed the
951 physical properties and signal of the continental basement (e.g. in the Norwegian margin; Péron-Pinvidic et al.,
952 2016). While the southern margin is not so well defined due to lack of data in the distal parts, volcanism is also
953 more developed in the western part than in the eastern part of the margins (Fig. 13.a). These observations show
954 that the conjugate margins evolve gradually from a more magmatic near the XAMFZ, characterized by significant
955 volcanism (Fig. 10.a) and the development of SDRs in the OCT (Figs. 11) to magma-poor to the east of the BHFZ
956 (Figs. 7 to 9, 10.b, c, d). We propose then that the central Gulf of Aden is composed of hybrid margins, transitional
957 between magma-rich and magma-poor margins in the western and eastern parts of the Gulf of Aden,
958 respectively (e.g. Leroy et al., 2012). Offshore Aden city, the margins are typical volcanic margins with syn-rift
959 thick SDRs and underplated bodies in the west (Ahmed et al., 2013) whereas in the east volcanism occurred just
960 before the breakup (Lucazeau et al., 2009; Leroy et al., 2010b; Nonn et al., 2017). This hybrid-type margins has
961 also been described in West Greenland (Chalmers and Pulvertaft, 2001) or in the central domain of the
962 paleomargins of Pyrenean Cretaceous basin (at the transition between a cooler western domain and a hotter
963 eastern domain; Clerc and Lagabrielle, 2014).

964 Near XAMFZ, the SDR wedges (Figs. 11.b, d) shows that magmatic extrusions occurred during the thinning
965 of the continental crust and the development syn-extrusive growth detachments (Planke et al., 2000; Geoffroy

et al., 2015). The SDRs developed seaward on top of the intruded continental crust and migrated progressively toward the future oceanic spreading centre (Geoffroy, 2005). However, wedge-shape horizons of the U2(v) unit towards the OCT ridge (dipping continentward, zoom 2 Fig. 8) indicate that the volcanic units were deposited during the up doming of the OCT ridge. The wedge-shape U2(v) unit dipping continentward is strongly similar to the Continentward Dipping Reflectors (CDRs) described by Gillard et al. (2017) in the Gulf of Guinea. It suggests an increase of the extrusive magmatic supply during the formation of the OCT above the exhumed basement. In the Yemeni margins, two volcanic sub-units are recorded on U2(v) unit in the OCT (Fig. 8.a) and may be interpreted as two volcanic pulses in the OCT. Our results show that the stage of mantle exhumation is accompanied or followed quickly by the establishment of volcanic activity (Fig. 13), as proposed in the Iberian-Newfoundland margins by Shillington et al., (2006) or in the Tyrrhenian basin by Prada et al., (2016) and in the eastern part of the Gulf of Aden by Autin et al., (2010a). Thus, we highlight a gradual eastward decline in the amount of volcanic activity and a diachronous emplacement of volcanism, which seem to appear later eastward along the hybrid conjugate margins of the central Gulf of Aden (Figs. 7 to 13). This assumption is in agreement with a greater influence of the Afar plume towards the west and the channelling of material coming from Afar plume along the main tectonic corridors (Leroy et al., 2010a, 2012) until a final lithospheric breakup.

A significant and localized volcanic supply in the OCT can contribute to focus the extension (e.g. Buck, 1991; Ebinger and Casey, 2001), while diffuse volcanic supply favours a distributed extension (e.g. Corti et al., 2003). Due to a higher thermal regime in the Ahl Medo-Hami segment than in the Bosaso-Sayhut segment, we suggest that the deformation is localized in the west and more diffuse in the east, leading to an early emplacement of the OCT in the west (Fig. 13). The higher thermal regime and the greater degree of rift localisation in the Ahl Medo-Hami segment are consistent with a greater influence of the Afar plume westward (Leroy et al., 2010a). It is also accompanied by (i) the more elevated topography of the basement on both margins (Fig. 9.b); (ii) the greater amount of volcanism in the continental, transitional and oceanic domains (as shown by the higher topography of the volcanic substratum westward (Figs. 4.b, 11.a) volcanic structures on seismic line 1S, Fig. 10.a) and (iii) by a narrower OCT to the west of the BHFZ (Figs. 5, 13).

*5.2.3 Syn-OCT uplift*

Ali and Watts (2013) have argued by wells backstripping and gravity modelling that the Yemeni margin was underplated by magmatic material during rifting of the Gulf of Aden and that an uplift event could have been

superimposed. During the OCT formation, the distal margins located near AFFZ record significant erosion (see red square, Fig. 9.b). Indeed, a significant block was individualized and rotated toward the ocean during the rifting process. During this period, the syn-rift units R1 and R2 deposited in the newly formed half-graben (Fig. 9.c). Later, the deposited units were affected by normal faults rooted on the units R1(a) and sealed by the discontinuity D1. The head of this block was eroded during the syn-OCT stage (Fig. 9.c) and is coeval with the filling of the basin with the syn-OCT unit U2. In the eastern Gulf of Aden a major regional uplift occurred at the end of the OCT formation (Leroy et al., 2012; Nonn et al., 2017).

We propose that this erosion also occurred in the central Gulf of Aden and may have eroded distal margins near the AFFZ, suggesting a shallow basement at the time of the OCT formation. The locally buoyant mantle (Bellahsen et al., 2013a) and the thinning of the crust could induce dynamic topography and uplift of the margin. These buoyancy forces may have been enhanced (i) by the crustal breakup (rift-induced decompression melting associated with the development of large-scale low-angle detachment faults exhuming subcontinental mantle in the OCT; White and McKenzie, 1989; Driscoll and Karner, 1998), (ii) by the rift dynamics and by the channelling of Afar plume material along the major transform zones as proposed by Leroy et al., (2010a) and/or (iii) by small-scale convection in the lower mantle induced by the lithosphere showing various ages and thicknesses on either side of transform fault zones (i.e. XAMFZ, BHFZ or AFFZ; Korostelev et al., 2015a, 2016). The onshore Cenozoic volcanism (Fantozzi, 1996; Leroy et al., 2010b) outcropping at the edge of the BHFZ and AFFZ (Fig. 2) is also compatible with the channelling of material coming from Afar plume along the main fracture zones.

### 5.3 Tectono-sedimentary evolution of hybrid-type margins

In this section, we propose a chronological interpretation of the sedimentary sequences on the deep margin is constructed using the onshore observations and dating results (Fig. 3).

During the stretching phase (Rupelian-Chattian, Fig. 3) the first syn-rift unit (R1 corresponding to Buwaysh Fm or Ghaydah Fm on the onshore and offshore Yemeni margin, respectively and to Scimi Fm or Lower Bandar-Harshau Fm. on the onshore and offshore Somalian margin, respectively; Fig. 3) is deposited in a continental environment under episodic hyper-saline conditions (Bott et al., 1992). During the thinning phase (Lavier and Manatschal, 2006) (Fig. 3), the R1(a) unit acts as a layer for the decoupling of syn-rift units over the basement (Figs. 4, 6 to 8, 9.a, 10.c). The Upper-Chattian – Aquitanian is marked by the accumulation of deep-marine deposits (R2 in this study; Fuwwah Fm (onshore), Hami Fm (offshore) on the Yemeni margins; Scusciuban or

Dubar Fm (onshore) and Bandar Harshau (offshore) on the Somalian margin; Fig. 3) within the syn-rift basins. Two tectonic subsidence events are recorded: (i) the deposition of R2(a) in N70°E-trending syn-rift basins (Fig. 5.c), mainly on the distal margins; (2) the increased deepening of the margins and the deposition of the R2(b) subunit all along the margins (e.g. Fig. 4). The eastward-dipping deposition profile which is acquired since the Jurassic (Figs. 5.a, b) (Luger et al., 1994) is a sedimentary pattern of the conjugate margins.

During the OCT formation, the conjugate margins are affected by late tilting and steepening of the margin slope, provoking erosion of the onshore domains which supplies sediments supply to the distal margins (Platel and Roger, 1989; Autin et al., 2010b; Razin et al., 2010; Leroy et al., 2012). Flat syn-OCT sediments (U2(s); Figs. 7 to 11) are deposited on both margins and onlap the OCT ridge on the northern margin (Figs. 7, 8).

The post-rift phase starts when an oceanic ridge is established in the asthenosphere, leading to steady-state oceanic spreading (Cannat et al., 2009). The post-rift sequence (U3 to U5, Figs. 3, 4, 7 to 10, 11.b) is thicker on the northern margin (up to 4000 m) than on the southern side (up to 1600 m). We argue that this difference may be due to tectonic factors (less subsidence on the southern margin) or environmental factors (poor drainage network in Somalian margin). According to (Watchorn et al., 1998), the post-rift sequence records at least three uplift pulses. We link first the uplift event to the end of the syn-OCT stage. Then the deposition of the U3 in distal parts of the margins occurred (Figs. 7.a, 8 to 10, 11.b), similar to the U3 unit recorded in the eastern Gulf of Aden (Autin et al., 2010b; d'Acremont et al., 2005; Bache et al., 2011; Leroy et al., 2012). If this event is synchronous throughout the Gulf of Aden, U3 could have been deposited between 17.6 and 10 Ma (Bache et al., 2011). However, U3 in the eastern Gulf of Aden displays more frequent occurrence of MTCs than the central margin unit. This discrepancy may be explained by increased subsidence and destabilization of the eastern margin (Leroy et al., 2012). Finally, the top of U3 is an erosional discontinuity (D3, Figs. 7.a, 8 to 10, 11.b) that we correlate to the second uplift recorded by Watchorn et al. (1998). A new subsidence phase (younger than 10 Ma) allows the deposition of U4 defined by the sudden occurrence of current-formed features that indicate an intensification of hydrodynamic regime. These features are consistent with a deep-sea domain and clearly imply the steepening of the margin slope as observed in the eastern Gulf of Aden (Ziegler, 2001; Bache et al., 2009; Baurion, 2012). The presence of significant progradations in the Bosaso-Sayhut segment (Fig. 9.a) suggests that deepening increases toward the east. U3 and U4 are tilted and faulted and the top of U4 is eroded, especially toward the continent (discontinuity D4, Figs. 7.a, 8, 9). This event can be correlated with the third uplift pulse recorded by sediments onlap (Watchorn et al., 1998). All these observations are interpreted as being related to a major uplift also recorded in the eastern Gulf of Aden

(Platel and Roger, 1989; Bache et al., 2011; Leroy et al., 2012; Nonn et al., 2017). Finally, U5 is characterized by sub-parallel deposits onlapping the eroded U4 and sealed at the surface by the present-day seabed (Figs.4, 7 to 11).

## 5. Conclusion

Our analysis of marine geophysical and geological data from the central Gulf of Aden contributes to a better understanding of the formation of hybrid margins system located at the transition between volcanic margins (offshore Aden city) and magma-poor margins in the east. We determine seismic stratigraphy and structural patterns and map the three main crustal domains (continental, Ocean-Continent Transition (OCT), oceanic domains) in order to propose a tectonic evolution of the Yemeni and Somalian conjugate margins. This study reveals that the conjugate margins formed during the oblique rifting of the central Gulf of Aden are narrow, asymmetrical (as the continental domain and the OCT of the southern margin is narrower than the northern one) and highly segmented. We highlight an eastward gradual decrease in intensity of magmatic activity and a diachronous set up of volcanic formations related to a strong influence of hot material coming probably from the Afar plume. At the western boundary of the studied zone near the XAMFZ, magmatic processes are predominant. The higher thermal regime is associated with the development of SDRs wedges from the late phase of the thinning of the continental crust (early Miocene-~21 Ma) up to the exhumation phase (Burdigalian-~18 Ma) that lead to the OCT development. Farther east, tectonic processes are predominant and evidence of volcanism appears later eastward, occurring during and shortly after the unroofing of sub-continental mantle along low-angle detachment faults (Burdigalian) in the OCT basement. The early syn-rift phase (Oligocene) is marked by the development of the main segmentation (XAMFZ, BHFZ and AFFZ). Between the XAMFZ and the BHFZ, the Ahl Medo-Hami segment (in the western part) experiences a greater influence of the Afar plume than the Bosaso-Sayhut segment between the BHFZ and the AFFZ (in the eastern part). The central Gulf of Aden is subject to a major uplift during the final syn-rift stage and up to OCT emplacement, associated with a major erosion in the east and gravitational deformation taking place on decoupling surfaces at the base of the syn-rift sequence (lower Ghaydah Fm) in the west.

## Acknowledgments

Partnership - TOTAL - UNIVERSITE PIERRE ET MARIE CURIE - CENTRE NATIONAL DE LA RECHERCHE SCIENTIFIQUE. This study is a contribution from Actions Marges (Total, CNRS-INSU, IFREMER and BRGM). We

are especially grateful to Total S.A. for their support during the project. We thank Thomas Maurin, Xavier du Bernard for valuable discussions. We are grateful to the editor Adam Bumby and the anonymous reviewer for their very helpful comments improving the manuscript. Dr M.S.N. Carpenter post-edited the English style and grammar.

**Bibliography**

Ahlbrandt, T.S., 2002. Madbi Amran/Qishn Total Petroleum System of the Ma'Rib-Al Jawf/Shabwah, and Masila-Jeza Basins, 1st ed. U.S. Geological Survey Bulletin.

Ahmed, A., Leroy, S., Keir, D., Korostelev, F., Khanbari, K., Rolandone, F., Stuart, G., Obrebski, M., 2014. Crustal structure of the Gulf of Aden southern margin: Evidence from receiver functions on Socotra Island (Yemen). Tectonophysics 637, 251–267. https://doi.org/10.1016/j.tecto.2014.10.014

Ahmed, A., Tiberi, C., Leroy, S., Stuart, G.W., Keir, D., Sholan, J., Khanbari, K., Al-Ganad, I., Basuyau, C., 2013. Crustal structure of the rifted volcanic margins and uplifted plateau of Western Yemen from receiver function analysis. Geophys. J. Int. 193, 1673–1690. https://doi.org/10.1093/gji/ggt072

Ali Kassim, M., 1991. Oligo-Miocene sedimentation in the Boosaaso and Qandala Basin, Gulf of Aden, NE Somalia. Geol. Basamento Ital. - Convegno Onore Tommaso Cocozza 87.

Ali, M.Y., 2015. Petroleum Geology and Hydrocarbon Potential of the Guban Basin, Northern Somaliland. J. Pet. Geol. 38, 433–457. https://doi.org/10.1111/jpg.12620

Ali, M.Y., Watts, A.B., 2016. Tectonic evolution of sedimentary basins of northern Somalia. Basin Res. 28, 340–364. https://doi.org/10.1111/bre.12113

Ali, M.Y., Watts, A.B., 2013. Subsidence history, crustal structure, and evolution of the Somaliland-Yemen conjugate margin. J. Geophys. Res. Solid Earth 118, 1638–1649. https://doi.org/10.1002/jgrb.50113

As-Saruri, M.A., Sorkhabi, R., Baraba, R., 2010. Sedimentary basins of Yemen: their tectonic development and lithostratigraphic cover. Arab. J. Geosci. 3, 515–527. https://doi.org/10.1007/s12517-010-0189-z

Autin, J., Bellahsen, N., Husson, L., Beslier, M.O., Leroy, S., d'Acremont, E., 2010a. Analog models of oblique rifting in a cold lithosphere. Tectonics 29, TC6016, doi:10.1029/2010TC002671.

Autin, J., Bellahsen, N., Leroy, S., Husson, L., Beslier, M.-O., d'Acremont, E., 2013. The role of structural inheritance in oblique rifting: Insights from analogue models and application to the Gulf of Aden. Tectonophysics, The Gulf of Aden rifted margins system : Special Issue dedicated to the YOCMAL project (Young Conjugate Margins Laboratory in the Gulf of Aden) 607, 51–64. https://doi.org/10.1016/j.tecto.2013.05.041

Autin, J., Leroy, S., Beslier, M.-O., D'Acremont, E., Razin, P., Ribodetti, A., Bellahsen, N., Robin, C., Al Toubi, K., 2010b. Continental break-up history of a deep magma-poor margin based on seismic reflection data (northeastern Gulf of Aden margin, offshore Oman). Geophys. J. Int. 180, 501–519. https://doi.org/10.1111/j.1365-246X.2009.04424.x

Azzaroli, A., 1958. L'oligocene e il Miocene della Somalia: stratigrafia, tettonica, paleontologia (macroforaminiferi, coralli, molluschi), Paleontolongia Italiana. Tipografia moderna, Pisa.

Bache, F., Leroy, S., Baurion, C., Robinet, J., Gorini, C., Lucazeau, F., Razin, P., d'Acremont, E., Al-Toubi, K., 2011. Post-rift uplift of the Dhofar margin (Gulf of Aden). Terra Nova 23, 11–18. https://doi.org/10.1111/j.1365-3121.2010.00975.x

Bache, F., Olivet, J.L., Gorini, C., Rabineau, M., Baztan, J., Aslanian, D., Suc, J.P., 2009. Messinian erosional and salinity crises: View from the Provence Basin (Gulf of Lions, Western Mediterranean). Earth Planet. Sci. Lett. 286, 139–157.

Baurion, C., 2012. Architecture sédimentaire et dynamique post-rift des marges conjuguées du Golfe d'Aden oriental. Université Pierre et Marie Curie (Paris VI), Paris.

Bellahsen, N., Husson, L., Autin, J., Leroy, S., d'Acremont, E., 2013a. The effect of thermal weakening and buoyancy forces on rift localization: Field evidences from the Gulf of Aden oblique rifting. Tectonophysics, The Gulf of Aden rifted margins system : Special Issue dedicated to the YOCMAL project (Young Conjugate Margins Laboratory in the Gulf of Aden) 607, 80–97. https://doi.org/10.1016/j.tecto.2013.05.042

Bellahsen, N., Leroy, S., Autin, J., Razin, P., d'Acremont, E., Sloan, H., Pik, R., Ahmed, A., Khanbari, K., 2013b. Pre-existing oblique transfer zones and transfer/transform relationships in continental margins: New insights from the southeastern Gulf of Aden, Socotra Island, Yemen. Tectonophysics, The Gulf of Aden rifted margins system : Special Issue dedicated to the YOCMAL project (Young Conjugate Margins Laboratory in the Gulf of Aden) 607, 32–50. https://doi.org/10.1016/j.tecto.2013.07.036

Beslier, M.-O., Cornen, G., Girardeau, J., 1996. Tectono-metamorphic evolution of peridotites from the ocean/continent transition of the Iberia Abyssal Plain margin. Proc. Ocean Drill. Program Sci. Results 149, 397–412. https://doi.org/10.2973/odp.proc.sr.149.218.1996

Beydoun, Z.R., 1997. Introduction to the revised Mesozoic stratigraphy and nomenclature for Yemen. Mar. Pet. Geol., Special Issue on Mesozoic Rift Basins of Yemen 14, 617–629. https://doi.org/10.1016/S0264-8172(96)00049-9

Beydoun, Z.R., 1970. Southern Arabia and Northern Somalia: Comparative Geology. Philos. Trans. R. Soc. Lond. Math. Phys. Eng. Sci. 267, 267–292. https://doi.org/10.1098/rsta.1970.0036

Beydoun, Z.R., As-Saruri, M.A.L., El-Nakhal, H., Al-Ganad, I.N., Baraba, R.S., Nani, A., Al-Aawah, M.H., 1998. International lexicon of stratigraphy : Republic of Yemen. 3, Asia, fasc 10 b 2. IUGS and Ministry of Oil and Mineral Resources, Republic of Yemen.

Beydoun, Z.R., As-Saruri, M.L., Baraba, R.S., 1996. Sedimentary Basins of the Republic of Yemen : Their Structural Evolution and Geological Characteristics. Oil Gas Sci. Technol. - Rev IFP 51, 763–775.

Birse, A.C.R., Bott, W.F., Morrison, J., Samuel, M.A., 1997. The Mesozoic and early tertiary tectonic evolution of the Socotra area, eastern Gulf of Aden, Yemen. Mar. Pet. Geol., Special Issue on Mesozoic Rift Basins of Yemen 14, 675–684. https://doi.org/10.1016/S0264-8172(96)00043-8

Boillot, G., Féraud, G., Recq, M., Girardeau, J., 1989. Undercrusting by serpentinite beneath rifted margins. Nature 6242.

Boillot, G., Grimaud, S., Mauffret, A., Mougenot, D., Kornprobst, J., Mergoil-Daniel, J., Torrent, G., 1980. Ocean-continent boundary off the Iberian margin: A serpentinite diapir west of the Galicia Bank. Earth Planet. Sci. Lett. 48, 23–34. https://doi.org/10.1016/0012-821X(80)90166-1

Bosence, D., Nichols, G., Al-Subbary, A.-K., Al-Thour, K.A., Reeder, M., 1996. Synrift continental to marine depositional sequences, Tertiary, Gulf of Aden, Yemen. J. Sediment. Res. 66, 766–777. https://doi.org/10.1306/D4268400-2B26-11D7-8648000102C1865D

Bosence, D.W.J., 1997. Mesozoic rift basins of Yemen. Mar. Pet. Geol., Special Issue on Mesozoic Rift Basins of Yemen 14, 611-IN6. https://doi.org/10.1016/S0264-8172(97)00039-1

Bosworth, W., Huchon, P., McClay, K., 2005. The Red Sea and Gulf of Aden Basins. J. Afr. Earth Sci. 43, 334–378. https://doi.org/:10.1016/j.jafrearsci.2005.07.020

Bott, W. f., Smith, B. a., Oakes, G., Sikander, A.H., Ibraham, A.I., 1992. The Tectonic Framework and Regional Hydrocarbon Prospectivity of the Gulf of Aden. J. Pet. Geol. 15, 211-243. https://doi.org/10.1111/j.1747-5457.1992.tb00963.x

Brannan, J., Gerdes, K.D., Newth, I.R., 1997. Tectono-stratigraphic development of the Qamar basin, eastern Yemen. Mar. Pet. Geol., Special Issue on Mesozoic Rift Basins of Yemen 14, 701-IN12. https://doi.org/10.1016/S0264-8172(96)00048-7

Brichau, S., Ring, U., Carter, A., Monié, P., Bolhar, R., Stockli, D., Brunel, M., 2007. Extensional faulting on Tinos Island, Aegean Sea, Greece: How many detachments? Tectonics 26, TC4009. https://doi.org/10.1029/2006TC001969

Buck, W.R., 1991. Modes of continental lithospheric extension. J. Geophys. Res. Solid Earth 96, 20,161-20,178. https://doi.org/10.1029/91JB01485

Cannat, M., Manatschal, G., Sauter, D., Péron-Pinvidic, G., 2009. Assessing the conditions of continental breakup at magma-poor rifted margins: What can we learn from slow spreading mid-ocean ridges? Comptes Rendus Geosci., Transition Océan-Continent 341, 406–427. https://doi.org/10.1016/j.crte.2009.01.005

Chalmers, J.A., Pulvertaft, T.C.R., 2001. Development of the continental margins of the Labrador Sea: a review. Geol. Soc. Lond. Spec. Publ. 187, 77–105. https://doi.org/10.1144/GSL.SP.2001.187.01.05

Clerc, C., Lagabrielle, Y., 2014. Thermal control on the modes of crustal thinning leading to mantle exhumation: Insights from the Cretaceous Pyrenean hot paleomargins. Tectonics 33, 2013TC003471. https://doi.org/10.1002/2013TC003471

Clerc, C., Lagabrielle, Y., Labaume, P., Ringenbach, J.-C., Vauchez, A., Nalpas, T., Bousquet, R., Ballard, J.-F., Lahfid, A., Fourcade, S., 2016. Basement – Cover decoupling and progressive exhumation of metamorphic sediments at hot rifted margin. Insights from the Northeastern Pyrenean analog. Tectonophysics 686, 82–97. https://doi.org/10.1016/j.tecto.2016.07.022

Coffin, M.F., Eldholm, O., 1994. Large igneous provinces: Crustal structure, dimensions, and external consequences. Rev. Geophys. 32, 1–36. https://doi.org/10.1029/93RG02508

Corti, G., Bonini, M., Conticelli, S., Innocenti, F., Manetti, P., Sokoutis, D., 2003. Analogue modelling of continental extension: a review focused on the relations between the patterns of deformation and the presence of magma. Earth-Sci. Rev. 63, 169–247. https://doi.org/10.1016/S0012-8252(03)00035-7

Courtillot, V., Jaupart, C., Manighetti, I., Tapponnier, P., Besse, J., 1999. On causal links between flood basalts and continental breakup. Earth Planet. Sci. Lett. 166, 177–195. https://doi.org/10.1016/S0012-821X(98)00282-9

d'Acremont, E., Leroy, S., Beslier, M.-O., Bellahsen, N., Fournier, M., Robin, C., Maia, M., Gente, P., 2005. Structure and evolution of the eastern Gulf of Aden conjugate margins from seismic reflection data. Geophys. J. Int. 160, 869–890. https://doi.org/10.1111/j.1365-246X.2005.02524.x

d'Acremont, E., Leroy, S., Maia, M., Gente, P., Autin, J., 2010. Volcanism, jump and propagation on the Sheba ridge, eastern Gulf of Aden: segmentation evolution and implications for oceanic accretion processes. Geophys. J. Int. 180, 535–551. https://doi.org/10.1111/j.1365-246X.2009.04448.x

d'Acremont, E., Leroy, S., Maia, M., Patriat, P., Beslier, M.-O., Bellahsen, N., Fournier, M., Gente, P., 2006. Structure and evolution of the eastern Gulf of Aden: insights from magnetic and gravity data (Encens-Sheba MD117 cruise). Geophys. J. Int. 165, 786–803. https://doi.org/10.1111/j.1365-246X.2006.02950.x

Direen, N.G., Stagg, H.M.J., Symonds, P.A., Colwell, J.B., 2011. Dominant symmetry of a conjugate southern Australian and East Antarctic magma-poor rifted margin segment. Geochem. Geophys. Geosystems 12, Q02006. https://doi.org/10.1029/2010GC003306

Dix, C.H., 1955. Seismic velocities from surface measurements. Geophysics 20, 68–86. https://doi.org/10.1190/1.1438126

Drewes, H., Hornik, H., Adams, J., Szabolcs, R., 2012. The International Gravimetric Bureau. In: "IAG Goedesist's handbook 2012." J. Geod., springer 86, 787–974. https://doi.org/10.1007/s00190-012-0584-1

Driscoll, N.W., Karner, G.D., 1998. Lower crustal extension across the Northern Carnarvon basin, Australia: Evidence for an eastward dipping detachment. J. Geophys. Res. Solid Earth 103, 4975–4991. https://doi.org/10.1029/97JB03295

Duval, B., Cramez, C., Jackson, M.P.A., 1992. Raft tectonics in the Kwanza Basin, Angola. Mar. Pet. Geol. 9, 389–404. https://doi.org/10.1016/0264-8172(92)90050-O

Ebinger, C.J., Casey, M., 2001. Continental breakup in magmatic provinces: An Ethiopian example. Geology 29, 527–530. https://doi.org/10.1130/0091-7613(2001)029<0527:CBIMPA>2.0.CO;2

Ellis, A.C., Kerr, H.M., Cornwell, C.P., Williams, D.O., 1996. A tectono-stratigraphic framework for Yemen and its implications for hydrocarbon potential. Pet. Geosci. 2, 29–42.

1225 Espurt, N., Callot, J.-P., Roure, F., Totterdell, J.M., Struckmeyer, H.I.M., Vially, R., 2012. Transition from
1226 symmetry to asymmetry during continental rifting: an example from the Bight Basin–Terre Adélie
1227 (Australian and Antarctic conjugate margins). Terra Nova 24, 167–180. https://doi.org/10.1111/j.1365-
1228 3121.2011.01055.x

1229 Espurt, N., Callot, J.-P., Totterdell, J., Struckmeyer, H., Vially, R., 2009. Interactions between continental
1230 breakup dynamics and large-scale delta system evolution: Insights from the Cretaceous Ceduna delta
1231 system, Bight Basin, Southern Australian margin. Tectonics 28, TC6002.
1232 https://doi.org/10.1029/2009TC002447

1233 Fantozzi, P.L., 1996. Transition from continental to oceanic rifting in the Gulf of Aden: structural evidence from
1234 field mapping in Somalia and Yemen. Tectonophysics 259, 285–311. https://doi.org/10.1016/0040-
1235 1951(95)00208-1

1236 Fantozzi, P.L., Ali-Kassim, M., 2002. Geological mapping in northeastern Somalia (Midjiurtinia region): Field
1237 evidence of the structural and paleogeographic evolution of the northern margin of the Somalian plate. J.
1238 Afr. Earth Sci., Horn of Africa 34, 21–55. https://doi.org/10.1016/S0899-5362(01)00100-2

1239 Fantozzi, P.L., Sgavetti, M., 1998. Tectonic and sedimentary evolution of the eastern Gulf of Aden continental
1240 margins: new structural and stratigraphic data from Somalia and Yemen, in: Purser, B., Bosence, D.J. (Eds.),
1241 Sedimentation and Tectonics in Rift Basins Red Sea:- Gulf of Aden. Springer Netherlands, pp. 56–76.

1242 Fort, X., Brun, J.-P., Chauvel, F., 2004. Salt tectonics on the Angolan margin, synsedimentary deformation
1243 processes. AAPG Bull. 88, 1523–1544. https://doi.org/10.1306/06010403012

1244 Fournier, M., Patriat, P., Leroy, S., 2001. Reappraisal of the Arabia-India-Somalia Triple Junction kinematics.
1245 Earth Planet Sci Lett 189, 103–114.

1246 Geoffroy, L., 2005. Volcanic passive margins. Comptes Rendus Geosci. 337, 1395–1408.
1247 https://doi.org/10.1016/j.crte.2005.10.006

1248 Geoffroy, L., Burov, E.B., Werner, P., 2015. Volcanic passive margins: another way to break up continents. Sci.
1249 Rep. 5. https://doi.org/10.1038/srep14828

1250 Gillard, M., 2015. Tectonomagmatic evolution of the final stages of rifting along the deep conjugate Australian-
1251 Antarctic magma-poor rifted margins: Constraints from seismic observations: Australian-Antarctic margins
1252 evolution. Tectonics 34. https://doi.org/10.1002/2015TC003850

1253 Gillard, M., Manatschal, G., Autin, J., 2016. How can asymmetric detachment faults generate symmetric Ocean
1254 Continent Transitions? Terra Nova 28, 27–34. https://doi.org/10.1111/ter.12183

1255 Gillard, M., Sauter, D., Tugend, J., Tomasi, S., Epin, M.-E., Manatschal, G., 2017. Birth of an oceanic spreading
1256 center at a magma-poor rift system. Sci. Rep. 7, 15072. https://doi.org/10.1038/s41598-017-15522-2

1257 Hakimi, M.H., Abdulah, W.H., Shalaby, M.R., 2010. Organic Geochemistry, Burial History and Hydrocarbon
1258 Generation Modelling of the Upper Jurassic Madbi Formation, Masila Basin, Yemen. J. Pet. Geol. 33, 299–
1259 318. https://doi.org/10.1111/j.1747-5457.2010.00481.x

1260 Hayward, N.J., Ebinger, C.J., 1996. Variations in the along-axis segmentation of the Afar Rift system. Tectonics
1261 15, 244–257. https://doi.org/10.1029/95TC02292

1262 Huchon, P., Khanbari, K., 2003. Rotation of the syn-rift stress field of the northern Gulf of Aden margin, Yemen.
1263 Tectonophysics 364, 147–166. https://doi.org/10.1016/S0040-1951(03)00056-8

1264 Hughes, G.W., Beydoun, Z.R., 1992. The Red Sea — Gulf of Aden: Biostratigraphy, Lithostratigraphy and
1265 Palaeoenvironments. J. Pet. Geol. 15, 135–156. https://doi.org/10.1111/j.1747-5457.1992.tb00959.x

1266 Jammes, S., Tiberi, C., Manatschal, G., 2010. 3D architecture of a complex transcurrent rift system: The
1267 example of the Bay of Biscay–Western Pyrenees. Tectonophysics 489, 210–226.
1268 https://doi.org/10.1016/j.tecto.2010.04.023

1269 Jarvis, A., Reuter, H.I., Nelson, A., Guevara, E., 2008. Hole-filled SRTM for the globe Version 4, available from
1270 the CGIAR-CSI SRTM 90m Database.

1271 Jestin, F., Huchon, P., Gaulier, J.M., 1994. The Somalia plate and the East African Rift System: present-day
1272 kinematics. Geophys. J. Int. 116, 637–654. https://doi.org/10.1111/j.1365-246X.1994.tb03286.x

Jolivet, L., Gorini, C., Smit, J., Leroy, S., 2015. Continental breakup and the dynamics of rifting in back-arc basins: The Gulf of Lion margin. Tectonics 34, 662–679. https://doi.org/10.1002/2014TC003570

Kane, K.E., Jackson, C.A.-L., Larsen, E., 2010. Normal fault growth and fault-related folding in a salt-influenced rift basin: South Viking Graben, offshore Norway. J. Struct. Geol. 32, 490–506. https://doi.org/10.1016/j.jsg.2010.02.005

Karner, G.D., Driscoll, N.W., McGinnis, J.P., Brumbaugh, W.D., Cameron, N.R., 1997. Tectonic significance of syn-rift sediment packages across the Gabon-Cabinda continental margin. Mar. Pet. Geol. 14, 973–1000. https://doi.org/10.1016/S0264-8172(97)00040-8

Korostelev, F., Leroy, S., Keir, D., Ahmed, A., Boschi, L., Rolandone, F., Stuart, G.W., Obrebski, M., Khanbari, K., El-Hussain, I., 2015. Upper mantle structure of the southern Arabian margin: Insights from teleseismic tomography. Geosphere 11, 1262–1278. https://doi.org/10.1130/GES01159.1

Korostelev, F., Leroy, S., Keir, D., Weemstra, C., Boschi, L., Molinari, I., Ahmed, A., Stuart, G.W., Rolandone, F., Khanbari, K., Al-Lazki, A., 2016. Magmatism at continental passive margins inferred from Ambient-Noise Phase-velocity in the Gulf of Aden. Terra Nova 28, 19–26. https://doi.org/10.1111/ter.12182

Kröner, A., Sassi, F.P., 1996. Evolution of the northern Somali basement: new constraints from zircon ages. J. Afr. Earth Sci. 22, 1–15. https://doi.org/10.1016/0899-5362(95)00121-2

Lagabrielle, Y., 2009. Mantle exhumation and lithospheric spreading: An historical perspective from investigations in the Oceans and in the Alps-Apennines ophiolites. Boll. Della Soc. Geol. Ital. 128, 279–293. https://doi.org/10.3301/IJG.2009.128.2.279

Lagabrielle, Y., Labaume, P., de Saint Blanquat, M., 2010. Mantle exhumation, crustal denudation, and gravity tectonics during Cretaceous rifting in the Pyrenean realm (SW Europe): Insights from the geological setting of the lherzolite bodies. Tectonics 29, TC4012. https://doi.org/10.1029/2009TC002588

Lavier, L.L., Manatschal, G., 2006. A mechanism to thin the continental lithosphere at magma-poor margins. Nature 440, 324–328. https://doi.org/10.1038/nature04608

Leroy, S., d'Acremont, E., Tiberi, C., Basuyau, C., Autin, J., Lucazeau, F., Sloan, H., 2010a. Recent off-axis volcanism in the eastern Gulf of Aden: Implications for plume–ridge interaction. Earth Planet. Sci. Lett., b 293, 140–153. https://doi.org/10.1016/j.epsl.2010.02.036

Leroy, S., Gente, P., Fournier, M., D'Acremont, E., Patriat, P., Beslier, M.-O., Bellahsen, N., Maia, M., Blais, A., Perrot, J., Al-Kathiri, A., Merkouriev, S., Fleury, J.-M., Ruellan, P.-Y., Lepvrier, C., Huchon, P., 2004. From rifting to spreading in the eastern Gulf of Aden: a geophysical survey of a young oceanic basin from margin to margin. Terra Nova 16, 185–192. https://doi.org/10.1111/j.1365-3121.2004.00550.x

Leroy, S., Lucazeau, F., d'Acremont, E., Watremez, L., Autin, J., Rouzo, S., Bellahsen, N., Tiberi, C., Ebinger, C., Beslier, M.-O., Perrot, J., Razin, P., Rolandone, F., Sloan, H., Stuart, G., Al-Lazki, A., Al-Toubi, K., Bache, F., Bonneville, A., Goutorbe, B., Huchon, P., Unternehr, P., Khanbari, K., 2010b. Contrasted styles of rifting in the eastern Gulf of Aden: A combined wide-angle, multichannel seismic, and heat flow survey. Geochem. Geophys. Geosystems 11, Q07004. https://doi.org/10.1029/2009GC002963

Leroy, S., Razin, P., Autin, J., Bache, F., d'Acremont, E., Watremez, L., Robinet, J., Baurion, C., Denèle, Y., Bellahsen, N., Lucazeau, F., Rolandone, F., Rouzo, S., Kiel, J.S., Robin, C., Guillocheau, F., Tiberi, C., Basuyau, C., Beslier, M.-O., Ebinger, C., Stuart, G., Ahmed, A., Khanbari, K., Al-Ganad, I., Clarens, P. de, Unternehr, P., Al-Toubi, K., Al-Lazki, A., 2012. From rifting to oceanic spreading in the Gulf of Aden: a synthesis. Arab. J. Geosci., Frontiers in Earth Sciences 5, 859–901. https://doi.org/10.1007/s12517-011-0476-3

Lister, G.S., Etheridge, M.A., Symonds, P.A., 1986. Detachment faulting and the evolution of passive continental margins. Geology 14, 246–250. https://doi.org/10.1130/0091-7613(1986)14<246:DFATEO>2.0.CO;2

Lucazeau, F., Leroy, S., Autin, J., Bonneville, A., Goutorbe, B., Watremez, L., D'Acremont, E., Düsünur, D., Rolandone, F., Huchon, P., Bellahsen, N., Tuchais, P., 2009. Post-rift volcanism and high heat-flow at the ocean-continent transition of the eastern Gulf of Aden. Terra Nova 21, 285–292. https://doi.org/10.1111/j.1365-3121.2009.00883.x

Luger, P., Gröschke, M., Bussmann, M., Dina, A., Mette, W., Uhmann, A., Kallenbach, H., 1994. Comparison of the Jurassic and Cretaceous sedimentary cycles of Somalia and Madagascar: implications for the Gondwana breakup. Geol. Rundsch. 83, 711–727. https://doi.org/10.1007/BF00251070

Masini, E., Manatschal, G., Tugend, J., Mohn, G., Flament, J.-M., 2014. The tectono-sedimentary evolution of a hyper-extended rift basin: the example of the Arzacq–Mauléon rift system (Western Pyrenees, SW France). Int. J. Earth Sci. 103, 1569–1596. https://doi.org/10.1007/s00531-014-1023-8

Menzies, M., Al-Kadasi, M., Al-Khirbash, S., A.K, A.-S., Baker, J., Blakey, S., Bosence, D., Davison, I., Dart, C., Owen, L., McClay, K.R., Nichols, G., Yelland, A., 1994. Geology of the Republic of Yemen. In: McCombe, D.A., Fernette, G.L., and Alawi, A.J. (compilers). The geological and mineral resources of Yemen. Ministry of Oil and Mineral Resources, Geology and Minerals Exploration Board,Yemen Mineral Sector Project, World Bank Technical Report.

Menzies, M., Baker, J., Bosence, D., Dart, C., Davison, I., Hurford, A., Al'Kadasi, M., McClay, K., Nichols, G., Al'Subbary, A., Yelland, A., 1992. The timing of magmatism, uplift and crustal extension: preliminary observations from Yemen. Geol. Soc. Lond. Spec. Publ. 68, 293–304. https://doi.org/10.1144/GSL.SP.1992.068.01.18

Menzies, M., Gallagher, K., Yelland, A., Hurford, A.J., 1997. Volcanic and nonvolcanic rifted margins of the Red Sea and Gulf of Aden: Crustal cooling and margin evolution in Yemen. Geochim. Cosmochim. Acta 61, 2511–2527.

Nichols, G., Watchorn, F., 1998. Climatic and geomorphic controls on rift sedimentation: Oligo-Miocene syn-rift facies in the Gulf of Aden, Yemen. Mar. Pet. Geol. 15, 505–518. https://doi.org/10.1016/S0264-8172(98)80001-9

Nonn, C., Leroy, S., Khanbari, K., Ahmed, A., 2017. Tectono-sedimentary evolution of the eastern Gulf of Aden conjugate passive margins: Narrowness and asymmetry in oblique rifting context. Tectonophysics 721, 322–348. https://doi.org/10.1016/j.tecto.2017.09.024

Péron-Pinvidic, G., Manatschal, G., Osmundsen, P.T., 2013. Structural comparison of archetypal Atlantic rifted margins: A review of observations and concepts. Mar. Pet. Geol. 43, 21–47. https://doi.org/10.1016/j.marpetgeo.2013.02.002

Péron-Pinvidic, G., Osmundsen, P.T., 2016. Architecture of the distal and outer domains of the Mid-Norwegian rifted margin: Insights from the Rån-Gjallar ridges system. Mar. Pet. Geol. 77, 280–299. https://doi.org/10.1016/j.marpetgeo.2016.06.014

Péron-Pinvidic, G., Osmundsen, P.T., Ebbing, J., 2016. Mismatch of geophysical datasets in distal rifted margin studies. Terra Nova 28, 340–347. https://doi.org/10.1111/ter.12226

Pickup, S.L.B., Whitmarsh, R.B., Fowler, C.M.R., Reston, T.J., 1996. Insight into the nature of the ocean-continent transition off West Iberia from a deep multichannel seismic reflection profile. Geology 24, 1079–1082. https://doi.org/10.1130/0091-7613(1996)024<1079:IITNOT>2.3.CO;2

Pik, R., Bellahsen, N., Leroy, S., Denèle, Y., Razin, P., Ahmed, A., Khanbari, K., 2013. Structural control of basement denudation during rifting revealed by low-temperature (U–Th–Sm)/He thermochronology of the Socotra Island basement—Southern Gulf of Aden margin. Tectonophysics, The Gulf of Aden rifted margins system : Special Issue dedicated to the YOCMAL project (Young Conjugate Margins Laboratory in the Gulf of Aden) 607, 17–31. https://doi.org/10.1016/j.tecto.2013.07.038

Planke, S., Symonds, P.A., Alvestad, E., Skogseid, J., 2000. Seismic volcanostratigraphy of large-volume basaltic extrusive complexes on rifted margins. J. Geophys. Res. Solid Earth 105, 19335–19351. https://doi.org/10.1029/1999JB900005

Platel, J.P., Roger, J., 1989. Evolution géodynamique du Dhofar (sultanat d'Oman) pendant le Crétace et le Tertiaire en relation avec l'ouverture du golfe d'Aden. Bull. Soc. Geol. Fr. V, 253–263. https://doi.org/10.2113/gssgfbull.V.2.253

Prada, M., Ranero, C.R., Sallarès, V., Zitellini, N., Grevemeyer, I., 2016. Mantle exhumation and sequence of magmatic events in the Magnaghi–Vavilov Basin (Central Tyrrhenian, Italy): New constraints from geological and geophysical observations. Tectonophysics. https://doi.org/10.1016/j.tecto.2016.01.041

Razin, P., Leroy, S., Robin, C., Robinet, J., Serra Kiel, J., Bellahsen, N., Grelaud, C., 2010. Dispositifs tecto-sédimentaires syn-rift et post-rift oligo-miocènes sur la marge sud du golfe d'Aden-Ile de Socotra (Yémen).

Redfern, P., Jones, J.A., 1995. The interior rifts of the Yemen - analysis of basin structure and stratigraphy in a regional plate tectonic context. Basin Res. 7, 337–356. https://doi.org/10.1111/j.1365-2117.1995.tb00121.x

Reston, T., Manatschal, G., 2011. Rifted margins: building blocks of later collision, in: Arc-Continent Collision, Frontiers in Earth Sciences. Springer Berlin Heidelberg, pp. 3–21. https://doi.org/10.1007/978-3-540-88558-0_1

Richardson, N.J., Underhill, J.R., Lewis, G., 2005. The role of evaporite mobility in modifying subsidence patterns during normal fault growth and linkage, Halten Terrace, Mid-Norway. Basin Res. 17, 203–223. https://doi.org/10.1111/j.1365-2117.2005.00250.x

Robinet, J., Razin, P., Serra-Kiel, J., Gallardo-Garcia, A., Leroy, S., Roger, J., Grelaud, C., 2013. The Paleogene pre-rift to syn-rift succession in the Dhofar margin (northeastern Gulf of Aden): Stratigraphy and depositional environments. Tectonophysics, The Gulf of Aden rifted margins system : Special Issue dedicated to the YOCMAL project (Young Conjugate Margins Laboratory in the Gulf of Aden) 607, 1–16. https://doi.org/10.1016/j.tecto.2013.04.017

Roger, J., Platel, J.P., Cavelier, C., Bourdillon-de-Grissac, C., 1989. Donnees nouvelles sur la stratigraphie et l'histoire geologique du Dhofar (sultanat d'Oman). Bull. Soc. Geol. Fr. V, 265–277. https://doi.org/10.2113/gssgfbull.V.2.265

Rosenbaum, G., Weinberg, R.F., Regenauer-Lieb, K., 2008. The geodynamics of lithospheric extension. Tectonophysics, Geodynamics of Lithospheric Extension 458, 1–8. https://doi.org/10.1016/j.tecto.2008.07.016

Sauter, D., Cannat, M., Rouméjon, S., Andreani, M., Birot, D., Bronner, A., Brunelli, D., Carlut, J., Delacour, A., Guyader, V., MacLeod, C.J., Manatschal, G., Mendel, V., Ménez, B., Pasini, V., Ruellan, E., Searle, R., 2013. Continuous exhumation of mantle-derived rocks at the Southwest Indian Ridge for 11 million years. Nat. Geosci. 6, 314–320. https://doi.org/10.1038/ngeo1771

Sengör, A.M.C., Burke, K., 1978. Relative timing of rifting and volcanism on Earth and its tectonic implications. Geophys. Res. Lett. 5, 419–421. https://doi.org/10.1029/GL005i006p00419

Shillington, D.J., Holbrook, W.S., Van Avendonk, H.J.A., Tucholke, B.E., Hopper, J.R., Louden, K.E., Larsen, H.C., Nunes, G.T., 2006. Evidence for asymmetric nonvolcanic rifting and slow incipient oceanic accretion from seismic reflection data on the Newfoundland margin. J. Geophys. Res. Solid Earth 111, B09402. https://doi.org/10.1029/2005JB003981

Stab, M., Bellahsen, N., Pik, R., Quidelleur, X., Ayalew, D., Leroy, S., 2016. Modes of rifting in magma-rich settings: Tectono-magmatic evolution of Central Afar. Tectonics 2015TC003893. https://doi.org/10.1002/2015TC003893

Tard, F., Masse, P., Walgenwitz, F., Gruneisen, P., 1991. The volcanic passive margin in the vicinity of Aden, Yemen. Bull. Cent. Rech. Explor.-Prod. Elf Aquitaine 15, 1–9.

Tari, G., Molnar, J., Ashton, P., Hedley, R., 2000. Salt tectonics in the Atlantic margin of Morocco. Lead. Edge 19, 1074–1078. https://doi.org/10.1190/1.1438481

Teixell, A., Labaume, P., Lagabrielle, Y., 2016. The crustal evolution of the west-central Pyrenees revisited: Inferences from a new kinematic scenario. Comptes Rendus Geosci., From rifting to mountain building: the Pyrenean Belt 348, 257–267. https://doi.org/10.1016/j.crte.2015.10.010

Tucholke, B.E., Sawyer, D.S., Sibuet, J.-C., 2007. Breakup of the Newfoundland Iberia rift. Geol. Soc. Lond. Spec. Publ. 282, 9–46. https://doi.org/10.1144/SP282.2

Tugend, J., Manatschal, G., Kusznir, N.J., Masini, E., Mohn, G., Thinon, I., 2014. Formation and deformation of hyperextended rift systems: Insights from rift domain mapping in the Bay of Biscay-Pyrenees. Tectonics 33, 2014TC003529. https://doi.org/10.1002/2014TC003529

Vendeville, B.C., Ge, H., Jackson, M.P.A., 1995. Scale models of salt tectonics during basement-involved extension. Pet. Geosci. 1, 179–183. https://doi.org/10.1144/petgeo.1.2.179

1417 Warden, A.J., Horkel, A.D., 1984. The geological evolution of the NE-branch of the Mozambique Belt (Kenya,
1418 Somalia, Ethiopia). Mitteilungen Osterreichischen Geol. Ges. 77, 161–184.

1419 Watchorn, F., Nichols, G.J., Bosence, D. W. J., 1998. Rift-related sedimentation and stratigraphy, southern
1420 Yemen (Gulf of Aden), in: Purser, B.H., Bosence, Dan W. J. (Eds.), Sedimentation and Tectonics in Rift Basins
1421 Red Sea:- Gulf of Aden. Springer Netherlands, pp. 165–189.

1422 Watremez, L., Leroy, S., Rouzo, S., d'Acremont, E., Unternehr, P., Ebinger, C., Lucazeau, F., Al-Lazki, A., 2011.
1423 The crustal structure of the north-eastern Gulf of Aden continental margin: insights from wide-angle seismic
1424 data. Geophys. J. Int. 184, 575–594. https://doi.org/10.1111/j.1365-246X.2010.04881.x

1425 White, R., McKenzie, D., 1989. Magmatism at rift zones: The generation of volcanic continental margins and
1426 flood basalts. J. Geophys. Res. Solid Earth 94, 7685–7729. https://doi.org/10.1029/JB094iB06p07685

1427 Whitmarsh, R.B., Manatschal, G., Minshull, T.A., 2001. Evolution of magma-poor continental margins from
1428 rifting to seafloor spreading. Nature 413, 150–154. https://doi.org/10.1038/35093085

1429 Ziegler, M.A., 2001. Late Permian to Holocene Paleofacies Evolution of the Arabian Plate and its Hydrocarbon
1430 Occurrences, in: GeoArabia. GulfPetroLink, pp. 445–504.

1431